

1997

Photoinduced metalloprotein electron-transfer in solid and in solution

Chengyu Shen
Iowa State University

Follow this and additional works at: <https://lib.dr.iastate.edu/rtd>

 Part of the [Inorganic Chemistry Commons](#)

Recommended Citation

Shen, Chengyu, "Photoinduced metalloprotein electron-transfer in solid and in solution" (1997). *Retrospective Theses and Dissertations*. 12035.
<https://lib.dr.iastate.edu/rtd/12035>

This Dissertation is brought to you for free and open access by the Iowa State University Capstones, Theses and Dissertations at Iowa State University Digital Repository. It has been accepted for inclusion in Retrospective Theses and Dissertations by an authorized administrator of Iowa State University Digital Repository. For more information, please contact digirep@iastate.edu.

INFORMATION TO USERS

This manuscript has been reproduced from the microfilm master. UMI films the text directly from the original or copy submitted. Thus, some thesis and dissertation copies are in typewriter face, while others may be from any type of computer printer.

The quality of this reproduction is dependent upon the quality of the copy submitted. Broken or indistinct print, colored or poor quality illustrations and photographs, print bleedthrough, substandard margins, and improper alignment can adversely affect reproduction.

In the unlikely event that the author did not send UMI a complete manuscript and there are missing pages, these will be noted. Also, if unauthorized copyright material had to be removed, a note will indicate the deletion.

Oversize materials (e.g., maps, drawings, charts) are reproduced by sectioning the original, beginning at the upper left-hand corner and continuing from left to right in equal sections with small overlaps. Each original is also photographed in one exposure and is included in reduced form at the back of the book.

Photographs included in the original manuscript have been reproduced xerographically in this copy. Higher quality 6" x 9" black and white photographic prints are available for any photographs or illustrations appearing in this copy for an additional charge. Contact UMI directly to order.

UMI

A Bell & Howell Information Company
300 North Zeeb Road, Ann Arbor, MI 48106-1346 USA
313/761-4700 800/521-0600

Photoinduced metalloprotein electron-transfer in solid and in solution

by

Chengyu Shen

A dissertation submitted to the graduate faculty
in partial fulfillment of the requirements for the degree of

DOCTOR OF PHILOSOPHY

Major: Inorganic Chemistry

Major Professor: Nenad M. Kostić

Iowa State University

Ames, Iowa

1997

UMI Number: 9814696

UMI Microform 9814696
Copyright 1998, by UMI Company. All rights reserved.

This microform edition is protected against unauthorized
copying under Title 17, United States Code.

UMI
300 North Zeeb Road
Ann Arbor, MI 48103

Graduate College
Iowa State University

This is to certify that the doctoral dissertation of
Chengyu Shen
has met the dissertation requirements of Iowa State University

Signature was redacted for privacy.

Major Professor

Signature was redacted for privacy.

For the Major Program

Signature was redacted for privacy.

For the Graduate College

TABLE OF CONTENTS

| | Pages |
|--|-------|
| GENERAL INTRODUCTION | 1 |
| Dissertation Organization | 2 |
| References | 3 |
| CHAPTER 1 CHARACTERIZATION OF ZINC-SUBSTITUTED CYTOCHROME C BY CIRCULAR DICHROISM AND RESONANCE RAMAN SPECTROSCOPIC METHODS | 6 |
| Abstract | 6 |
| Introduction | 7 |
| Experimental Procedures | 8 |
| Chemicals | 8 |
| Preparation of Zinc Cytochrome c | 9 |
| Measurements | 11 |
| Results and Discussions | 11 |
| Preparation of Zinc Cytochrome c | 11 |
| Circular Dichroism Spectra | 12 |
| Resonance Raman Spectra | 15 |

| | |
|---|----|
| The Case For Six-Coordination | 20 |
| Conclusions | 21 |
| Acknowledgement | 22 |
| References | 22 |
| CHAPTER 2: KINETICS OF PHOTOINDUCED ELECTRON- TRANSFER REACTIONS WITHIN SOL-GEL GLASS DOPED WITH ZINC CYTOCHROME C. STUDY OF ELECTROSTATIC EFFECTS IN CONFINED LIQUIDS | 27 |
| Abstract | 27 |
| Introduction | 28 |
| Experimental Procedures | 30 |
| Chemicals | 30 |
| The Sol-Gel Process | 30 |
| Kinetic Experiments | 31 |
| Spectroscopic Measurements | 33 |
| Porosity of the Glass | 33 |
| Protein Adsorption on Silica | 34 |
| Results and Discussions | 34 |
| Doped Silica Glass | 34 |
| Quenching of $^3\text{Zncyt}$ by the $[\text{Fe}(\text{CN})_6]^{3-}$ Anion | 42 |
| Quenching of $^3\text{Zncyt}$ by Electroneutral Molecules | 57 |
| Hindrance of Diffusion in Glasses | 59 |

| | |
|--|-----------|
| Conclusions | 61 |
| Acknowledgements | 62 |
| References | 62 |
| Supporting Information | 67 |
| CHAPTER 3: REDUCTIVE QUENCHING OF THE: TRIPLET STATE OF ZINC CYTOCHROME C BY HEXACYANOFERRATE(II) ANION AND BY CONJUGATE BASES OF ETHYLENEDIAMINETETRAACETIC ACID | 75 |
| Abstract | 75 |
| Introduction | 76 |
| Experimental Procedures | 78 |
| Chemicals | 78 |
| Kinetics | 78 |
| Purity of $K_4[Fe(CN)_6]$ | 79 |
| Results and Discussions | 79 |
| The Triplet State, 3Zncyt | 79 |
| Redox Potentials and Quenching Modes | 80 |
| Optical Absorption of the Anion Radical $Zncyt^-$ | 82 |
| Requirements For Reductive Quenching | 83 |
| Reductive Quenching of 3Zncyt by EDTA | 85 |
| Reductive Quenching of 3Zncyt by the $[Fe(CN)_6]^{4-}$ Ion | 90 |

| | |
|--|-----------|
| Conclusions | 93 |
| Acknowledgment | 93 |
| References | 94 |
| CHAPTER 4: EFFECTS OF MUTATION IN PLASTOCYANIN ON THE KINETICS OF THE PROTEIN REARRANGEMENT GATING THE ELECTRON-TRANSFER REACTION WITH ZINC CYTOCHROME C. ANALYSIS OF THE REARRANGEMENT PATHWAY | 99 |
| Abstract | 99 |
| Introduction | 101 |
| Materials and Methods | 104 |
| Chemicals | 104 |
| Buffers | 104 |
| Temperature and Viscosity | 104 |
| Zinc cytochrome c | 104 |
| Plastocyanin | 105 |
| Flash Kinetic Spectrophotometry | 105 |
| Kinetic Effects of Viscosity | 106 |
| Fittings of Data | 106 |
| Results | 106 |
| Natural Decay of the Triplet State, $^3\text{Zncyt}$ | 106 |
| Quenching of $^3\text{Zncyt}$ by Cupriplastocyanin | 108 |

| | |
|---|-----|
| The Slowest Component of Quenching and the Magnitude of Transient Absorbance | 109 |
| Kinetic Effects of Viscosity | 112 |
| Discussions | 112 |
| Plastocyanin Mutants | 112 |
| Mechanism of Quenching and the Rate Constants | 116 |
| Kinetic Effects of Viscosity | 117 |
| Analysis of the Viscosity Effects | 117 |
| Kinetics of the Rearrangement | 120 |
| Conclusions and Prospects | 122 |
| Acknowledgments | 122 |
| References | 123 |
| GENERAL CONCLUSIONS | 128 |
| ACKNOWLEDGMENTS | 129 |

GENERAL INTRODUCTION

Metal derivatives of cytochrome *c* have been extensively used in the studies of electron-transfer reactions. Among them, the most useful has been that containing the zinc(II) ion, designated Zncyt.¹⁻³ The zinc(II) ion has $3d^{10}$ configuration and is redox inactive. The inactivity of zinc porphyrin in the ground electronic state and redox activity in the excited state have proven useful in the study of cytochrome *c* complexes with small redox reagents or metalloproteins.⁴⁻¹⁰

Despite decades of study, the properties and reactivities of Zncyt remain incompletely understood. It is not known yet in what way replacement of Fe with Zn in Cytc may affect the protein structure. In terms of size and charge Zn(II) resembles Fe(II), but their other chemical properties differ. Iron porphyrins are mostly six-coordinated, but zinc porphyrins are only four- or five-coordinated in aqueous solution.¹¹⁻¹⁴ While native Fecyt is found to be six-coordinated, the coordination state of Zn(II) in Zncyt is controversial.¹⁵ Since the immediate environment of the porphyrin is of prime importance in determining reactivity, a more detailed characterization on this issue is needed.

Sol-gel glasses (silica hydrogel) doped with enzymes and other proteins hold promise as sensors or catalysts.¹⁶⁻²⁵ Sol-gel glasses and composite materials obtained from them have two main properties. Because they are porous, relatively small molecules can move through the pores and reach the large molecules that are trapped inside. Because these glasses are transparent in the UV-visible range, the chemicals and their reactions can be studied by optical spectroscopic methods.¹⁶

We studied the reaction of Zncyt with inorganic/organic quenchers in glass. We found interesting electrostatic effects that govern the reaction of metalloproteins in glass. These electrostatic effects should be taken into account in further research with doped glasses and in their applications as sensors and catalysts.

All of the previous studies on Zncyt in aqueous solution have dealt with oxidative quenching by various quenchers.⁴⁻¹⁰ The products of these reactions are zinc cytochrome *c* cation radical and the reduced form of the quencher. But Zncyt, once excited to its triplet state, is a strong oxidizing agent as well as a strong reducing agent. Here we explored the possibility of reductive quenching, products of which are cytochrome *c* anion radical and the oxidized form of the quencher.

Another topic discussed is the photoinduced electron transfer between two metalloproteins, zinc cytochrome *c* and plastocyanin. Kinetic studies carried out previously in our lab revealed the interplay between the structural rearrangement and the electron transfer.²⁶⁻²⁹ The gating process seems to be configurational fluctuation of the diprotein complex. Here we studied systematically the reaction of Zncyt with wild-type form and nine mutants of spinach plastocyanin. We studied this reaction at different viscosity to probe the dynamics of the process.

Dissertation Organization

This dissertation consists of four chapters. Chapter 1 deals with zinc cytochrome *c* characterization, Chapter 2 deals with electron transfer reactions in solid, Chapters 3 and 4 focus on electron transfer reaction in aqueous solution. Each chapter is self-contained with

its own equations, figures, tables, and references. Following the last chapter is general conclusions. With the exception of resonance Raman measurements (Chapter I and II) which were collected by Mr. George Chumanov and Mrs. Shuyu Ye, all the work in this dissertation was performed by the author of this thesis.

References

- (1). Vanderkooi, J. M. and Erecinska, M. *Eur. J. Biochem.* **1975**, *60*, 199.
- (2). Vanderkooi, J. M.; Adar, F.; and Erecinska, M. *Eur. J. Biochem.* **1976**, *64*, 381.
- (3). Erecinska, M. and Vanderkooi, J. M. *Meth. Enzymol.* **1978**, *53*, 165.
- (4). Vanderkooi, J. M.; Landesberg, R.; Haydon, G.; and Owen, C. *Eur. J. Biochem.* **1977**, *81*, 377.
- (5). Vanderkooi, J. M.; Glatz, P.; Casadei, J.; and Woodrow III, G. V. *Eur. J. Biochem.* **1980**, *110*, 189.
- (6). Koloczek, H.; Horie, T.; Yonetani, T.; Anni, H.; Maniara, M.; and Vanderkooi, J. M. *Biochemistry* **1987**, *26*, 3142.
- (7). Dixit, S. N.; Waring, A. J.; and Vanderkooi, J. M. *FEBS Lett.* **1981**, *125*, 86.
- (8). Dixit, B. B. S. N.; Moy, V. T.; and Vanderkooi, J. M. *Biochemistry* **1984**, *23*, 2103.
- (9). Horie, T.; Maniara, G.; and Vanderkooi, J. M. *FEBS Lett.* **1985**, *177*, 287.
- (10). Conklin, K. T. and McLendon, G. *J. Am. Chem. Soc.* **1988**, *110*, 3345.
- (11). Vogel, G. G. and Stahlbush, J. R. *Inorg. Chem.* **1977**, *16*, 950.
- (12). Nappa, M. and Valentine, J. S. *J. Am. Chem. Soc.* **1978**, *100*, 5075.

- (13). Scheidt, W. R.; Kastner, M. E.; and Hatano, K. *Inorg. Chem.* **1978**, *17*, 706.
- (14). Scheidt, W. R.; Mondal, J. U.; Eigenbrot, C. W.; Adler, A.; Radonovich, L. J.; and Hoard, J. L. *Inorg. Chem.* **1986**, *25*, 795.
- (15). Anni, H.; Vanderkooi, J. M.; and Mayne, L. *Biochemistry* **1995**, *34*, 5744.
- (16). Yamanaka, S. A.; Nishida, F.; Ellerby, L. M.; Nishida, C. R.; Dunn, B.; Valentine, J. S.; Zink, J. I. *Chem. Mater.* **1992**, *4*, 495.
- (17). Wu, S.; Ellerby, L. M.; Cohan, J. S.; Dunn, B.; Valentine, J. S.; Zink, J. I. *Chem. Mater.* **1993**, *5*, 115.
- (18). Akbarian, F.; Dunn, B.; Zink, J. I. *J. Mater. Chem.* **1993**, *3*, 1041.
- (19). Lopez, T.; Moran, M.; Navarrete, J.; Herrera, L.; Gomez, J. *J. Non-Cryst. Solids* **1992**, *147*, 753.
- (20). Matsui, K.; Tominaga, M.; Arai, Y.; Satoh, H.; Kyoto, M. *J. Non-Cryst. Solids* **1994**, *169*, 295.
- (21). Matsui, K. *Langmuir* **1992**, *8*, 673.
- (22). Ellerby, L. M.; Nishida, C. R.; Nishida, F.; Yamanaka, S. A.; Dunn, B.; Valentine, J. S. *J. Am. Chem. Soc.* **1995**, *117*, 9505.
- (23). Dave, B. C.; Soye, H.; Miller, J. M.; Dunn, B.; Valentine, J. S.; Zink, J. I. *Chem. Mater.* **1995**, *7*, 1431.
- (24). Yamanaka, S. A.; Dunn, B.; Valentine, J. S.; Zink, J. I. *J. Am. Chem. Soc.* **1995**, *117*, 9095.
- (25). Dave, B. C.; Dunn, B.; Valentine, J. S.; Zink, J. I. *Anal. Chem.* **1994**, *66*, 1120A.

- (26). Zhou, J. S. and Kostić, N. M. *J. Am. Chem. Soc.* **1992**, *114*, 3562.
- (27). Zhou, J. S. and Kostić, N. M. *Biochemistry* **1992**, *31*, 7543.
- (28). Zhou, J. S. and Kostić, N. M. *The Spectrum* **1992**, *5*, No. 2, 1.
- (29). Peerey, L. M. and Kostić, N. M. *Biochemistry* **1989**, *28*, 1861.

CHAPTER 1

CHARACTERIZATION OF ZINC-SUBSTITUTED CYTOCHROME *C* BY CIRCULAR DICHROISM AND RESONANCE RAMAN SPECTROSCOPIC METHODS

Chengyu Shen and Nenad M. Kostić

Abstract

Iron(III) in cytochrome *c* is replaced with zinc(II) by a modification of a method published by others, and the procedure is described in full detail. Three forms of cytochrome *c* — those containing iron(III), iron(II), and zinc(II)—are examined by circular dichroism spectroscopy and resonance Raman spectroscopy. Circular dichroism spectra show that introduction of zinc(II) ions does not appreciably alter the conformation of cytochrome *c*. Resonance Raman spectra indicate the size of the porphyrin "core" that is inconsistent with six-coordination and consistent with five-coordination. Unlike the iron(III) and iron(II) ions, which are bound to two axial ligands (His 18 and Met 80), the zinc(II) ion in cytochrome *c* seems to be bound to only one, most probably His 18. Evidence pertaining to the question of axial coordination is discussed.

Introduction

Because metalloproteins act as electron carriers and redox enzymes in photosynthesis and respiration, chemical mechanisms of their electron-transfer reactions are being studied vigorously.¹⁻⁵ Various cytochrome *c* are ubiquitous in biological systems.⁶⁻⁸ Structures of several of these heme proteins are known in detail. Because of their biological roles and favorable chemical and spectroscopic properties, mammalian cytochromes *c* have proved invaluable in numerous biochemical and biophysical studies of general importance.⁶⁻⁸

Just as the organic part of proteins can be modified by mutagenesis, the active sites of metalloproteins can be modified by methods of coordination chemistry. Despite the great stability of the macrocyclic complex that iron(II) and iron(III) ions form with protoporphyrin IX, these ions can be replaced by several other transition-metal ions.⁹⁻¹⁰ Among the so-called reconstituted derivatives of cytochrome *c*, the most useful has been that containing the zinc(II) ion, designed Zncyt.¹¹⁻¹³ Whereas iron ions contain partially filled 3d orbitals and undergo thermal redox reactions, the zinc(II) ion has 3d¹⁰ configuration and is redox-inactive. This inactivity of zinc porphyrin in the ground electronic state has proven useful in the study of cytochrome *c* complexes with other metalloproteins.¹⁴⁻¹⁶ It is the properties of the porphyrin excited states that make zinc cytochrome *c* very useful. The fluorescent singlet state, with a lifetime of ca. 3 ns, and the phosphorescent triplet state, with a lifetime of ca. 10 ms, are monitored in studies of porphyrin-protein interactions, protein-protein complexes, and photoinduced electron-transfer reactions between proteins.¹⁷⁻³²

Despite these important applications, zinc cytochrome *c* remains incompletely characterized. An earlier study³³ indicated that metal replacement does not noticeably perturb the overall structure of the porphyrin, but the coordination sphere of the zinc(II) ion was not explored in detail. Zinc(II) porphyrins in noncoordinating solvents remain four-coordinate; in coordinating solvents or in the presence of good ligands they tend to form

five-coordinate complexes by binding one axial ligand.³⁴⁻³⁷ Six-coordinate complexes, which contain two axial ligands, have not been detected in solution; we know of two such complexes,^{38,39} both of which exist only in crystals. The number and identity of the axial ligand(s) in the zinc cytochrome *c* was long unknown. Several recent studies testify to the continuing need for characterization of this protein.⁴⁰⁻⁴³ In one of them,⁴³ NMR and optical spectroscopic evidence was interpreted in terms of axial ligation of the zinc(II) ion with both His 18 and Met 80 residues. Although this claim is reasonable, it was received skeptically because six-coordinate zinc(II) porphyrin complexes are rare and because an earlier spectroscopic study⁹ claimed that only one axial ligand is present. Coordination numbers of non-iron metal ions in cytochrome *c* has been controversial.⁴³ Some derivatives that were initially believed to be six-coordinate on close examination turned out to be five-coordinate.^{43,44} Since the complete three-dimensional structure of zinc cytochrome *c* has not been determined by either X-ray crystallography or NMR spectroscopy, additional spectroscopic studies of zinc(II) coordination are needed.

To our knowledge, this is the first report of resonance Raman and circular dichroism spectra of zinc cytochrome *c*. Their analysis furthers our understanding of this important protein.

Experimental Procedures

Chemicals

Distilled water was further demineralized and purified to a resistance greater than $17 \text{ M } \Omega \text{ cm}^{-1}$. All the chemicals were of reagent grade. Sodium phosphate buffers had pH of 7.0 and the concentration specified. Hydrogen fluoride in bottles was obtained from Air Products and Chemicals, Inc. Ultrapure argon was obtained from Air Products Co. Horse-heart cytochrome *c* was the product of type III from Sigma Chemical Company. The

protein for spectroscopic experiments was oxidized by a small excess of $K_3[Fe(CN)_6]$ and purified by cation-exchange chromatography on a column of CM-52, with 85 mM sodium phosphate buffer at pH 7.0 as an eluent⁴⁵. The major (middle) band was concentrated by ultrafiltration, purified on a Bio-Rad desalting column sized 1.5 × 4.0 cm with a 10 mM sodium phosphate buffer at pH 7.0 as an eluent and used for further experiments.

Ferrocytochrome *c* was obtained by reduction with ascorbic acid and removal of this reagent with a Bio-Rad desalting column, as just described.

Preparation of Zinc Cytochrome *c*

This method is a modification of published ones.^{11, 12, 20, 21} All experiments involving hydrogen fluoride were done inside a strong hood; the body was protected with a respiration mask, eye goggles, a face shield, gloves, a laboratory coat, and a plastic apron. All experiments involving metal-free (so-called free-base) cytochrome *c*, designed H₂cyt, and its zinc(II) derivative, designed Zncyt, were done in the dark, as quickly as possible.

A 50-mg sample of ferricytochrome *c* was added to a 50-mL Teflon beaker through a cone of glassy paper, so that no particles stuck to the beaker wall. The beaker was suspended in a dewar holding liquid nitrogen. Hydrogen fluoride gas from a bottle was passed into the open beaker, close to the solid cytochrome *c*, for at least 40 s. The gas condensed into the liquid. The bottle was kept upright, to avoid spilling the liquid hydrogen fluoride. The content of the open beaker was stirred with a Teflon rod for ca. 10 min, until a purple, viscous solution was obtained. Most of the hydrogen fluoride was consumed in the formation of FeF_3 . If necessary, more hydrogen fluoride gas was added and stirring was continued until cytochrome *c* completely dissolved. The Teflon beaker was removed from the liquid-nitrogen bath, a small aliquot of the solution was dissolved in a 150 mM phosphate buffer at pH 7.0, and its visible absorption spectrum was recorded. Metal-free

cytochrome *c* (H₂cyt) has characteristic peaks at 506, 540, 568, and 620 nm. A small amount of residual HF in the Teflon beaker was removed by a current of ultrapure argon. The argon flow was stopped when white fumes no longer emerged from the beaker. The metal-free cytochrome *c* was dissolved in a minimum volume of 50 mM phosphate buffer at pH 7.0. The resulting solution, which was still purple, was desalted by elution with 50 mM phosphate buffer at pH 7.0 through a Bio-Rad desalting column sized 1.5 × 4.0 cm. Subsequent operations were done in common glassware. The effluent was acidified with 1/10 to 1/20 of its volume of glacial acetic acid, approximately tenfold molar excess of zinc acetate was added, and the mixture was kept in a water bath at 50-60 °C for 30 min. The solution became saturated with zinc acetate, and a small amount of this solid remained. Reconstitution was checked by visible absorption spectra. As H₂cyt was converted to Zn₂cyt, the bands of the former disappeared and those of the latter, at 423, 549, and 585 nm, appeared. The solution was brought to 4 < pH < 6 by addition of solid Na₂HPO₄, and undissolved zinc acetate was removed by centrifugation at 6000 rpm, in a table-top centrifuge. The resulting clear solution was desalted and concentrated by ultrafiltration in an Amicon cell, with a YM-5 membrane, at 4 °C. This solution was chromatographed on a CM-52 column sized 2.5 × 8 cm, with a 85 mM sodium phosphate buffer at pH 7.0 as the eluent. Usually only one band was evident. The first and the last portions of it were discarded, and only the middle portion was saved. In rare cases when some ferricytochrome *c* remained, it migrated as a distinct second band and was discarded. The effluent was diluted tenfold with water and concentrated by ultrafiltration, as described above. The phosphorescence (emission from the triplet state) had the lifetime of 10 ms, corresponding to the natural decay with the rate constant of 100 s⁻¹. The yield was 35%. Zinc cytochrome *c* can be stored for months at 77 K, in the dark.

Measurements

Protein solutions were made in a 2.5 mM phosphate buffer at pH 7.0. Circular dichroism spectra and UV-visible spectra at room temperature were measured with JASCO 710 and IBM 9420 instruments, respectively. Concentrations of the Fe(III), Fe(II), and Zn(II) forms of cytochrome *c* in the circular dichroism samples were as follows: 3.8, 2.4, and 2.9 M in the interval 200-350 nm; and 17.5, 18.6, and 9.7 μ M in the interval 350-500 nm. Resonance Raman spectra were measured with a Spex Triplemate spectrometer equipped with a Princeton Instruments CCD detector, model LN 1152, cooled to -120 °C. The excitation source was the 413.1-nm line of a Coherent 100 Kr⁺ laser. The laser power at the sample was ca. 10 mW, and scattered radiation was collected in the so-called backscattered configuration. In order to suppress luminescence of zinc cytochrome *c* the samples were kept in an optical dewar vessel containing liquid nitrogen, and the measurements were made at 77 K. The protein concentration was 0.10 mM.

Results and Discussions

Preparation of Zinc Cytochrome *c*

This useful derivative of cytochrome *c* can be prepared by several variations of the same method.^{11, 12, 20, 21} Our procedure shortens the time of handling H₂cyt and Zncyt, both of which are unstable. Any ferricytochrome *c* that might remain after incubation with zinc acetate is removed from zinc cytochrome *c* at the end, by cation-exchange chromatography. Our account of the procedure is based on numerous repetitions by several researchers. The instructions are sufficiently detailed to ensure success without unnecessary failures.

Circular Dichroism Spectra

Circular dichroism (CD) spectroscopy has proven useful in the study of proteins, especially of heme proteins⁴⁶⁻⁵³. We compare the spectra of cytochrome *c* containing iron(III), iron(II), and zinc(II) ions in the porphyrin. The spectra in two wavelength intervals, shown in Figures 1 and 2, were recorded with protein solutions of different concentrations but in the same buffer.

Intrinsic Bands. The negative peaks at 209 and 222 nm are due to the $\pi - \pi^*$ and $n - \pi^*$ transitions in the amide group, respectively.^{54, 55} Circular dichroism in the far-UV range is a property of the polypeptide backbone and is a sensitive indicator of the protein conformation. The three common types of secondary structure (α -helix, antiparallel β -sheet, and random coil) and even the less-common types can be recognized and quantitated on the basis of the intrinsic CD intensities. As the superimposable spectra in Figure 1 show, the three forms of cytochrome *c* have nearly identical conformations. This was known for the two iron forms,^{7, 8, 46, 48, 49} and the same is true also for the zinc(II) form. Our finding agrees with the results of a recent NMR spectroscopic study,⁴³ which showed that replacement of iron(II) by zinc(II) does not cause any significant conformational change in cytochrome *c*.

Soret Bands. Circular dichroism corresponding to the Soret absorption band is caused by interaction of the heme chromophore, which itself is achiral, with the chiral protein surrounding it. Aromatic side chains and peptide carbonyl groups do, and aliphatic side chains apparently do not, contribute to the induced CD of the heme.^{51, 52} Because the intensity, shape, and sign of a CD band all depend on these interactions, Soret spectra are

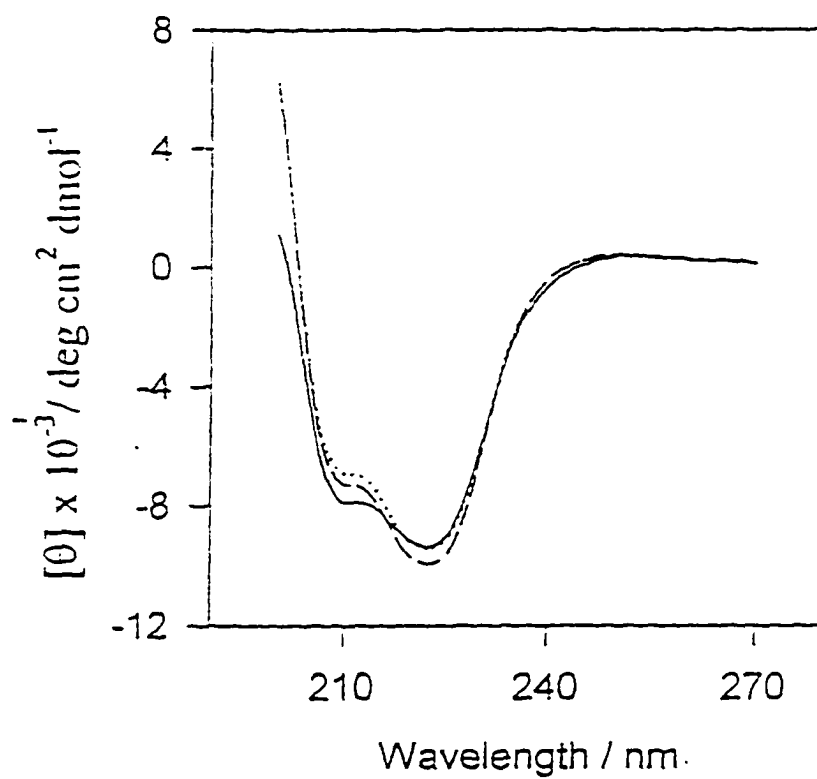


Figure 1. Circular dichroism spectra of the protein matter in ferricytochrome *c* (dashed line), ferri-ferrocytochrome *c* (solid line), and zinc cytochrome *c* (dashed-dotted line)

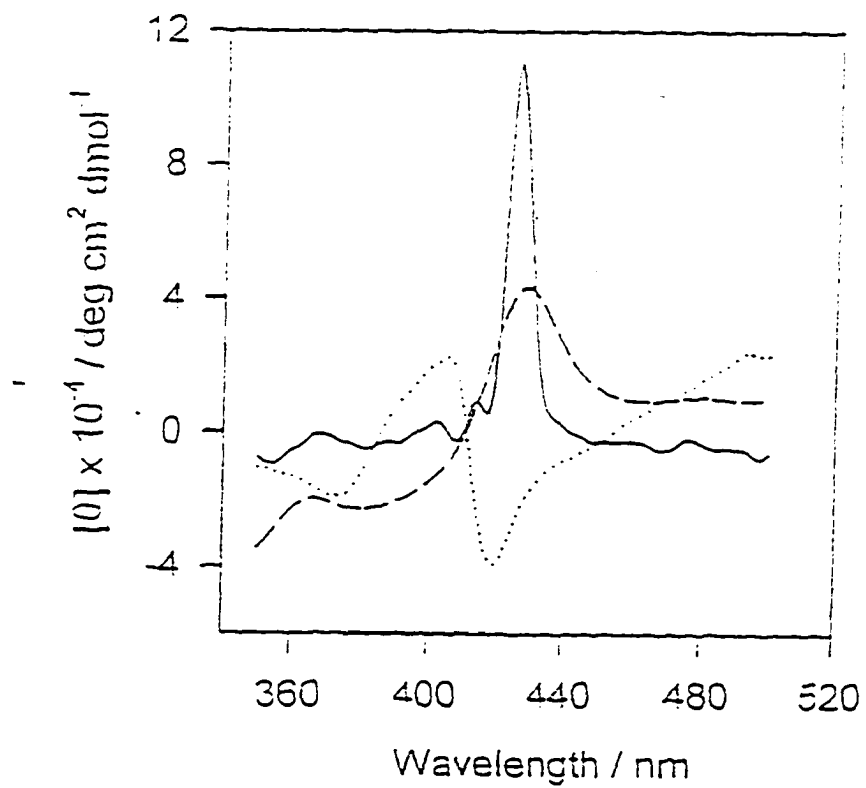


Figure 2. Circular dichroism spectra of the heme in ferricytochrome *c* (dashed line), ferrocytochrome *c* (solid line), and zinc cytochrome *c* (dashed-dotted line).

As Figure 2 shows, mere reduction of iron(III) to iron(II) causes a split band to change to a relatively narrow, single band. This change can be a result of different factors in different derivatives of cytochrome *c*.⁴⁶ The band maxima of the iron(II) and zinc(II) proteins nearly coincide, but the band widths differ somewhat. This spectral similarity may indicate that electron densities are similar.

Resonance Raman Spectra

Resonance Raman spectroscopy has successfully been applied in various studies of metalloporphyrins, their complexes, and proteins containing these complexes.⁵⁶⁻⁵⁸ Laser excitation at wavelengths within electronic absorption bands of the heme can cause great enhancement of the vibrational modes of the heme.⁵⁹ To our knowledge, this powerful experimental method has not been applied to zinc cytochrome *c*.

Because the excitation wavelength of 413.1 nm falls in the Soret range, totally-symmetric vibrational modes are enhanced.⁶⁰ Assignments in Table 1 are based on a thorough, recent study of resonance Raman spectra of cytochrome *c*⁵⁸ and on a detailed, earlier study of nickel(II) octaethylporphyrin by normal-coordinate analysis.^{61, 62}

Higher Frequencies. Even though most of the vibrational modes in Table 1 do not directly involve the metal ion, their wavenumbers indirectly depend on the identity of this ion and its axial ligands. This dependence is most evident in the porphyrin skeletal modes, (table 1) those having wavenumbers greater than 1350 cm^{-1} . Some of the bands, so-called markers, are diagnostic of the oxidation state and the spin state of the metal ion. The prominent band 4, corresponding to a A_{1g} mode, is sensitive to the oxidation state of the metal ion and the π - electron density of the porphyrin ring.⁶³⁻⁶⁸ Its wavenumber in zinc

Table 1. Resonance Raman Bands³ and Their Wavenumbers for Cytochrome *c*
Containing Three Metal Ions

| Band ^b | Wavenumbers / cm ⁻¹ | | | Band ^b | Wavenumbers / cm ⁻¹ | | |
|------------------------------------|--------------------------------|--------|--------|---|--------------------------------|---------|---------|
| | Fe(III) | Fe(II) | Zn(II) | | Fe(III) | Fe(II) | Zn(II) |
| * v ₁₀ | 1641 | 1626 | 1614 | v ₄₆ | | 925 | 920 |
| v ₃₈ | | 1609 | 1608 | γ ₁₀ | 840 | 837 | |
| v ₂ | | 1598 | 1591 | γ ₄ | 818 | 826 | 822 |
| * v ₁₉ | 1589 | 1586 | 1579 | v ₆ | 799 | 797,791 | 799 |
| v ₁₁ | 1564 | 1552 | 1557 | v ₁₅ | 748 | 750 | 756 |
| * v ₃ | 1507 | 1496 | 1481 | γ ₅ | 731 | 731 | 728 |
| v ₂₉ | 1406 | 1409 | 1407 | γ ₁₁ | | 724 | |
| v ₂₀ | | 1397 | 1388 | v ₇ | 701 | 700 | 698 |
| * v ₄ | 1375 | 1364 | 1369 | v(C _a S) | 679 | 692,682 | 682 |
| δ(C _a H) _{2,4} | 1318 | 1315 | 1321 | γ ₂₀ | 656 | 667,652 | 664 |
| δ(C ₂ H) _{2,4} | 1306 | 1301 | 1305 | v ₄₈ | 641,631 | 643,632 | 642 |
| v ₁₃ | 1234 | 1231 | | γ ₂₁ | 569 | 569 | 577 |
| v ₃₀ | 1177 | 1174 | 1176 | v ₄₉ | | 537 | |
| v ₄₃ | | 1154, | 1141 | γ ₁₂ | 522 | 520 | 520,510 |
| | | 1143 | | | | | |
| v ₁₄ | 1129 | 1131 | | v ₃₃ | 481 | 479 | |
| v ₂₂ | | 1131 | | γ ₂₂ | 445 | 466 | 451 |
| v ₅ | | 1118 | 1118 | δ(C _β C _a C _b) _{2,4} | 415 | 421,413 | 421,411 |
| v ₄₄ | | 1118 | | δ(C _β C _a S) | 400 | 402,393 | |

| Table 1 | (continued) | | | (continued) | | | |
|--------------------------------------|-------------|--------|------|--|-----|---------|---------|
| $\delta(\text{C}_b\text{H}_3)_{2,4}$ | 1092 | 1093 | 1089 | $\delta(\text{C}_\beta\text{C}_c\text{C}_d)_{6,7}$ | 379 | 381,375 | 384,375 |
| ν_{23} | | 1080 | | ν_{50} | 363 | 360 | 363 |
| $\delta(\text{CH}_3)$ | | 1063 | | * ν_8 | 355 | 349 | 342 |
| $\delta(\text{C}_b\text{H}_3)_{2,4}$ | 1056 | 1055 | 1052 | ν_{51} | 307 | 308 | 315 |
| ν_{31} | 1030 | 1031 | 1029 | ν_9 | 270 | 267 | 265 |
| $\nu(\text{C}_a\text{C}_b)_{2,4}$ | | 1017 | 1019 | ν_{53} | | 203 | 191 |
| ν_{45} | | 990 | | ν_{34} | | 182 | 184 |
| $\nu(\text{C}_c\text{C}_d)_{6,7}$ | 971 | 972.96 | 969 | ν_{18} | 165 | 161 | 171 |
| | | 8 | | | | | |
| ν_{32} | | 946 | | | | | |

a Assignments are in Ref.

b the most informative bands are marked with an asterisk.

cytochrome *c* falls between the wavenumbers in ferricytochrome *c* and ferrocycytochrome *c*. This finding may reflect the net charges of the three ions, which are related to, but smaller than, the oxidation states. The iron(III) ion has the highest actual charge. Of the two ions with the oxidation state of II, zinc(II) ion, which forms bonds that are largely electrostatic, has a higher charge than the iron(II) ion, which forms bonds that are partially covalent.

Axial Ligation. The size of the porphyrin "core," i.e., the distance from the center of the "hole" to the nitrogen atoms, can be deduced from the positions of the bands ν_3 , ν_{10} , and ν_{19} .⁶⁹⁻⁷³ As Table 1 shows, the corresponding wavenumbers for zinc cytochrome *c* are 7-15 cm^{-1} lower than those for ferrocyclochrome *c* and 10-27 cm^{-1} lower than those for ferricytochrome *c*. The core sizes calculated⁷⁴ from the ν_3 , ν_{10} , and ν_{19} wavenumbers generally agree. This general consistency in the results obtained by applying empirical relationships give us confidence in both the results and the relationships. The average values of the core sizes, based on the three wavenumbers, are the following: 1.981, 2.001, and 2.025 Å for the Fe(III), Fe(II), and Zn(II) forms of cytochrome *c*.

Stretching vibrations involving the iron atom and its axial ligands, His 18 and Met 80, could not be detected in the most thorough study of resonance Raman spectra of native cytochrome *c*.⁵⁸ We could not detect them in the spectra of zinc cytochrome *c*, either. Because of this limitation, we cannot directly determine the axial ligation of the zinc(II) ion in the protein. Structures of four-coordinate and five-coordinate zinc(II) porphyrin complexes showed that addition of one axial ligand brings about an expansion of the core.⁴³ ⁶³ If addition of another axial ligand has a similar effect, the core size of a six-coordinate complex is expected to be ca. 2.050 Å. Indeed, actual structures of two six-coordinate complexes revealed such an expansion even when the axial ligands are weakly bonded to the zinc(II) ion in the porphyrin: 2.052 Å when the axial Zn-N distances are 2.432 Å³⁹ and 2.057 Å when the axial Zn-O distances are 2.380 Å.³⁸ Clearly, the stronger the axial bonds, the wider the porphyrin core. Even a moderately strong axial bonding to a six-coordinate zinc(II) atom in cytochrome *c* would be expected to result in a core size of ca. 2.060 Å, far larger than the actual value of 2.025 Å. Zinc(II) porphyrins inserted into apomyoglobin acquire one axial histidine ligand, most likely His 93.^{10, 43} Resonance Raman spectra of myoglobin so reconstituted with zinc(II) complexes containing two different porphyrins

indicated the core size of 2.035 Å,⁶³ which is similar to the value that we find in zinc cytochrome *c*. The position of the band ν_4 depends on the core size as well as the factors mentioned above. We note that the wavenumber predicted for the five-coordinate zinc(II) porphyrin complex with imidazole as the axial ligand is 1369 cm⁻¹,⁶³ exactly the value that we found in zinc cytochrome *c* (Table 1). To summarize, the shifts in the marker bands expected of a hexacoordinate complex would be much greater than those that we observed in our spectra, which are well resolved. On the basis of this indirect evidence, we suggest that the zinc(II) ion in the reconstituted cytochrome *c* has only one axial ligand. Since imidazole and similar nitrogen bases are common, and thio ethers are rare, as axial ligands in zinc porphyrin complexes,³⁴⁻³⁹ the likely axial ligand in zinc cytochrome *c* is His 18. Similarity of the core sizes in zinc(II) derivatives of cytochrome *c* and myoglobin further corroborates this conclusion.

Lower Frequencies. As Table 1 shows, the spectrum of zinc cytochrome *c* retains the bands found in the native protein, in some cases with somewhat altered relative intensities. The bands in the intervals 731-632 and 421-342 cm⁻¹ are broader for the iron(III) and zinc(II) forms of the protein than for the iron(II) form; the bands of the latter are nicely resolved. The band ν_{15} , corresponding to the pyrrole breathing mode, is much weaker and broader in the first two forms than in the third. The band ν_{21} has a higher wavenumber and lower intensity for the zinc(II) form than for the iron(II) form. The band ν_8 , corresponding to a mixture of the stretching of the metal-nitrogen bonds and bending of the porphyrin-substituent bonds in the zinc(II) lies 7 cm⁻¹ below that in the iron(II) form and 13 cm⁻¹ below that in the iron(III) form. This band, too, seems to be sensitive to the size of the porphyrin core. Five-coordination of the zinc(II) ion in myoglobin is accepted.⁷⁵ That the wavenumbers ν_8 in the spectra of zinc cytochrome *c* and zinc myoglobin⁶³ are identical is additional evidence in favor of five-coordination of the zinc(II) ion in cytochrome *c*.

The Case for Six-Coordination

Having suggested that Met 80 may not be coordinated to the zinc(II) ion in cytochrome *c*, we are obligated to consider the evidence against our suggestion. Position of a near-UV absorption band indicates axial ligation but does not allow determination of either the number or the chemical nature of the axial ligands.⁴³ Absorption spectra, therefore, are consistent with our proposal. Contrary evidence comes from ¹H NMR spectra, in which well over 200 resonances, corresponding to 67 out of 104 amino-acid residues, were assigned and compared in the spectra of the iron(II) and zinc(II) forms of the protein.⁴³ "Close identity" was reported for the resonances corresponding to the side chains of His 18 and Met 80 in the two forms, and this was taken as evidence that both of these ligands are bound to the zinc(II) ion. Only three (out of 67) residues have more than one proton whose chemical shifts in the two forms of cytochrome *c* differ by more than 0.21 ppm. Significantly, both His 18 and Met 80 belong to this small group. Only three (out of well over 200) resonances are perturbed by as much as 0.30-0.32 ppm when iron(II) is replaced by zinc(II). Again, one of them corresponds to Met 80, the residue whose coordination is in question. These facts, combined with the abundance of zinc(II) porphyrin complexes having one axial ligand and the rarity of those having two, require a skeptical analysis of the NMR spectra.

Without attempting such an analysis, we offer some thoughts that may be relevant to it. The relatively small perturbation of His 18 upon replacement of iron(II) with zinc(II) may be a symptom of an indirect effect of the removal of the other axial ligand, Met 90. Electronic effects are easily transmitted between trans ligands in metal complexes. The relatively large perturbations of Met 80 are tellingly localized in the CH (0.30 ppm) and CH₃ (0.21 ppm) groups. These two groups are directly bonded to the sulfur atom and are expected to feel the presence or absence of the sulfur-metal bond. Indeed, coordination of

aliphatic thio ethers of the type CH_2SCH_3 to platinum(II), a metal that forms many thioether complexes, brings about perturbations of 0.33 ± 0.07 ppm;⁷⁶⁻⁷⁹ this is an average of 14 values, and the variation given is one standard deviation. Clearly, the perturbations found in Met 80 resemble those in magnitude. Very few iron(II) porphyrin complexes containing axially coordinated thioethers are known, and we found NMR spectroscopic data for only one realistic model of the active site in cytochrome *c*.⁸⁰ The aryl alkyl sulfide ligand in it, however, differs from the dialkyl sulfide group in methionine. Chemical shifts of the methyl group are 2.20 ppm when it is free and 3.56 ppm when it is coordinated to iron(II) porphyrin in the six-coordinate complex. The largeness of this change may corroborate the conclusion⁴³ that the smaller change observed in zinc cytochrome *c* is not caused by detachment of Met 80 from the metal ion and refute our claim of five-coordination. Because, however, the chemical shift and its changes are affected much more by the ring current in the porphyrin group than by coordination, it is conceivable that Met 80 held above the heme but not coordinated to the zinc(II) ion may have approximately the same chemical shift as Met 80 coordinated to the iron(II) ion. In this case, the small differences of 0.21 and 0.30 ppm may still be due to the absence of direct coordination.

Conclusions

Our analyses of circular dichroism and resonance Raman spectra show that replacement of iron(II) or iron(III) by zinc(II) in cytochrome *c* causes little, if any, structural perturbation of the protein conformation and a large change of ligation at the active site. Even though one of the axial ligands in native cytochrome *c*, most likely Met 80, does not seem to be coordinated in the zinc(II) form of this protein, the protein structure remains essentially unchanged. This finding supports the recent notion of the structure of

metalloproteins. According to this view, the coordination geometry of the metal site is governed more by the protein structure than by the intrinsic structural preferences of the metal atom. In this case, one axial metal-ligand bond, which is present in native cytochrome *c* but apparently absent in its zinc(II) form, is not essential for the preservation of the overall protein conformation and of the structure of its active site.

Acknowledgement. We thank Maja Ivković-Jensen, Milan Crnogorac, and Ekaterina V. Sokerina for their suggestions about preparation of zinc cytochrome *c*.

References

- (1). Hoffman, B. M.; Natan, M. J.; J. Nocek, J. M.; and Wallin, S. A. *Struc. Bonding* **1991**, *75*, 86.
- (2). McLendon, G. and Hake, R. *Chem. Rev.* **1992**, *92*, 481.
- (3). Winkler, J. R. and Gray, H. B. *Chem. Rev.* **1992**, *92*, 369.
- (4). Mauk, A. G. *Struct. Bonding* **1991**, *75*, 131.
- (5). Kostić, N. M. *Metal Ions Biol. Syst.* **1991**, *27*, 129.
- (6). Pettigrew, G. W. and Moore, G. R. *Cytochromes c: Biological Aspects*, Springer-Verlag: Berlin, 1987.
- (7). Moore, G. R. and Pettigrew, G. W. *Cytochromes c: Evolutionary, Structural and Physicochemical Aspects*, Spinger-Verlag: Berlin, 1990.
- (8). Scott, R. A. and Mauk, A. G. Editors, *CytochromeĖc: A Multidisciplinary Approach*, University Science Books: Mill Valley, CA, 1996.
- (9). Chien, J. C. W. *J. Phys. Chem.* **1978**, *82*, 2171.
- (10). Chien, J. C. W. *J. Am. Chem. Soc.* **1978**, *100*, 1310.
- (11). Vanderkooi, J. M. and Erecinska, M. *Eur. J. Biochem.* **1975**, *60*, 199.

- (12). Vanderkooi, J. M.; Adar, F.; and Erecinska, M. *Eur. J. Biochem.* **1976**, *64*, 381.
- (13). Erecinska, M. and Vanderkooi, J. M. *Meth. Enzymol.* **1978**, *53*, 165.
- (14). Vanderkooi, J. M.; Landesberg, R.; Haydon, G.; and Owen, C. *Eur. J. Biochem.* **1977**, *81*, 377.
- (15). Vanderkooi, J. M.; Glatz, P.; Casadei, J.; and Woodrow III, G. V. *Eur. J. Biochem.* **1980**, *110*, 189.
- (16). Koloczek, H.; Horie, T.; Yonetani, T.; Anni, H.; Maniara, M.; and Vanderkooi, J. M. *Biochemistry* **1987**, *26*, 3142.
- (17). Dixit, S. N.; Waring, A. J.; and Vanderkooi, J. M. *FEBS Lett.* **1981**, *125*, 86.
- (18). Dixit, B. B. S. N.; Moy, V. T.; and Vanderkooi, J. M. *Biochemistry* **1984**, *23*, 2103.
- (19). Horie, T.; Maniara, G.; and Vanderkooi, J. M. *FEBS Lett.* **1985**, *177*, 287.
- (20). Conklin, K. T. and McLendon, G. *J. Am. Chem. Soc.* **1988**, *110*, 3345.
- (21). Elias, H.; Chou, M. H.; and Winkler, J. R. *J. Am. Chem. Soc.* **1988**, *110*, 429.
- (22a). Vos, K.; Lavalette, D.; and Visser, A. J. W. G. *Eur. J. Biochem.* **1987**, *169*, 269.
- (22b). Zhou, J. S. and Hoffman, B. M. *Science* **1994**, *265*, 1693.
- (23). Zhou, J. S. and Kostić, N. M. *J. Am. Chem. Soc.* **1991**, *113*, 6067.
- (24). Zhou, J. S. and Kostić, N. M. *J. Am. Chem. Soc.* **1991**, *113*, 7040.
- (25). Zhou, J. S. and Kostić, N. M. *J. Am. Chem. Soc.* **1992**, *114*, 3562.
- (26). Zhou, J. S. and Kostić, N. M. *Spectrum* **1992**, *5*, 1.
- (27). Zhou, J. S. and Kostić, N. M. *Biochemistry* **1993**, *32*, 4539.
- (28). Zhou, J. S. and Kostić, N. M. *J. Am. Chem. Soc.* **1993**, *115*, 10796.
- (29). Qin, L. and Kostić, N. M. *Biochemistry* **1994**, *33*, 12592.
- (30). Zhou, J. S. and Kostić, N. M. *Biochemistry* **1992**, *31*, 7543.
- (31). Qin, L. and Kostić, N. M. *Biochemistry* **1996**, *35*, 0000.
- (32). Shen, C. and Kostić, N. M. *Inorg. Chem.* **1996**, *35*, 2780.

- (33). Moore, G. R.; Williams, R. J. P.; Chien, J. C. W.; and Dickinson, L. C. *J. Inorg. Chem.* **1980**, *12*, 1.
- (34). Vogel, G. G. and Stahlbush, J. R. *Inorg. Chem.* **1977**, *16*, 950.
- (35). Nappa, M. and Valentine, J. S. *J. Am. Chem. Soc.* **1978**, *100*, 5075.
- (36). Scheidt, W. R.; Kastner, M. E.; and Hatano, K. *Inorg. Chem.* **1978**, *17*, 706.
- (37). Scheidt, W. R.; Mondal, J. U.; Eigenbrot, C. W.; Adler, A.; Radonovich, L. J.; and Hoard, J. L. *Inorg. Chem.* **1986**, *25*, 795.
- (38). Schauer, C. K.; Anderson, O. P.; Eaton, S. S.; and Eaton, G. R. *Inorg. Chem.* **1985**, *24*, 4082.
- (39). Scheidt, W. R.; Eigenbrot, C. W.; Ogiso, M.; and Hatano, K. *Bull. Chem. Soc. Jpn.* **1987**, *60*, 3529.
- (40). Logovinsky, V.; Kaposi, A. D.; and Vanderkooi, J. M. *Biochim. Biophys. Acta* **1993**, *1161*, 149.
- (41). Angiolillo, P. J. and Vanderkooi, J. M. *Biophys. J.* **1995**, *68*, 2505.
- (42). Anni, H.; Vanderkooi, J. M.; Sharp, K. A.; Yonetani, T.; Hopkins, S. C.; Herenyi, L.; and Fidy, J. *Biochemistry* **1994**, *33*, 3475.
- (43). Anni, H.; Vanderkooi, J. M.; and Mayne, L. *Biochemistry* **1995**, *34*, 5744.
- (44). Shelnut, J. A.; Straub, K. D.; Rentzepis, P. M.; Gouterman, M.; and Davidson, E. R. *Biochemistry* **1984**, *23*, 3946.
- (45). Brautigan, D. L.; Ferguson-Miller, S.; and Margoliash, E. *Methods Enzymol.* **1978**, *53*, 129.
- (46). Myer, Y. P. *Methods Enzymol.* **1978**, *54*, 249.
- (47). Myer, Y. P. *Biochem. Biophys. Acta* **1968**, *154*, 84.
- (48). Pal, P. K.; Verma, B.; and Myer, Y. P. *Biochemistry* **1975**, *14*, 4325.
- (49). O'Hern, D. J.; Pal, P. K.; and Myer, Y. P. *Biochemistry* **1975**, *14*, 382.

- (50). Myer, Y. P. *Biochemistry* **1968**, *7*, 765.
- (51). Hsu, M-C. and Woody, R. W. *J. Am. Chem. Soc.* **1971**, *93*, 3515.
- (52). Mizutani, T.; Ema, T.; Yoshida, M.; and Ogoshi, H. *Inorg. Chem.* **1994**, *33*, 3558.
- (53). Pielak, G. J.; Oikawa, K.; Mauk, A. G.; Smith, M. and Kay, G. M. *J. Am. Chem. Soc.* **1986**, *108*, 2724.
- (54). Holzwarth G. and Doty, P. *J. Am. Chem. Soc.* **1965**, *87*, 218.
- (55). Chen, Y-H.; Yang, J-T.; and Martinez, H. M. *Biochemistry* **1972**, *11*, 4120.
- (56). Felton, R. H. and Yu, N.-T. in *The Porphyrins*, D. Dolphin, Ed., Academic, New York, 1978, Vol. III, pp. 347-388.
- (57). Spiro, T. G. In *Methods in Enzymology*, S. Fleischer and L. Packer, Ed., Academic, New York, 1978, Vol. 54, pp. 233-249.
- (58). Hu, S.; Morris, I. K.; Singh, J. P.; Smith, K. M. and Spiro, T. G. *J. Am. Chem. Soc.* **1993**, *115*, 12446.
- (59). Tang, J. and Albrecht, A. C. In *Raman Spectroscopy*, H. A. Szymanski, Ed., Plenum, New York, 1970, Vol. 2, Chap. 2.
- (60). Spiro, T. G. *Biochim. Biophys. Acta* **1975**, *416*, 169.
- (61). Li, X.; Czernuszewicz, R. S.; Kincaid, J. R.; Su, Y. O.; and Spiro, T. G. *J. Phys. Chem.* **1990**, *94*, 31.
- (62). Li, X.; Czernuszewicz, R. S.; Kincaid, J. R.; Stein, P.; and Spiro, T. G. *J. Phys. Chem.* **1990**, *94*, 47.
- (63). Feitlson, J. and Spiro, T. G. *Inorg. Chem.* **1986**, *25*, 861.
- (64). Shelnut, J. A. *J. Phys. Chem.* **1983**, *87*, 605.
- (65). Shelnut, J. A. *J. Am. Chem. Soc.* **1983**, *105*, 774.
- (66). Shelnut, J. A. *Inorg. Chem.* **1983**, *22*, 2535.
- (67). Spiro, T. G. and Streckas, T. C. *J. Am. Chem. Soc.* **1974**, *96*, 338.

- (68). Spiro, T. G. in *Iron Porphyrins*, A. B. P. Lever and H. B. Gray, Ed., Addison-Wesley, Reading, MA., Vol. II, Chap. 3.
- (69). Spiro, T. G. *Adv. Prot. Chem.* **1985**, *37*, 111.
- (70). Spaulding, L. D.; Chang, C. C.; Yu, N.-T.; and Felton, R. H. *J. Am. Chem. Soc.* **1976**, *97*, 2517.
- (71). Spiro, T. G.; Stong, T. C.; and Stein, P. *J. Am. Chem. Soc.* **1979**, *101*, 2648.
- (72). Parthasarathi, N.; Hansen, C.; Yamaguchi, S.; and Spiro, T. G. *J. Am. Chem. Soc.* **1987**, *109*, 3865.
- (73). Prendergast, K. and Spiro, T. G. *J. Am. Chem. Soc.* **1992**, *114*, 3793.
- (74). Spiro, T. G. and Li, X. in *Biological Applications of Raman Spectroscopy*, Spiro, T. G. Ed., John Wiley & Sons, New York, 1987, Vol. 3, Chap. 1.
- (75). Cheng, J.; Zhou, J. S.; and Qin, L. and Kostić, N. M. *Inorg. Chem.* **1994**, *33*, 1600. and references cited therein.
- (76). Roulet, R. and Barbey, C. *Helv. Chim. Acta* **1973**, *56*, 2179.
- (77). Goggin, P. L.; Goodfellow, R. J.; Haddock, S. R.; Reed, F. J. S.; Smith, J. G.; and Thomas, K. M. *J. Chem. Soc., Dalton Trans.* **1972**, 1904.
- (78). Scott, J. D. and Puddephatt, R. J. *Organometallics* **1983**, *2*, 1643.
- (79). Galbraith, J. A.; Menzel, K. A.; Ratilla, E. M. A.; and Kostić, N. M. *Inorg. Chem.* **1987**, *26*, 2073.
- (80). Matile, S. and Woggon, W.-D. *J. Chem. Soc., Chem. Commun.* **1990**, 774.

CHAPTER 2

KINETICS OF PHOTOINDUCED ELECTRON-TRANSFER
REACTIONS WITHIN SOL-GEL SILICA GLASS DOPED WITH
ZINC CYTOCHROME *c*. STUDY OF ELECTROSTATIC EFFECTS
IN CONFINED LIQUIDS

Chengyu Shen and Nenad M. Kostić

Abstract

Silica hydrogel (glass) was doped with native (iron-containing) cytochrome *c* and with its zinc derivative. Ultraviolet-visible, circular dichroism, and resonance Raman spectra of both proteins and the lifetime of the triplet state of the zinc protein show that encapsulation in the sol-gel glass only slightly perturbs the polypeptide backbone and does not detectably perturb the heme group. Because thermal (ground-state) redox reactions of the encapsulated native cytochrome *c* are very slow, we take advantage of the transparency of the silica to study, by laser flash spectrometry, photoinduced (excited-state) redox reactions of zinc cytochrome *c*, which occur in milliseconds. The triplet state, $^3\text{Zncyt}$, is oxidatively quenched by $[\text{Fe}(\text{CN})_6]^{3-}$, dioxygen, and *p*-benzoquinone. These reactions are monophasic in bulk solutions but biphasic in solutions confined in glass. Changes in ionic strength and

in bulk solutions but biphasic in solutions confined in glass. Changes in ionic strength and pH differently affect the kinetics in these two environments. Adsorption of cytochrome *c*, which is positively-charged, to the pore walls, which are negatively-charged at pH 7.0, affects the kinetics in the doped glass. Exclusion of the $[\text{Fe}(\text{CN})_6]^{3-}$ anions from the glass interior also affects the kinetics. Even at equilibrium the anion concentration is lower inside the glass than in the external solution. This exclusion can be lessened or eliminated by raising ionic strength and lowering the pH value. The electroneutral quenchers are not excluded from the glass. Diffusion of all three quenchers is slower in the confined solution than in bulk solution. The smaller the molecule, the lesser this hindrance by the glass matrix. In light of these findings, the assumption that porosity of sol-gel glasses ensures uniform penetration of relatively small molecules into the pores must be taken skeptically and tested for each solute (or analyte) of interest, especially for the charged ones. These considerations are important in the design of sensors.

Introduction

Inorganic oxides with chemical compositions of traditional glasses and ceramics can be prepared at room temperature, by polymerization of appropriate precursors.¹⁻⁴ This, the sol-gel method, became especially important when it was shown, in the middle 1980s, that the new materials can be doped by various chemicals.⁵⁻¹³ Since then, many chemical reactions have been effected inside these hydrogels, which we will refer to simply as glasses.^{5-11,14-19} The sol-gel method proved compatible with proteins, and several of them, mostly enzymes, have recently been encapsulated in silica glass.^{5,14,15,20-32} The method of Avnir and

coworkers²⁴ has been modified by Dunn, Valentine, Zink, and their coworkers,^{14,15,20-23} so that noninvasive entrapment of proteins can be achieved relatively easily. Because the pores of hydrogels (partially dried gels) contain water, the protein molecules are solvated and retain their properties.

Sol-gel glasses and composite materials obtained from them have two main properties. Because they are porous, relatively small molecules can move through the pores and reach the relatively large molecules that are trapped inside. Because these glasses are transparent in the UV-visible range, the chemicals and their reactions can be studied by optical spectroscopic methods. A general conclusion from the previous studies is that the trapped compounds retain most of their physical and chemical properties.^{6,14,15,20-23}

It is known, however, that liquids confined in porous matrices have special properties.^{33,34} In this study we contrast glass interior and bulk solution as media for oxidative quenching of the triplet state of the protein zinc cytochrome *c* by three agents. This work has several features that, to our knowledge, have not been combined before in studies of doped glasses. Transparency has often been used for monitoring, but seldom for initiation, of chemical reactions;^{7-10,35-37} we take advantage of transparency and study photoinduced electron transfer from the excited state of a protein to various small molecules.

Sol-gel glasses doped with enzymes and other proteins hold promise as sensors, especially for biomolecules.^{20,22,23,27,31,38-41} Quality of these sensors depends on the rate and specificity of protein-analyte interactions, and we report some findings pertinent to this problem. There have been only several quantitative kinetic studies in glasses^{14,15,22,42}, much

needs to be done in this area. We chose reactions having relatively simple kinetics in aqueous solution and studied kinetics of these reactions inside glass. We found interesting electrostatic effects, which caused unexpected but explainable dependence of rate constants on ionic strength and pH value. These electrostatic effects should be taken into consideration in further research with doped glasses and in their applications as sensors.

Experimental Procedures

Chemicals. Horse-heart cytochrome *c* was obtained from Sigma Chemical Co. Iron(III) ions in the protein were replaced by zinc(II) ions, and the reconstituted protein, designated Zncyt, was purified by a standard procedure, in the dark.⁴³ The compounds $K_3[Fe(CN)_6]$, tetramethylorthosilicate (also called tetramethoxysilane), hydroquinone, and *p*-benzoquinone of reagent grade were obtained from Aldrich Chemical Co. The last chemical, which is photolabile, was kept and handled in the dark.^{44,45} Ultrapure argon was obtained from Air Products, Inc. Distilled water was demineralized to electrical resistivity greater than $17\text{ M } \Omega \cdot \text{cm}$. Sodium phosphate buffer was used throughout; it had pH of 7.0 and concentration of 2.5 mM, unless stated otherwise. Ionic strength (μ) was raised with NaCl and lowered by dilution; it (not the phosphate concentration) is specified.

The Sol-Gel Process. The silica gel was prepared by a published procedure.¹⁵ A 15.76-g sample of tetramethylorthosilicate and a mixture of 3.38 g water and 0.22 g of 0.040 M HCl were kept in an ice-cooled ultrasonic bath for 45 min. Clear, homogeneous sol of orthosilicic acid was formed. Upon addition of a 10 mM sodium phosphate buffer at pH 7.0 gelation began. Solutions in the same buffer containing different concentrations of

ferricytochrome *c* (the native protein) or of zinc cytochrome *c* (the reconstituted protein) were promptly added to the polymerizing gel. In some experiments the protein was omitted, so that undoped glasses were eventually obtained. The sol, whether doped or undoped, was quickly poured to the height of 10 mm into polystyrene cuvettes sized 10 x 10 mm that had all the sides transparent. Rapid polymerization was accompanied by a great increase in viscosity in less than 5 min. Aging and drying continued at 4 °C. During the aging the samples were kept sealed with parafilm, except when methanol was removed, several times a day, by washing with the same sodium phosphate buffer. After 14 d the samples were exposed to air. Drying lasted until 40% by weight of the initially added water evaporated, typically 14-21 d. The hydrogel, which is usually referred to as glass, retained 60% of the water added initially and had 50% of the original volume. The square prismatic slabs sized 7.5 x 7.5 x 9.0 mm were stored in a buffer.

Kinetic Experiments. Flash kinetic spectrometry (so-called laser flash photolysis) was done with a standard apparatus.⁴⁶ A Phase-R (now Lumenex) laser DL1100 containing a 50 μ M solution of rhodamine 590 in methanol delivered 400-ns pulses of excitation light perpendicular to the monochromatic probing beam from a tungsten-halogen lamp. The sample was kept under ultrapure argon, in a fluorescence cell sized 10 x 10 mm. The absorbance-time curves were analyzed with kinetic software from OLIS, Inc. Each signal was an average of eight pulses. Appearance and disappearance of the triplet state of zinc cytochrome *c*, designated $^3\text{Zncyt}$, were monitored at 460 nm, where the transient absorbance reaches the maximum. Appearance and disappearance of the corresponding cation radical, designated Zncyt^+ , was monitored at 675 nm, where the difference in absorbance between it

and the triplet state is greatest. The concentration of zinc cytochrome *c* in the fresh glass (fully hydrated gel) was 10 μM . This concentration in the partially-dried glass, which had shrunk to 50% of its initial volume, was 20 μM .

The slabs were soaked for 2-3 d in buffered solutions of a quencher, $\text{K}_3[\text{Fe}(\text{CN})_6]$ or *p*-benzoquinone. These solutions were changed several times a day, for complete equilibration with the porous glass. The buffer ions, which are relatively small and highly mobile, are assumed to have the same concentration inside the glass and in the external solution. Because the buffer is colorless, movement of its ions between the solution and glass cannot be studied by common experimental methods. Concentrations of the quenchers will be discussed in detail below. Between soakings in different solutions, the slab was thoroughly rinsed by soaking in water.

Each sample for kinetic experiments was thoroughly and noninvasively deaerated in a fluorescence cuvette by gentle flushing with ultrapure argon that had been passed through water in order to avoid evaporation of the solvent and consequent increase in the concentrations of the solutes. When the sample was an aqueous solution, deaeration for ca. 15 min was more than sufficient. When the sample also contained a slab of glass, deaeration lasted 24 h, for complete removal of dioxygen from the pores. Experiments that were done relatively easily with solutions required more effort with glasses. Several days of work, mostly incubation and deaeration of samples, were needed for each point on the linear plots of the observed rate constant versus the quencher concentration, obtained under pseudo-first-order conditions. Three to five of these points defined each linear plot, the slope of which is the second-order rate constant. Finally, these determinations were made at

different ionic strengths and pH values. The intricate kinetic experiments with glasses are somewhat less precise than the straightforward experiments with solutions. The estimated errors in the second-order rate constants are $\pm 30\%$ and $\pm 10\%$, respectively.

Spectroscopic Measurements. Ultraviolet-visible spectra were recorded with an IBM 9430 spectrophotometer. A doped glass in the sample beam was examined against an undoped glass in the reference beam. Each slab was kept in a standard quartz cuvette sized 10 x 10 mm. The light beams were small enough to pass entirely through the slabs. Circular dichroism spectra at room temperature, measured with a JASCO 710 instrument, gave the ellipticity of protein samples. Ultraviolet-visible spectra of these same samples, measured immediately afterwards, gave the protein concentrations; then molar ellipticity was calculated. Because optical activity decreases with increasing wavelength, progressively higher concentrations were used for the spectra in the following ranges: 200-350, 350-500, and 500-650 nm.

Resonance Raman spectra were measured with a Spex 1807 triple spectrometer equipped with a Princeton Instruments CCD detector, model LN1152, cooled by liquid nitrogen. The excitation source was an Innova 100 Kr⁺ laser from Coherent, Inc., emitting at 413.1 nm. The laser power at the samples was less than 5 mW, and radiation was collected in the so-called backscattered configuration, by an f/1.2 camera lens. Calibration was done with indene; the resolution was 5 cm⁻¹. The samples were kept in an optical dewar vessel containing liquid nitrogen, and the measurements were made at 77 K.

Porosity of the Glass. Slabs of undoped glass were soaked for several days in solutions containing 100 or 250 μM K₃[Fe(CN)₆] ($\epsilon_{422} = 1025 \text{ M}^{-1}\text{cm}^{-1}$) or 500 μM hydroquinone

($\epsilon_{297} = 1100 \text{ M}^{-1}\text{cm}^{-1}$) in a 600 mM sodium phosphate buffer at pH 7.0. These solutions were changed several times a day. Ultraviolet-visible spectra of the slabs infused with the chromophore were recorded against undoped slabs in the reference beam and then compared with spectra of solutions containing this chromophore in the same buffer. Absorbance ratio for the slab and the solution of the same thickness equals the fraction of the optical path in the glass that passes through the pores, if the pores are filled with the solution. The measurements were repeated with both light beams passing through different parts of the slabs.

Protein Adsorption on Silica. Undoped glass was ground with a pestle in a mortar. To 2.0 mL of a 10 μM solution of ferricytochrome *c* in a 10 mM phosphate buffer at pH 7.0 contained in a spectrophotometric cuvette were added 50 mg of the powdered glass. The suspension was shaken occasionally during 1 d. The UV-vis spectrum of the clear supernatant was compared with the spectrum before addition of the powdered glass. Ionic strength of the supernatant was adjusted to 300 mM with NaCl, and the UV-vis spectra were compared again.

Results and Discussions

Doped Silica Glass

Formation of Glasses. The sol-gel process remains poorly understood despite many decades of research and application.^{1-4,47-52} Different procedures yield gels and glasses of different physical properties. We use a new method, developed by others,^{14,15,20} in which acid-catalyzed hydrolysis of $\text{Si}(\text{OCH}_3)_4$ to $\text{Si}(\text{OH})_4$ is promoted by sonication, subsequent

condensation polymerization of $\text{Si}(\text{OH})_4$ is catalyzed by base, and the gel is never completely dried. The product, sometimes termed hydrogel but usually simply glass, is believed to have properties different from those of xerogels and aerogels.^{3,20} In our experiments the rate of gelation increased as temperature and buffer concentration increased. These conditions and also relative volumes of the $\text{Si}(\text{OH})_4$ sol and of the sodium phosphate buffer solution at pH 7.0 were adjusted for optimal balance between the probability of cross-linking (i.e., formation of Si–O–Si bonds) and the catalytic efficacy of the phosphate anions. The protein added at the beginning of the gelation had enough time, about 3-5 min, to diffuse uniformly through the viscous solution. Because the polymerization reaction is incomplete, interconnected clusters of silica (SiO_2) are formed, leaving pores in between them. Some of the pores contain molecules of cytochrome *c*, which interrupt polymerization and serve as templates around which this process occurs. Throughout aging and partial drying mechanical strength of the gel increases. As the water evaporates, its fraction decreases and that of the solid increases. The whole gel, and the pores within it, shrink. Consequently, the concentration of the trapped cytochrome *c* doubles, from 10 to 20 μM . Water from the surface pores is lost, and silanol groups at the surface condense. The average pore size in silica xerogel, which is completely dried at high temperature, is ca. 20 Å.³ The average pores in our glass, which is only partially dried at 4 °C, must be larger than that but smaller than ca. 100 Å because our slabs do not scatter visible light.²⁰ The partially-dried glass retains enough water to maintain the structure of cytochrome *c*, as will be shown below. Zinc cytochrome *c*, which has very high absorptivity ($\epsilon_{423} = 2.43 \times 10^5 \text{ M}^{-1}\text{cm}^{-1}$),⁵³ was never found in the buffer surrounding the glass, and the absorption spectrum of the protein

in the doped glass was essentially the same before and after the incubation. Clearly, the protein does not leak out of the porous glass into the external solution.

Ultraviolet-visible Spectra and Thermal Oxidoreduction. We confirmed^{14,15,20-23} that the undoped glass is optically transparent except for some absorbance around 300 nm; see Supporting Information, Figure 1. Positions and intensities of the hyper, Soret, α , and β bands for both ferricytochrome *c* and zinc cytochrome *c* in the doped glasses remain unchanged throughout the aging and drying process; see Supporting Information, Figures 2 and 3. Uniform color and absorbance of different regions of the doped glass prove homogeneous distribution of the proteins.

When the glass doped with 20 μM ferricytochrome *c* were immersed first in a 200 μM solution of ascorbic acid and next in a 200 μM solution of $\text{K}_3[\text{Fe}(\text{CN})_6]$, each of them containing the same sodium phosphate buffer at pH 7.0 as the solvent, complete reduction and then oxidation of the heme iron were clearly evident by the characteristic changes in the UV-vis spectra. This cycle was repeated three times, and each time the spectra of the ferric and ferrous forms of the protein appeared unchanged. We thus confirmed²⁰ that the encapsulated protein remains capable of reversible redox reactions. Each reaction, however, took two days (and each cycle, four days) for completion because the redox agents diffused slowly into the porous glass. Much faster reactions are required for further study of doped silica glasses and for their practical applications as sensors. Photoinduced, rather than thermal, redox reactions are promising for both research and application. They are the main subject of this study.

Circular Dichroism Spectra. This spectroscopy has proved very useful in the study of conformation and ligation of heme proteins.⁵⁴⁻⁵⁷ This and other spectroscopic methods showed that introduction of zinc(II) ions does not appreciably alter the overall structure and conformation of cytochrome *c*.^{43,58}

The very strong bands at 209 and 222 nm are due to π - π^* and n - π^* transitions, respectively, in the amide group. These and other features in the so-called intrinsic region, below 300 nm, are the property of the polypeptide backbone and are sensitive indicators of the protein conformation. The strong features in the region 350-500 nm correspond to the Soret absorption band of the heme and are highly sensitive to interactions between this planar chromophore and its chiral environment. The weak circular dichroism in the region 500-650 nm corresponds to the π - π^* transitions of the heme that are traditionally designated α and β .

As Figure 1 shows, encapsulation of the native and reconstituted cytochrome *c* causes a change in the relative intensity, and a decrease in the absolute intensity, of the intrinsic bands. The approximate extent of α -helicity, estimated with the standard formula,^{55,59} is as follows: ferricytochrome *c*, 32 and 28 % in solution and glass, respectively; and zinc cytochrome *c*, 30 and 19 % in solution and glass, respectively. The spectral changes in zinc cytochrome *c* upon encapsulation are comparable to those caused by electrostatic association of ferricytochrome *c* with highly-charged anions in solution, changes known to be localized and relatively small.⁶⁰

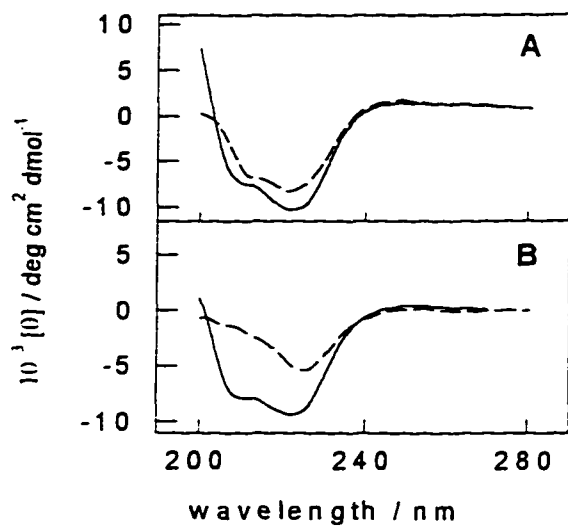


Figure 1. Intrinsic circular dichroism at 25 °C of (A) ferricytochrome *c* and (B) zinc cytochrome *c* in a sodium phosphate buffer at pH 7.0 adjusted with NaCl to ionic strength of 5.0 mM (solid line) and in sol-gel silica glass infused with the same buffer (dashed line). Molar ellipticity is normalized to the mean residue value.

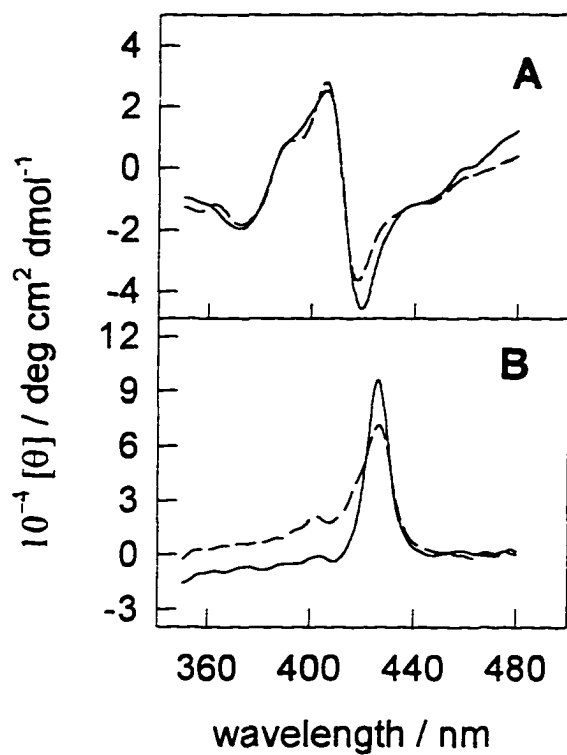


Figure 2. Circular dichroism in the Soret region at 25 °C of (A) ferricytochrome *c* and (B) zinc cytochrome *c* in a sodium phosphate buffer at pH 7.0 adjusted with NaCl to ionic strength of 5.0 mM (solid line) and in sol-gel silica glass infused with the same buffer (dashed line).

As Figure 2 shows, on encapsulation the Soret spectrum of ferricytochrome *c* changes only slightly, whereas that of zinc cytochrome *c* changes more. The main band in the spectrum of zinc cytochrome *c* broadens, but its position (λ_{max}) does not change. (Encapsulation causes a similar change in the CD spectrum of bacteriorhodopsin.)¹⁵ Because an edge of the heme group is partially exposed at the surface of cytochrome *c*, even a relatively small conformational change in the crevice containing the heme may affect the CD spectrum.^{56,61} If such a conformational change occurs, it must be slight because the spectra in Figure 3 almost overlap.

Resonance Raman Spectra. This spectroscopy has successfully been applied to heme proteins in numerous studies.^{62,63} Laser excitation at wavelengths within electronic absorption bands of the heme can cause great enhancement of the vibrational modes of the heme. In a recent study our collaborators and we applied this method for the first time to zinc cytochrome *c* and showed that the size of the porphyrin "core" is inconsistent with six-coordination and is consistent with five-coordination. Unlike the iron(II) and iron(III) ions, which have both His 18 and Met 80 as axial ligands, the zinc(II) ion in cytochrome *c* seems to have only one axial ligand, probably His 18. This difference in coordination number between the native and reconstituted proteins is retained in the glass.

This study concerns the effects of encapsulation. As Table 1 shows, all the vibrational bands have identical wavenumbers, within the error bounds of the experiment, in solution and in glass. Even the relative intensities of most of the bands remain unchanged. Clearly, the glass matrix does not alter the spin state, oxidation state, and geometry of the heme site.

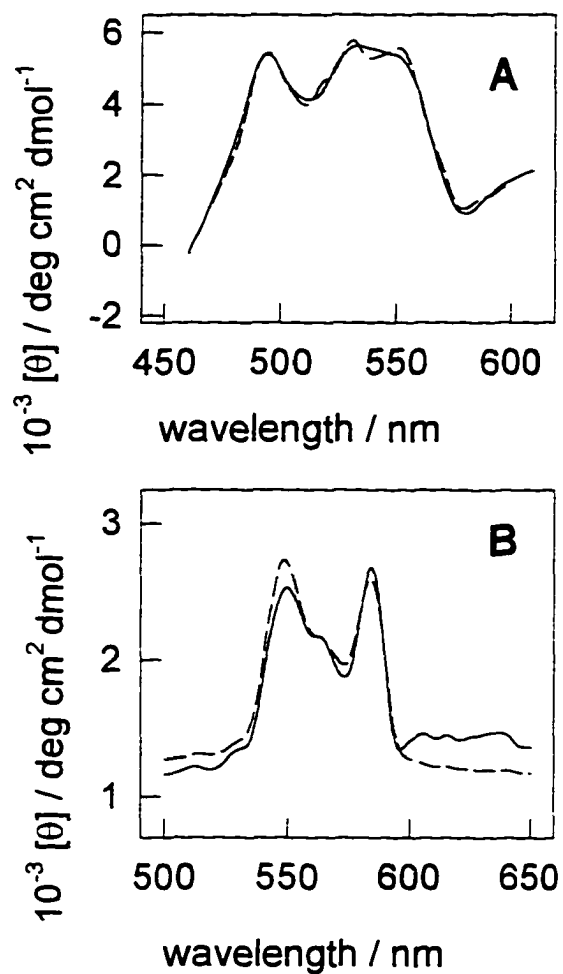
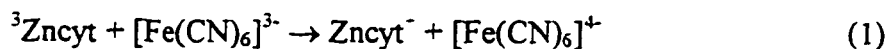


Figure 3. Circular dichroism spectra in the α , β region at 25 °C of (A) ferricytochrome *c* and (B) zinc cytochrome *c* in a sodium phosphate buffer at pH 7.0 adjusted with NaCl to ionic strength of 5.0 mM (solid line) and in sol-gel silica glass infused with the same buffer (dashed line).

Lifetime of the Triplet State. The rate constant for natural decay of $^3\text{Zncyt}$ in aqueous solution is $100 \pm 10 \text{ s}^{-1}$ throughout the intervals $5.0 \leq \text{pH} \leq 9.0$ and $2.5 \text{ mM} \leq \mu \leq 3.00 \text{ M}$.⁶⁴ The rate constant for the encapsulated zinc cytochrome *c* at pH 7.0 is $70 \pm 10 \text{ s}^{-1}$. This slight decrease, corresponding to a slight increase in the lifetime of the triplet state (Supporting Information, Figure 4), indicates a small stabilization of the protein in the glass. The decrease in the rate constant is probably caused by immobilization, which lessens the probability of collisions involved in quenching the excited state.

Quenching of $^3\text{Zncyt}$ by the $[\text{Fe}(\text{CN})_6]^{3-}$ Anion

The Reaction. Because zinc(II) is a redox-inactive ion, zinc cytochrome *c* in its ground electronic state cannot react with the $[\text{Fe}(\text{CN})_6]^{3-}$ ion. In other words, thermal electron-transfer reaction is not possible. Because, however, the triplet state of the porphyrin ring is a strong reducing agent, the reaction in eq 1 is readily induced by a laser pulse.⁶⁵ Because the cation radical of the porphyrin in $\text{Zncyt}^{\cdot+}$ is a strong oxidizing agent, reverse electron transfer regenerates zinc cytochrome *c* (in the ground state) and $[\text{Fe}(\text{CN})_6]^{3-}$. The next laser pulse triggers another sequence of two electron transfers in opposite directions, and so on.



The net charges of the two reactants in eq 1 are 6+ and 3- at pH 7.0. Effects of ionic strength on the second-order rate constant *k* give information about electrostatic interactions of these two molecules with each other and with their environment. We are particularly

Table 1. Resonance Raman Bands of Ferricytochrome *c* and of Zinc Cytochrome *c* in Solution and in Partially-dried Silica Gel

| assignment ^a | wavenumber / cm ⁻¹ | | | |
|---|-------------------------------|-------|----------|----------|
| | cyt(III) | | Zncyt | |
| | solution | glass | solution | glass |
| U ₁₀ | 1641 | 1642 | 1614 | 1613 |
| U ₂ | | | 1591 | 1591 |
| U ₁₉ | 1589 | 1591 | | |
| U ₃ | 1507 | 1508 | 1481 | 1481 |
| U ₄ | 1375 | 1376 | 1369 | 1369 |
| U ₃₀ | 1177 | 1176 | 1176 | 1176 |
| U ₄₃ | | | 1141 | 1142 |
| U ₁₄ | 1129 | 1128 | | |
| δ(C _b H ₃) _{2,4} | | | 1052 | 1052 |
| ν(C _c C _d) _{6,7} | 971 | 971 | 969 | 971 |
| U ₆ | | | 799 | 797 |
| U ₁₅ | 748 | 748 | 756 | 755 |
| γ ₅ | 731 | 731 | 728 | 726 |
| U ₇ | 701 | 701 | 698 | 697 |
| ν(C _s S) | | | 682 | 680 |
| γ ₂₁ | 569 | 568 | 577 | 576 |
| γ ₁₂ | 522 | 522 | 520, 510 | 511 |
| U ₃₃ | 481 | 480 | | |
| γ ₂₂ | 445 | 447 | 451 | 448 |
| δ(C _β C _a C _b) _{2,4} | 415 | 415 | 421, 411 | 411 |
| δ(C _β C _a S) | 400 | 399 | | |
| δ(C _β C _c C _d) _{6,7} | 379 | 381 | 384, 375 | 385, 374 |
| U ₈ | 351 | 350 | 342 | 342 |
| U ₅₁ | 307 | 307 | | |
| U ₉ | 270 | 270 | | |

^aRef 63.

interested in the properties of the glass interior, that is, in the possible difference between the hydrated pores and the bulk solution.

The Reaction in Solution. As Figure 4 shows, the rate constant k increases from $1.0 \times 10^9 \text{ M}^{-1}\text{s}^{-1}$ to $1.4 \times 10^{10} \text{ M}^{-1}\text{s}^{-1}$ as the ionic strength of the buffered solution decreases from 300 to 5.0 mM owing to the attraction between the reactants. Electrostatic interactions between redox

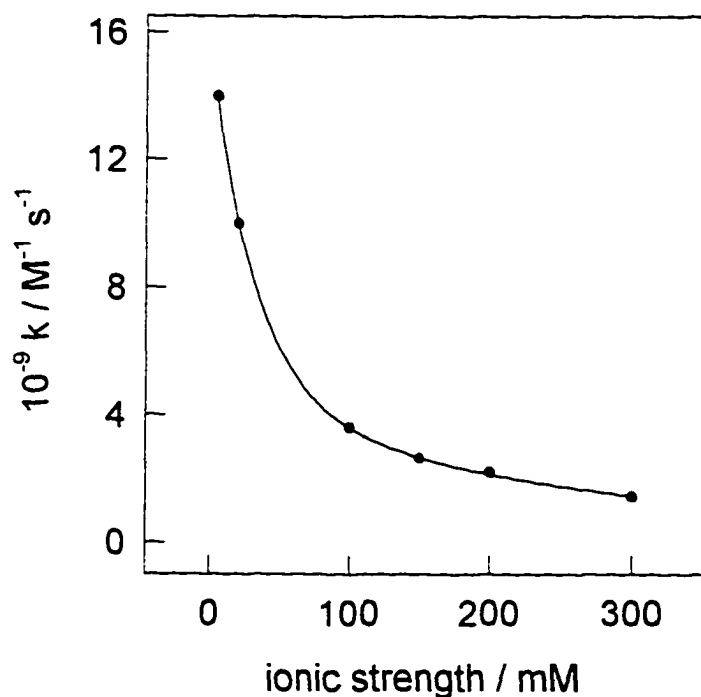


Figure 4. Dependence on ionic strength of the second-order rate constant for the reaction in eq 1 in a sodium phosphate buffer at pH 7.0 containing variable concentration of NaCl, at 25 °C.

metalloproteins and transition-metal complexes have been much studied in the past and are largely understood.^{66,67} Without revisiting solved problems, we point out that the disappearance of $^3\text{Zncyt}$ in bulk solution is a monoexponential process characterized by monotonic dependence of the rate constant on ionic strength. The only important interaction in solution seems to be the attraction between reactants in eq. 1

The Reaction in Glass. A slab of glass uniformly doped with 20 μM zinc cytochrome *c* was thoroughly equilibrated with $\text{K}_3[\text{Fe}(\text{CN})_6]$. The triplet state, $^3\text{Zncyt}$, is created in situ by a laser flash. Because its quenching is controlled by local diffusion within the pores, not by transfer of the $[\text{Fe}(\text{CN})_6]^{3-}$ ions from the bulk solution to the glass interior, the reaction in eq 1 is fast. It was followed by monitoring both the disappearance of the triplet state (see Figure 5) and the appearance of the cation radical (see Supporting Information, Figure 5). Experiments of the latter kind prove that $^3\text{Zncyt}$ is quenched by the electron-transfer reaction, according to eq 1.

The trace in Figure 5 cannot be fitted with one or two exponentials but can be fitted well with three exponentials of approximately equal amplitudes. Excellent fitting can, of course, be obtained also with more than three exponentials. The slowest process, having the rate constant of 100-200 s^{-1} in different experiments, is the natural decay of $^3\text{Zncyt}$, probably in somewhat different environments. The observed rate constants of the other two exponential components changed with varying concentration of the quencher, as expected, but that of the faster component remained approximately eight times greater than that of the slower. Both of these components correspond to the quenching according to eq 1. The contrast between the monophasic quenching in solution and multiphasic quenching in silica

glass highlights the difference between the homogeneous free solution and the microheterogeneous environment in the pores.

Kinetic Effects of Ionic Strength in Glass. Two typical pseudo-first-order kinetic plots (in each case, for the faster of the two exponential components) are shown in Supporting Information, Figure 6. The rate constant decreased from 6.3×10^7 to 2.5×10^7

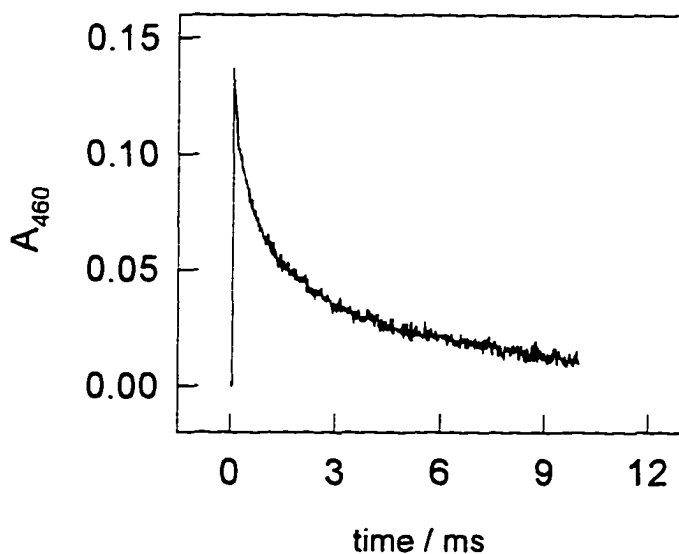


Figure 5. Decay of the triplet state $^3\text{Zncyt}$ in sol-gel glass, in the presence of $100 \mu\text{M}$ $[\text{Fe}(\text{CN})_6]^{3-}$ as the quencher. The solvent is a sodium phosphate buffer at pH 7.0 adjusted with NaCl to ionic strength of 20 mM.

$M^{-1}s^{-1}$ as the ionic strength decreased from 60 to 20 mM. (The slower component showed a similar decrease.) These findings, and others of their kind that are not shown in figures, define a trend opposite to that found in solution (Figure 4). Although the quenching reaction inside the glass is relatively fast, it is much slower than the reaction in solution. The respective rate constants at the ionic strength of 20 mM are 2.5×10^7 (for the faster component) and $1.1 \times 10^{10} M^{-1}s^{-1}$. The causes of this ca. 400-fold decrease will be discussed later. First, we discuss the surprising effect of ionic strength. Each quartet of data points in Figure 6 is the result of approximately 1 week's work. The second-order rate constants were obtained reproducibly with the same slab of doped glass, so that the concentration of encapsulated zinc cytochrome *c* be kept constant. Clearly, all the dialysis experiments were reversible, and the reaction in eq 1 did not cause any permanent change in the glass. As Figures 6A and 6B show, the rate constants for the two components depend identically on ionic strength (assumed to be the same inside the glass and in external solution): no change or a slight increase from 600 to 100 mM and a steep decrease to 10 mM. The rate constants of the two components remain in the approximate ratio of 8:1, and their amplitudes remain approximately equal, at all ionic strengths. In the following discussion we will offer an explanation for the intriguing contrast between the effects of ionic strength in solution and in the pores of the silica glass.

Adsorption of Cytochrome *c* on the Silica Surface. Silica surface, and therefore the pore walls, contain functional groups of several kinds: siloxane (Si–O–Si), silaketone (Si=O), silanol (Si–OH), and siloxide (Si–O⁻)⁶⁸. Because these groups exist in variable proportions and individually or in clusters of various sizes, the pK_a values of silica gel span

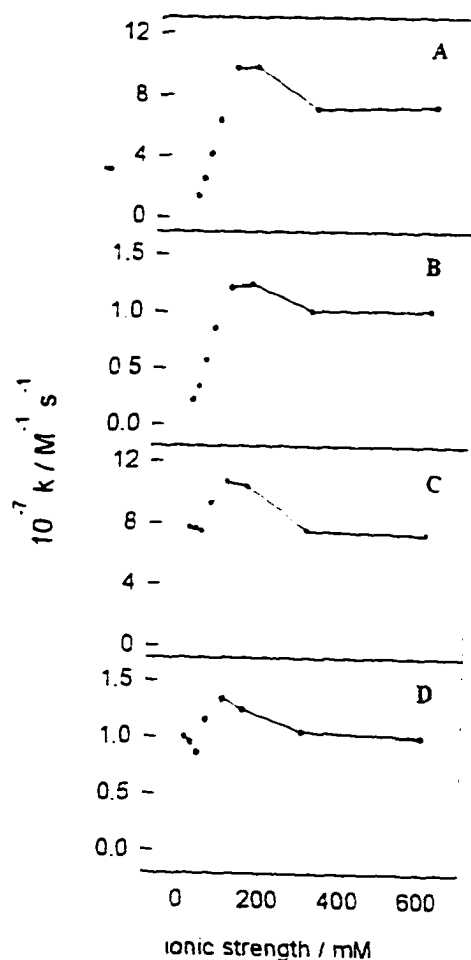


Figure 6. Dependence on ionic strength of the second-order rate constant for the faster (A, C) and slower (B, D) components of the reaction in eq 1 inside sol-gel silica glass infused with a sodium phosphate buffer at pH 7.0 containing variable concentration of NaCl. (A) and (B) Assuming that the $[\text{Fe}(\text{CN})_6]^{2-}$ concentration inside the glass equals that in the external solution of $\text{K}_3[\text{Fe}(\text{CN})_6]$. (C) and (D) Recognizing the partial exclusion of the $[\text{Fe}(\text{CN})_6]^{2-}$ ions from the glass interior at ionic strength lower than 600 mM and correcting their concentration inside the glass according to eq 2.

the interval $3 < \text{pH} < 9$.^{69,70} Silica gel and the sol-gel glass bear a net negative charge at pH 7.0. Ferricytochrome *c* and zinc cytochrome *c* have net charges of 7+ and 6+, respectively, at pH 7.0.⁶⁷ Very recent measurements of dipolar relaxation of ferricytochrome *c* in silica glass at pH 4.25 and ionic strength of 100 mM showed that encapsulation slightly restricts the movement of the protein molecules. Since the activation energy for this relaxation is only 1.1 kcal/mol greater inside the glass than in solution, rotation of the protein molecules inside the glass at pH 4.25 and ionic strength of 100 mM is almost as free as that in solution.²¹

In our experiments, at pH 7.0 and ionic strength of 10 mM, UV-vis absorption of ferricytochrome *c* solution disappeared upon incubation with powdered undoped glass, which became reddish. Evidently, the protein was completely removed from solution and adsorbed on the glass.^{71,72} Raising the ionic strength restored only a part of the original UV-vis absorbance. These qualitative experiments show that adsorption at pH 7.0 is relatively strong and only partially reversible.

Selected rate constants shown in Figures 6A and 6B were reproduced with the same slab of doped glass when the ionic strength was raised and then lowered. The apparent small increase in the rate constant *k* as the ionic strength decreases from 600 to 100 mM is qualitatively consistent with the behavior expected of oppositely-charged reactants in eq 1 that are mobile inside the glass pores. The steep decrease of the rate constant upon further lowering of ionic strength is consistent with the hypothesis of adsorption of zinc cytochrome *c* on the pore walls. The exposed heme edge, through which an electron is given to the $[\text{Fe}(\text{CN})_6]^{3-}$ ion, is surrounded by a ring of positively-charged amino-acid side chains.⁶⁷ If

this basic patch adhered to the negatively-charged surface of the pore, the heme edge would become less accessible to the quencher; this attraction is expected to be favored at low ionic strengths. The two components of the reaction cannot be due to the adsorbed and unadsorbed protein because the relative amplitudes of these components are independent of ionic strength.

Exclusion of $[\text{Fe}(\text{CN})_6]^{3-}$ Ions From the Glass. Partial adsorption of zinc cytochrome *c* on the pore walls is not the only possible cause of the unexpected dependence in Figures 6A and 6B. The second-order rate constant depends also on the concentration of the $[\text{Fe}(\text{CN})_6]^{3-}$ ion. Because this octahedral anion is much smaller than 20 Å, the estimated lower limit of the pore size, it is reasonable to assume that uniform diffusion of this quencher into the glass is not obstructed by steric factors. Considering relative sizes, prolonged immersion of a slab of glass in fresh batches of the same $\text{K}_3[\text{Fe}(\text{CN})_6]$ solution is expected to yield equal concentrations of the $[\text{Fe}(\text{CN})_6]^{3-}$ ions in the pores ("inside") and in the solution ("outside"). Sizes, however, are not the only relevant factor.

The kinetic experiments in this section were done with two different slabs of doped glass. The results are consistent, and only one set is shown in Figure 7. It was dialyzed against solutions containing various (constant) concentrations of $\text{K}_3[\text{Fe}(\text{CN})_6]$ in sodium phosphate buffers at pH 7.0 having various (constant) ionic strengths. Soaking was ended when the UV-vis spectrum of the glass ceased changing, i.e., when equilibrium was reached. Between dialyses against different solutions, the slab was thoroughly rinsed by soaking in water. For the same concentration of the $[\text{Fe}(\text{CN})_6]^{3-}$ ions in solution, the greater the ionic strength, the greater the absorbance of these ions inside the glass. Since the

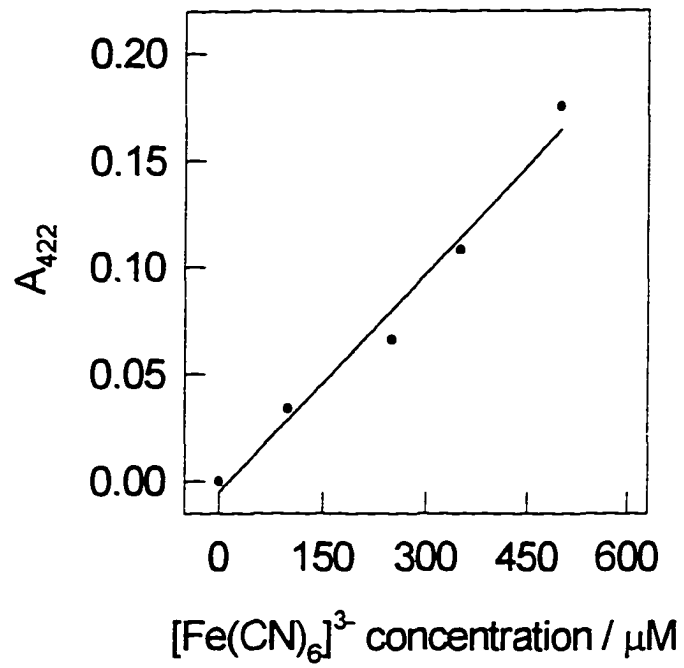


Figure 7. Uptake of $[\text{Fe}(\text{CN})_6]^{3-}$ complex by a slab of undoped sol-gel glass immersed in solutions containing different concentrations of the complex. The solvent is a sodium phosphate buffer at pH 7.0 adjusted with NaCl to ionic strength of 20 mM.

absorptivity ($\epsilon_{422} = 1025 \text{ M}^{-1} \text{ cm}^{-1}$) of $[\text{Fe}(\text{CN})_6]^{3-}$ is independent of ionic strength in the range used in these experiments, it is reasonable to assume that the absorptivity in bulk solution applies also to the confined solution. Evidently, uptake of $[\text{Fe}(\text{CN})_6]^{3-}$ by the glass increases as ionic strength increases. At a constant ionic strength (to which $\text{K}_3[\text{Fe}(\text{CN})_6]$ contributed much less than NaCl) absorbance at 422 nm of the glass was directly proportional to the concentration of $[\text{Fe}(\text{CN})_6]^{3-}$ ions in the external solution; see Figure 7. The slope of this plot of absorbance "inside" vs. concentration "outside" was, however, only about one-third the absorptivity of the $[\text{Fe}(\text{CN})_6]^{3-}$ ions. This was additional evidence for partial exclusion of the anion from the glass interior.

Porosity of the Glass. At the ionic strength of 600 mM electrostatic interactions are negligible. Repulsion between the silica surface and the $[\text{Fe}(\text{CN})_6]^{3-}$ anions, and therefore also exclusion, is presumed absent. Nevertheless, absorbance of these anions in undoped glass never equaled that of a surrounding solution having the same thickness (optical pathlength). Experiments with four different undoped slabs, prepared by the same procedure at different times, gave relative absorbances at 422 nm (in comparison with solutions in which they were incubated for 3 d) of 0.822, 0.843, 0.870, and 0.898. These values were independent of the $\text{K}_3[\text{Fe}(\text{CN})_6]$ concentration in the surrounding solution. Absorbances remained unchanged when different parts of each slab were probed by the light beam. Evidently, all the slabs were optically isotropic and uniformly infused with $[\text{Fe}(\text{CN})_6]^{3-}$ ions, but they differed in porosity. The solution can enter only into the pores of the glass; silica itself is transparent but impenetrable. Cubes of the aforementioned

pathlength factors (relative absorbances) yielded the following respective estimates of the pore volume as the percentage of the slab volume: 56, 60, 66, and 72%. Small variation in the pathlength factor corresponds to a larger variation in the estimated volume of the pores, but the results are qualitatively consistent.

Similar experiments, lasting 4 d, were done also with hydroquinone, an electroneutral species. Two different undoped slabs gave pathlength factors (relative absorbances) at 315 nm of 0.90 and 0.94, corresponding to the estimated pore volumes of 72 and 83%, respectively. The smaller molecules seem to penetrate the pores more fully, as might be expected.

Partitioning Coefficient. Given the pathlength factor, concentration C_{in} of a solute in the glass can be determined from its UV-visible spectrum. The concentration C_{out} in the external solution is known. Partitioning coefficient is defined simply in eq 2. This coefficient for $[\text{Fe}(\text{CN})_6]^{3-}$ ions is plotted in Figure 8. Consistent plots were obtained with two different slabs of glass; one of these is shown.

$$P = C_{in} / C_{out} \quad (2)$$

Corrected Effects of Ionic Strength in Glass. The second-order rate constants k in Figures 6A and 6B for the electron-transfer reaction in glass were calculated with $[\text{Fe}(\text{CN})_6]^{3-}$ concentrations in external solution, C_{out} . The unexpectedly low rate constants at low ionic strength may be due to partial exclusion of the $[\text{Fe}(\text{CN})_6]^{3-}$ ion from the glass interior. When the rate constants were recalculated with corrected concentrations of the quencher, C_{in} , Figures 6C and 6D were obtained. The surprising feature at low ionic strength disappeared, but Figures 6C and 6D still differ greatly from Figure 4 in that the rate

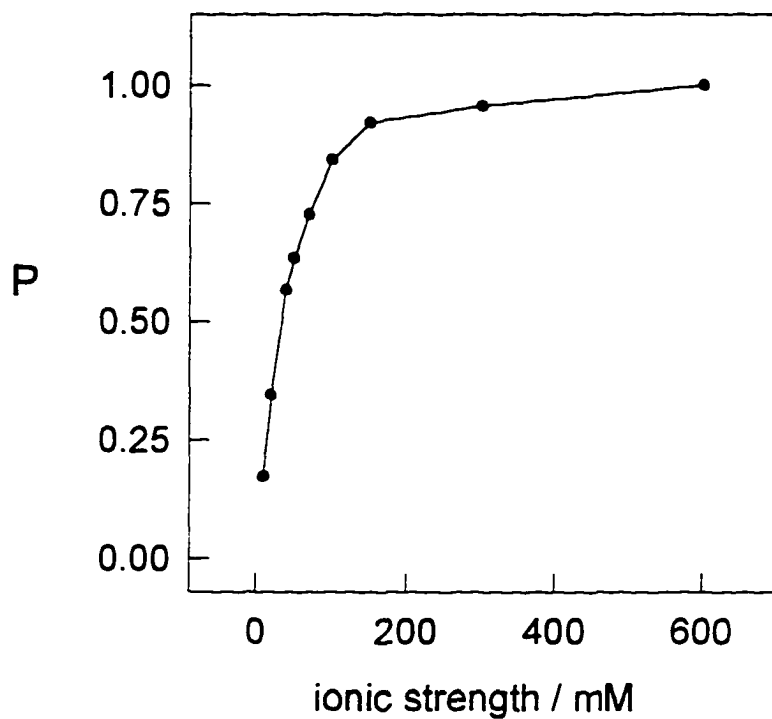


Figure 8. Dependence on ionic strength of the partitioning coefficient, P , for $[\text{Fe}(\text{CN})_6]^{2-}$ ions between the interior of the sol-gel glass and the external solution. For definition, see eq 2. The solvent was a sodium phosphate buffer at pH 7.0 containing variable concentration of NaCl.

constant in the glass does not significantly increase as ionic strength decreases. The remaining small hump in Figures 6C and 6D lies within the error bounds of the kinetic experiments with glasses; the rate constant can be considered virtually independent of ionic strength.

This independence may perhaps be attributed, at least in part, to adsorption of the protein to the pore walls at low ionic strength. Because the charge of the protein is neutralized by the charge of the surface, electrostatic interactions between the reactants are absent. When the protein is desorbed from the pore walls, its electrostatic interactions with $[\text{Fe}(\text{CN})_6]^{3-}$ ions are still weak or absent because of the high ionic strength required for desorption. Glass interior is intrinsically different from bulk solution as a medium for the reaction in eq 1 and possibly for other reactions.

Kinetic Effects of pH in Glass. Because the experiments discussed above were done mostly at medium and high ionic strengths, the reactions were relatively fast. The following experiments were done at a low ionic strength of 7.5 mM, so that exclusion effects be pronounced. As Figure 9A shows, the reaction in bulk solution does not depend on the pH value. Indeed, conformation of cytochrome *c* remains the same, and its net charge varies only slightly, in the interval $5.5 \leq \text{pH} \leq 9.0$. The reaction in glass, however, appears to be assisted by a decrease of pH; see Figure 9B. The partitioning coefficient (eq 2) for $[\text{Fe}(\text{CN})_6]^{3-}$ ions at the ionic strength of 7.5 mM and at $7.0 \leq \text{pH} \leq 9.5$ is very low. Consequently, the quenching reactions at the ionic strength of 7.5 mM are slow. The partitioning coefficient is larger in weakly acidic solutions: 0.35 and 0.38 at pH values of 6.0 and 5.5, respectively. Evidently, the exclusion discussed above can be lessened even at

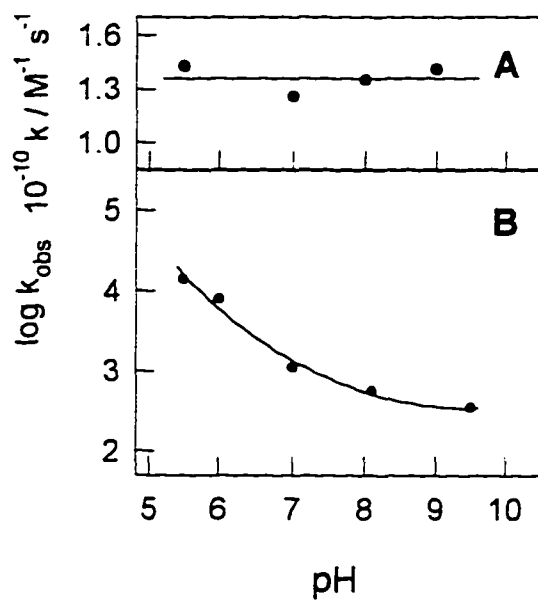
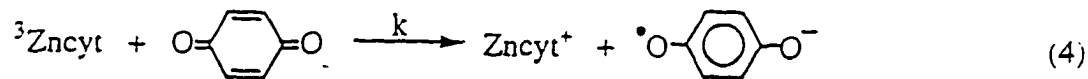
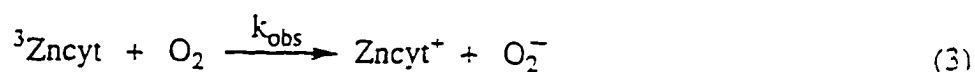


Figure 9. Kinetics of the reaction in eq 1 at various pH values of the bulk solution, at ionic strength of 7.5 mM. (A) Independence of the second-order rate constant for the reaction in bulk solution. (B) Dependence of the pseudo-first-order rate constant for the reaction in sol-gel silica glass.

low ionic strength by (partial) protonation of the negatively-charged siloxide groups on the silica surface. The difference between Figures 9A and 9B reflects an intrinsic difference between solution and sol-gel glass as reaction media.

Quenching of $^3\text{Zncyt}$ by Electroneutral Molecules

We showed above that cytochrome *c* can adsorb on the silica surface but explained the surprisingly low rate constants at low ionic strength (Figures 6A and 6B) in terms of other factors. To verify this explanation, we studied reactions with the electroneutral quenchers dioxygen (eq 3) and *p*-benzoquinone (eq 4). As before, the reverse electron-transfer reactions, which are not shown, regenerated the reactants and allowed repeated flashing of the same slab. As before, the slowest of the three exponential components was the natural decay of the triplet state. As before, the other two exponentials corresponded to the quenching reaction, and the faster component had the rate constant approximately seven times that of the slower.



Reaction with Dioxygen. Because concentration of dioxygen in water is fixed by the solubility of air, the quantities plotted in Figure 10 are the observed, not the second-order, rate constants for both components of the reaction in eq 3. Their independence of ionic

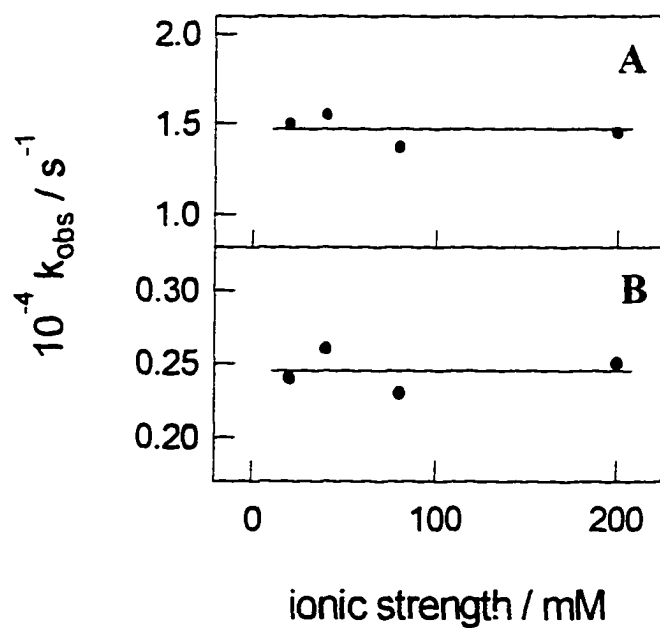


Figure 10. Independence of ionic strength of the pseudo-first-order rate constant for the reaction in eq 3 in sol-gel silica glass. (A) The faster component. (B) The slower component.

strength was an interesting, albeit preliminary, evidence concerning the interactions in the confined solution.

Reaction with *p*-Benzoquinone. Diffusion of this compound into glass was studied as described above for $K_3[Fe(CN)_6]$. Ultraviolet absorbance ($\epsilon_{305} = 225 \text{ M}^{-1}\text{cm}^{-1}$) inside the glass is directly proportional to concentration of *p*-benzoquinone in external solutions; see Supporting Information, Figure 7. There is no exclusion. Partitioning coefficient (eq 2) is equal to one, within the margins of experimental error, in the entire range 20 mM μ^2 300 mM; see Supporting Information, Figure 8. The second-order rate constants for the faster and the slower components of the reaction in eq 4 are 1.4×10^8 and $2.0 \times 10^7 \text{ M}^{-1}\text{s}^{-1}$ in the entire interval 20 mM μ^2 300 mM; see Figure 11.

The results in Figures 10 and 11 show that availability of zinc cytochrome *c* molecules for the reaction inside glass pores is not significantly affected by adsorption to the pore walls. If this is true also for the reaction in eq 1, then the small humps in Figures 6C and 6D, which lie within the error margins of the kinetic experiments with glass, are insignificant. Our conclusion above is now confirmed. The interesting effects of low ionic strength on the reaction in eq 1 within glass are due to partial exclusion of the anionic quencher from the glass interior.

Hindrance of Diffusion in Glasses

Even the solutes that are small enough to penetrate the glass uniformly may be somewhat retarded by this matrix in chemical reactions. We compared the rate constants for the reactions in eqs 1, 4, and 3 in bulk solution and in solution confined within glass. In each

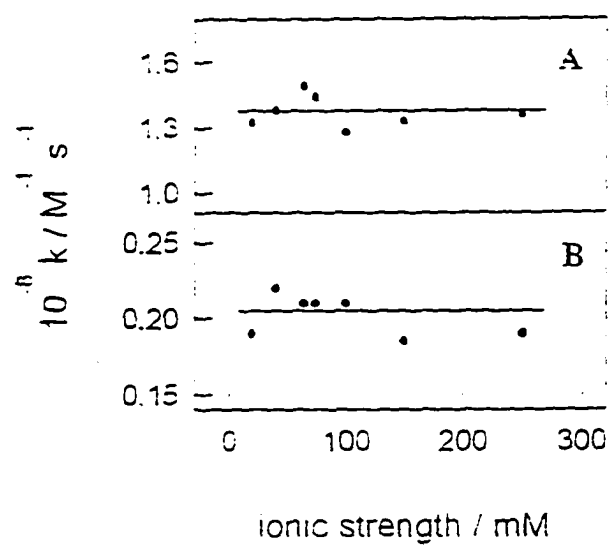


Figure 11. Independence of ionic strength of the second-order rate constant for the reaction in eq 4 in sol-gel silica glass. (A) The faster component. (B) The slower component.

case the latter reaction was slower than the former. The ratio of the rate constant in solution and the rate constant of the faster component in glass (the hindrance factor of the glass) decreased as the quencher for $^3\text{Zncyt}$ became smaller and more mobile. At the ionic strength of 20 mM these factors for $[\text{Fe}(\text{CN})_6]^{3-}$, *p*-benzoquinone, and O_2 are 400, 5, and 1.1, respectively. At the ionic strength of 300 mM, at which electrostatic effects are minimized, the hindrance factors are 20, 5, and 1.1, respectively. Although $[\text{Fe}(\text{CN})_6]^{3-}$ and *p*-benzoquinone are relatively small molecules, their movement is retarded by the glass environment. Again, solutes behave differently in bulk solution and in solution confined inside the pores.

Conclusions

This study confirms the utility of the new sol-gel method for doping silica glass with proteins. Because the glasses are optically transparent, they are well suited to the study of photoinduced chemical reactions. Kinetic investigation of these fast reactions revealed some interesting and important properties of sol-gel silica, which should be taken into account when it is used as a matrix for sensors.

Because the silica surface may be charged, diffusion of ions between the glass and surrounding solution may result in different ion concentrations in these two domains even when the system has reached equilibrium. The concentrations at equilibrium may depend on pH and ionic strength, factors that determine the surface charge. Quantitative theoretical study of these effects has only begun.⁷³⁻⁷⁵ Because of them, the common assumption that porosity of sol-gel glasses ensures uniform penetration of relatively small species into the

pores must be taken skeptically and tested for each solute of interest, preferably at different concentrations of this solute and under different conditions of ionic strength, pH, and other relevant factors. Microscopic heterogeneity of the glass interior and multiphasic kinetics of reactions occurring there should be considered.

Acknowledgements. This work was supported by the NSF, through Grant MCB-9222741. Chengyu Shen thanks Mrs. Neoma Wall for a graduate fellowship. We thank Dr. George Chumanov and Shuyu Ye, who recorded the resonance Raman spectra.

References

- (1) Brinker, C. J.; Scherer, G. *Sol-gel Science: The Physics and Chemistry of Sol-gel Processing*, Academic Press, San Diego, 1989.
- (2) Roy, R. *Science* **1987**, *238*, 1664.
- (3) Hench, L. L.; West, J. K. *Chem. Rev.* **1990**, *80*, 33.
- (4) Buckley, A. M.; Greenblatt, M. *J. Chem. Edu.* **1994**, *71*, 599.
- (5) Avnir, D.; Braun, S.; Lev, O.; Ottolenghi, M. *Chem. Mater.* **1994**, *6*, 1605.
- (6) Avnir, D. *Acc. Chem. Res.* **1995**, *28*, 328.
- (7) Slama-Schwok, A.; Ottolenghi, M.; Avnir, D. *Nature* **1992**, *355*, 240.
- (8) Samuel, J.; Plevaya, Y.; Ottolenghi, M.; Avnir, D. *Chem. Mater.* **1994**, *6*, 1457.
- (9) Slama-Schwok, A.; Avnir, D.; Ottolenghi, M. *J. Phys. Chem.* **1989**, *93*, 7544.
- (10) Slama-Schwok, A.; Avnir, D.; Ottolenghi, M. *J. Am. Chem. Soc.* **1991**, *113*, 3984.

- (11) Levy, D.; Reifeld, R.; Avnir, D. *Chem. Phys. Lett.* **1984**, *109*, 593.
- (12) Levy, D.; Avnir, D. *J. Phys. Chem.* **1988**, *92*, 4734.
- (13) Tour, J. M.; Cooper, J. P.; Pedalwar, S. L. *Chem. Mater.* **1990**, *2*, 647.
- (14) Yamanaka, S. A.; Nishida, F.; Ellerby, L. M.; Nishida, C. R.; Dunn, B.; Valentine, J. S.; Zink, J. I. *Chem. Mater.* **1992**, *4*, 495.
- (15) Wu, S.; Ellerby, L. M.; Cohan, J. S.; Dunn, B.; Valentine, J. S.; Zink, J. I. *Chem. Mater.* **1993**, *5*, 115.
- (16) Akbarian, F.; Dunn, B.; Zink, J. I. *J. Mater. Chem.* **1993**, *3*, 1041.
- (17) Lopez, T.; Moran, M.; Navarrete, J.; Herrera, L.; Gomez, J. *J. Non-Cryst. Solids* **1992**, *147*, 753.
- (18) Matsui, K.; Tominaga, M.; Arai, Y.; Satoh, H.; Kyoto, M. *J. Non-Cryst. Solids* **1994**, *169*, 295.
- (19) Matsui, K. *Langmuir* **1992**, *8*, 673.
- (20) Ellerby, L. M.; Nishida, C. R.; Nishida, F.; Yamanaka, S. A.; Dunn, B.; Valentine, J. S.; Zink, J. I. *Science* **1992**, *255*, 673.
- (21) Dave, B. C.; Soyeze, H.; Miller, J. M.; Dunn, B.; Valentine, J. S.; Zink, J. I. *Chem. Mater.* **1995**, *7*, 1431.
- (22) Yamanaka, S. A.; Dunn, B.; Valentine, J. S.; Zink, J. I. *J. Am. Chem. Soc.* **1995**, *117*, 9095.
- (23) Dave, B. C.; Dunn, B.; Valentine, J. S.; Zink, J. I. *Anal. Chem.* **1994**, *66*, 1120A.
- (24) Braun, S.; Rappoport, S.; Avnir, D.; Ottolenghi, M. *Mater. Lett.* **1990**, *10*, 1.
- (25) Guo, L-H.; Mukamel, S.; McLendon, G. *J. Am. Chem. Soc.* **1995**, *117*, 546.

- (26) Mabrouk, P. A. *J. Am. Chem. Soc.* **1995**, *117*, 2141.
- (27) Glezer, V.; Lev, O. *J. Am. Chem. Soc.* **1993**, *115*, 2533.
- (28) Audebert, P.; Demaille, C.; Sanchez, C. *Chem. Mater.* **1993**, *5*, 911.
- (29) Zusman, R.; Beckman, D. A.; Zusman, I.; Brent, R. L. *Anal. Biochem.* **1992**, *201*, 103.
- (30) Braun, S.; Shtelzer, S.; Rappoport, S.; Avnir, D.; Ottolenghi, M. *J. Non-Cryst. Solids* **1992**, *147*, 739.
- (31) Tatsu, Y.; Yamashita, K.; Yamagushi, M.; Yamamura, S.; Yamamoto, H.; Yoshikawa, S. *Chem. Lett.* **1992**, *8*, 1615.
- (32) Zink, J. I.; Valentine, J. S.; Dunn, B. *New J. Chem.* **1994**, *18*, 1109.
- (33) Xu, S.; Ballard, L.; Kim, Y. J.; Jonas, J. J. *Phys. Chem.* **1995**, *99*, 5787.
- (34) Korb, J.-P.; Delville, A.; Xu, S.; Demeulenaere, G.; Costa, P.; Jonas, J. J. *Chem. Phys.* **1994**, *101*, 7074.
- (35) Ueda, M.; Kim, H.-B.; Ikeda, T.; Ichimura, K. *Chem. Mater.* **1994**, *6*, 1771.
- (36) Ueda, M.; Kim, H.-B.; Ikeda, T.; Ichimura, K. *Chem. Mater.* **1992**, *4*, 1229.
- (37) Catellano, F. N.; Heimer, T. A.; Tandhasetti, M. T.; Meyer, G. J. *Chem. Mater.* **1994**, *6*, 1041.
- (38) Zusman, R.; Rottman, C.; Ottolenghi, M.; Avnir, D. *J. Non-Cryst. Solids* **1990**, *122*, 107.
- (39) Wang, R.; Narang, U.; Bright, F. V. *Anal. Chem.* **1993**, *65*, 2671.
- (40) Narang, U.; Prasad, P. N.; Bright, P. N. *Anal. Chem.* **1994**, *66*, 3139.
- (41) Dulebohn, J. I.; Haefner, S. C.; Dunber, K. R. *Chem. Mater.* **1992**, *4*, 506.

- (42) Hagen, S. J.; Hofrichter, J.; Eaton, W. A. *Science* **1995**, *269*, 959.
- (43) Ye, S.; Shen, C.; Cotton, T. M.; Kostic', N. M. *J. Inorg. Biochem.* **1997**, *65*, 219
and references therein.
- (44) Ononye, A. I. Bolten, J. R. *J. Phys. Chem.* **1986**, *90*, 6266.
- (45) Ononye, A. I., Bolten, J. R. *J. Phys. Chem.* **1986**, *90*, 6270.
- (46) Zhou, J. S.; Kostic', N. M. *Biochemistry* **1993**, *32*, 4539.
- (47) Mckiernan, J.; Pouxvier, J-C.; Dunn, B.; Zink, J. I. *J. Phys. Chem.* **1989**, *93*, 2129.
- (48) Pouxvier, J-C.; Dunn, B.; Zink, J. I. *J. Phys. Chem.* **1989**, *93*, 2134.
- (49) Hanna, S. D.; Dunn, B.; Zink, J. I. *J. Non-Cryst. Solids* **1994**, *167*, 239.
- (50) Nishida, F.; Mckiernan, J. M.; Dunn, B.; Zink, J. I. *J. Am. Ceram. Soc.* **1995**, *78*,
1640.
- (51) Mckiernan, J. M.; Simoni, E.; Dunn, B.; Zink, J. I. *J. Phys. Chem.* **1994**, *98*, 1006.
- (52) Audebert, P.; Griesmar, P.; Hapiot, P.; Sanchez, C. *J. Chem. Mater.* **1992**, *2*, 1293.
- (53) Vanderkooi, J. M.; Adar, F.; Erecinska, M. *Eur. J. Biochem.* **1976**, *64*, 381.
- (54) Hennessey, J. P.; Johnson, W. C. *Biochemistry* **1981**, *20*, 1085.
- (55) Chen, Y-H.; Yang J. T. *Biochem. Biophys. Res. Commun.* **1971**, *44*, 1285.
- (56) Hsu, M-C.; Woody, R. W. *J. Am. Chem. Soc.* **1971**, *93*, 3515.
- (57) Myer, Y. P. *Curr. Top. Bioenerg.* **1985**, *14*, 149.
- (58) Anni, H.; Vanderkooi, J. M.; Leland, M. *Biochemistry* **1995**, *34*, 5744.
- (59) Benson, D. R.; Bradley, R. H.; Doughty, M. B.; *J. Am. Chem. Soc.*, **1995**, *117*,
8502.

- (60) Chottard, G.; Michelon, M.; Herve, M.; Herve, G. *Biochem. Biophys. Acta* **1987**, *916*, 402.
- (61) Mizutani, T.; Tadashi, E.; Ogoshi, H. *Inorg. Chem.* **1994**, *33*, 3558.
- (62) Hildebrandt, P. In *Cytochrome c: a Multidisciplinary Approach*; Scott, R. A.; Mauk, A. G., Eds; University Science Books: Sausalito, CA, 1996; chapter 6.
- (63) Hu, S.; Morris, I. K.; Singh, J. P.; Smith, K. M.; Spiro, T. G. *J. Am. Chem. Soc.* **1993**, *115*, 12446 and references therein.
- (64) Zhou, J. S.; Kostic, N. M. *J. Am. Chem. Soc.* **1993**, *115*, 10796.
- (65) Shen, C.; Kostic, N. M. *Inorg. Chem.* **1996**, *35*, 2780.
- (66) Wherland, S.; Gray, H. B. In *Biological Aspects of Inorganic Chemistry*; Dolphin, D, Ed.; Wiley, 1977; p.298.
- (67) Moore, G. R.; Eley, C. S.; Williams, G.; *Adv. Inorg. Bioinorg. Mech.* **1984**, *3*, 1.
- (68) Ramsden, J. T. *Chem. Soc. Rev.* **1995**, *74*.
- (69) Hair, M. L.; Hertl, W. *J. Phys. Chem.* **1970**, *74*, 91.
- (70) Schindler, P.; Dick, R.; Wolf, P. *J. Colloid Interface Sci.* **1976**, *55*, 469.
- (71) Duinhoven, S.; Poort, R.; Van Der Voet, G.; Agterof, W. G. M.; Norde, W.; Lyklema, J. *J. Colloid Interface Sci.* **1995**, *170*, 340.
- (72) Duinhoven, S.; Poort, R.; Van Der Voet, G.; Agterof, W. G. M.; Norde, W.; Lyklema, J. *J. Colloid Interface Sci.* **1995**, *170*, 351.
- (73) Dubois, M.; Zemb, J.; Belloni, L.; Setton, R. *J. Chem. Phys.* **1992**, *96*, 2287.
- (74) Vlachy, V. I., Haymet, A. D. *Aust. J. Chem.*, **1990**, *43*, 1961.
- (75) Jamnik, B.; Vlachy, V. *J. Am. Chem. Soc.* **1995**, *117*, 8010.

Supporting Information

Figures 1-10

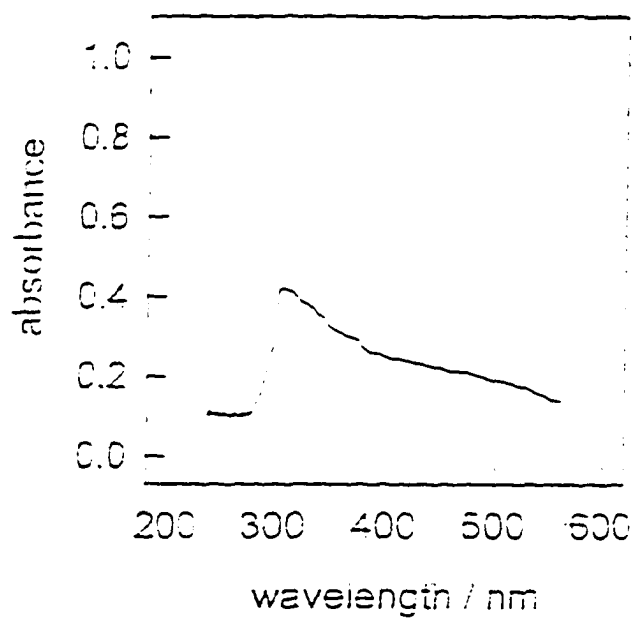


Figure 1: Absorption spectrum of a 0.75 cm thick slab of undoped glass

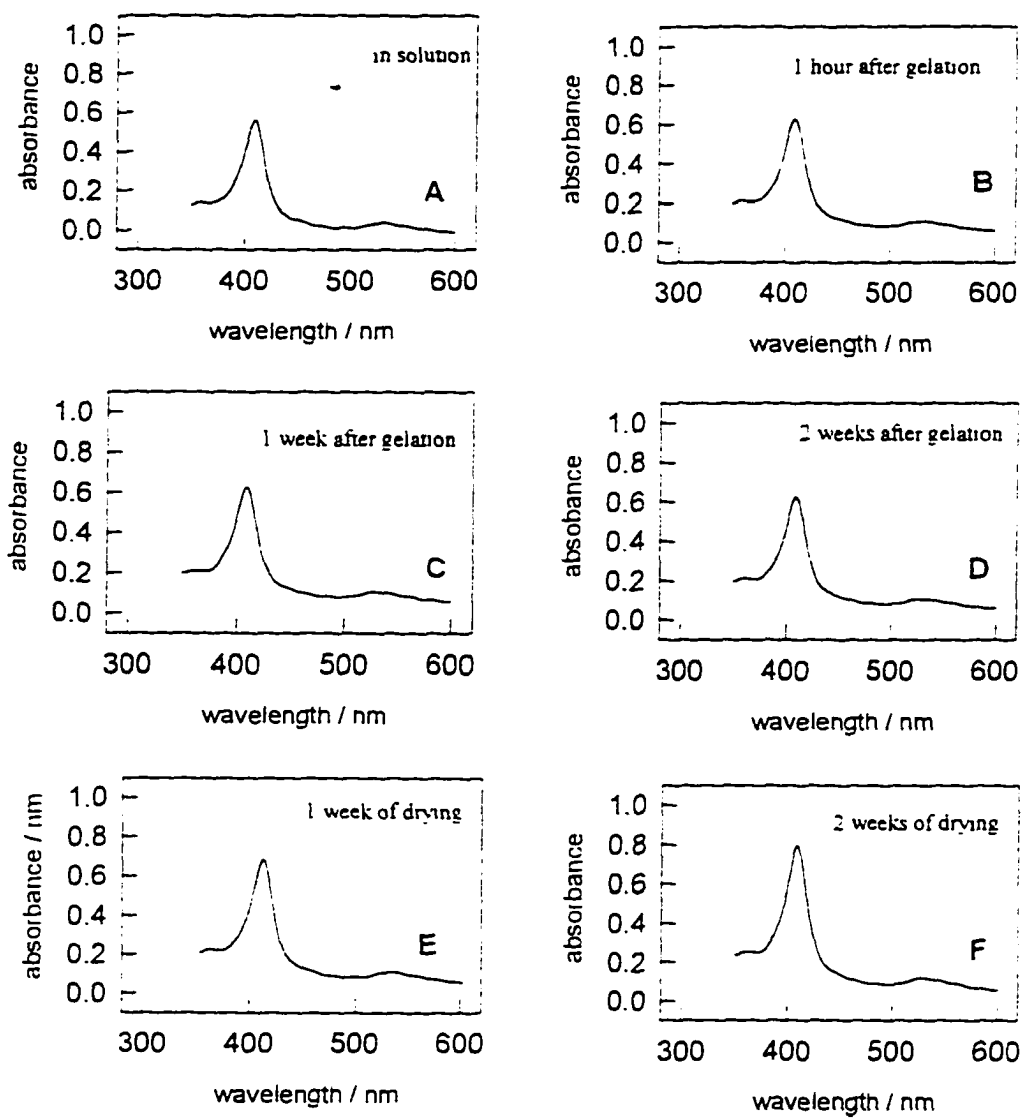


Figure 2: Absorption spectra of cyt(III) at different stages of glass preparation.

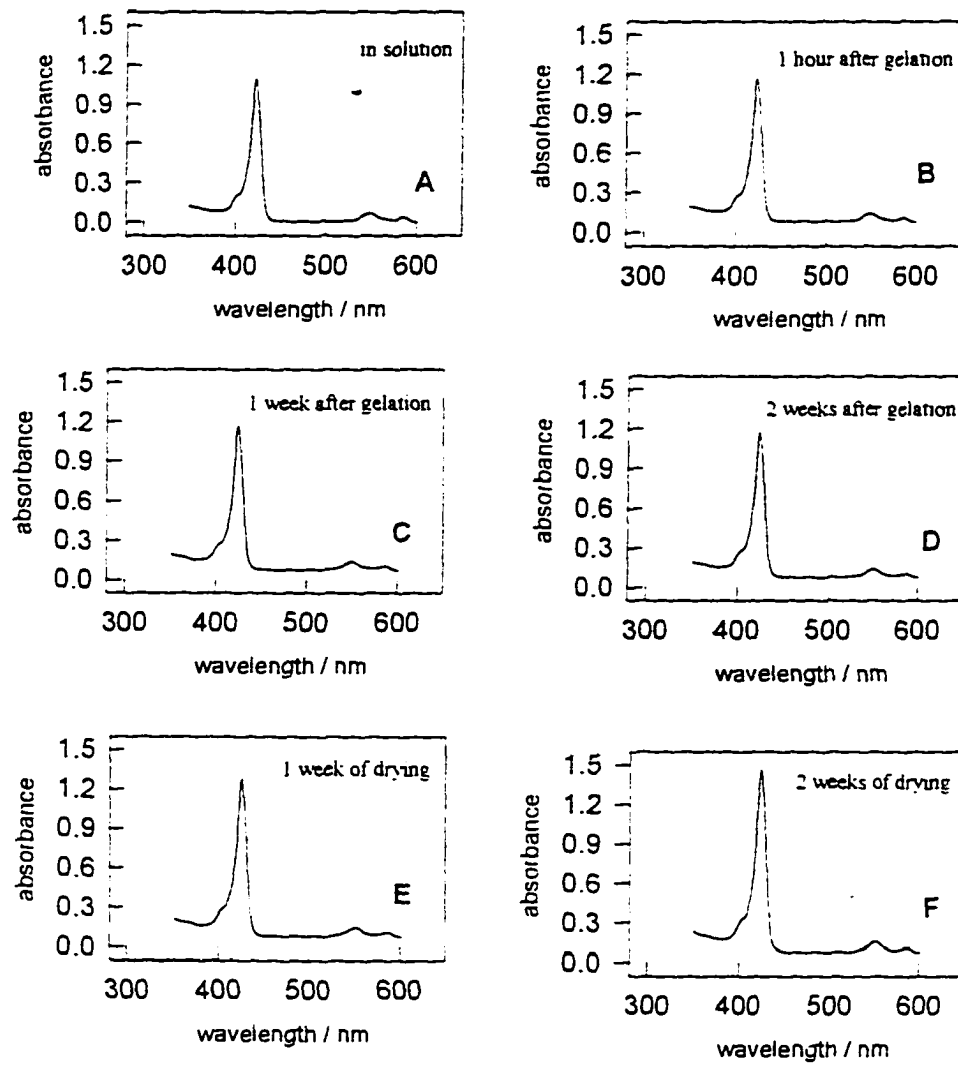


Figure 3: Absorption spectra of Zn cyt at different stages of Glass preparation.

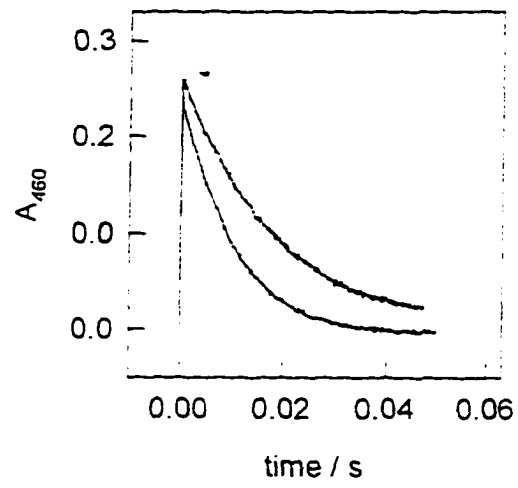


Figure 4: Natural decay of ^{60}Zn in solution (lower curve) and in sol-gel glass. (upper curve)

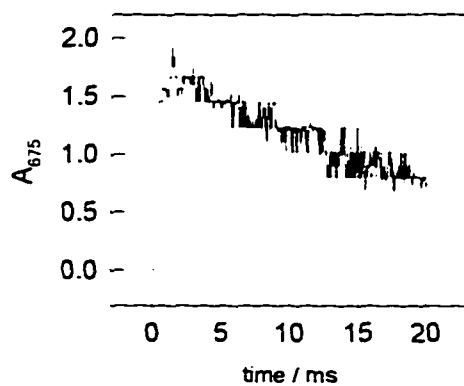


Figure 5: Formation and decay of Zn cyt⁺ in sol-gel glass, in the presence of 100 μM $\text{Fe}(\text{CN})_6^{3-}$, $\mu = 20$ mM.

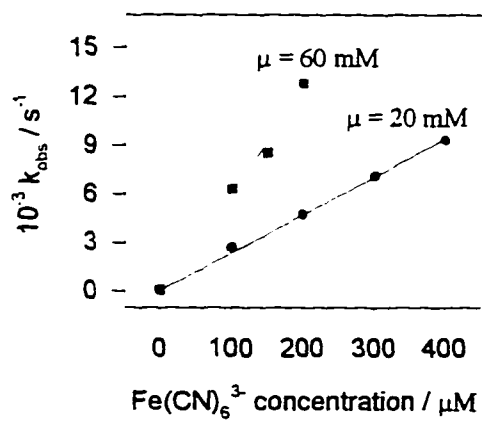


Figure 6: The fastest component of quenching of $^3\text{Zn cyt}^+$ by $\text{Fe}(\text{CN})_6^{3-}$ in sol-gel glass at two ionic strengths

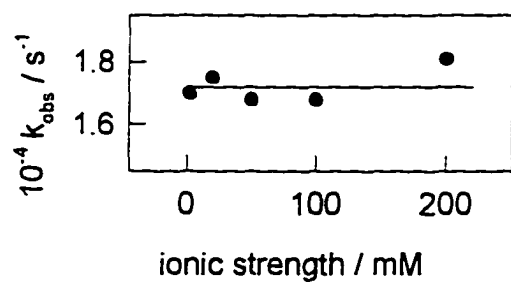


Figure 7: Quenching of $^3\text{Zncyt}$ by O_2 in bulk solutions of different ionic strengths

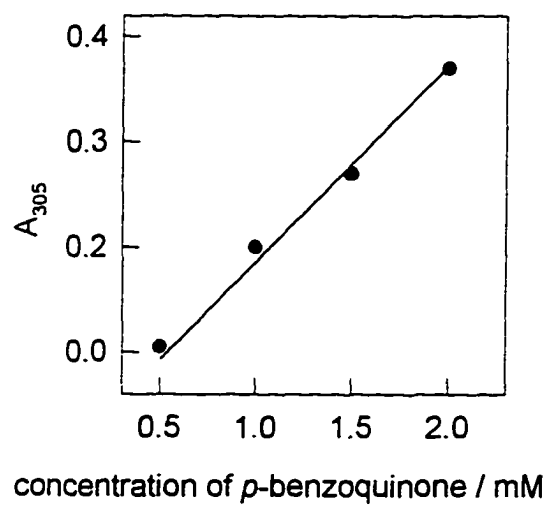


Figure 8: Uptake of *p*-benzoquinone by a slab of undoped glass immersed in solutions of different concentrations, at ionic strength of 20 mM

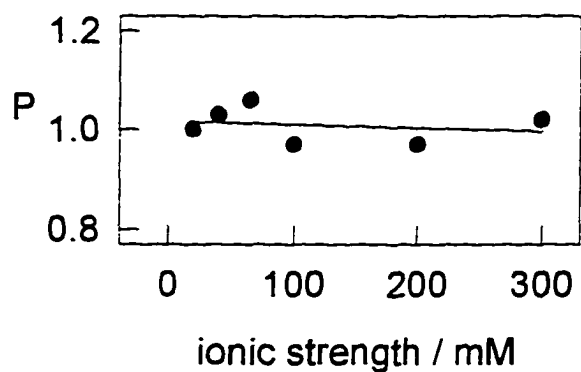


Figure 9: Partitioning coefficient for *p*-benzoquinone between sol-gel glass and surrounding solution

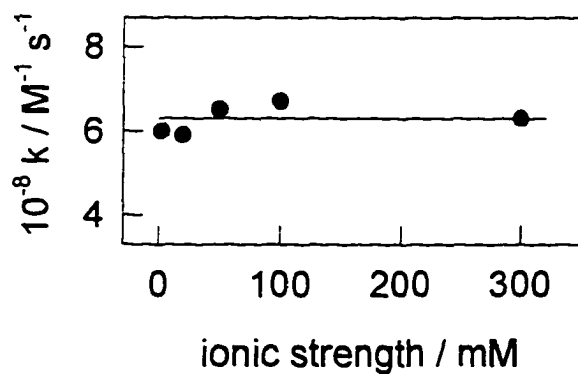


Figure 10: Quenching of 3Zncyt by *p*-benzoquinone in bulk solutions of different ionic strengths

CHAPTER 3**REDUCTIVE QUENCHING OF THE TRIPLET STATE OF ZINC
CYTOCHROME *c* BY HEXACYANOFERRATE(II) ANION AND
BY CONJUGATE BASES OF
ETHYLENEDIAMINETETRAACETIC ACID**

Chengyu Shen and Nenad M. Kostić

Abstract

The long-lived triplet state of zinc cytochrome *c*, designated $^3\text{Zncyt}$, has often been used as a reductant, in oxidative-quenching reactions. This article seems to be the first report of the use of $^3\text{Zncyt}$ as an oxidant, in two reductive-quenching reactions. Conjugate bases (anions) of EDTA quench $^3\text{Zncyt}$ at pH 6.5 with the observed rate constant that is two times greater than the rate constant for natural decay of this excited state. Electrostatic attraction between these quenchers and Zncyt is a necessary but not sufficient condition for quenching. A transient species observed at 690 nm has the absorbance and the time profile expected of the anion radical Zncyt^- . Detection of this species is possible because of the rapid decomposition of EDTA upon oxidation. The complex $[\text{Fe}(\text{CN})_6]^+$ quenches $^3\text{Zncyt}$ at

pH 7.0 with the rate constant of $(1.5 \pm 0.3) \times 10^8 \text{ M}^{-1} \text{ s}^{-1}$. This fast quenching is not caused by electrostatic association of $^3\text{Zncyt}$ and $[\text{Fe}(\text{CN})_6]^{4-}$ nor by energy transfer from the former to the latter. The complex $[\text{Fe}(\text{CN})_6]^{4-}$ is not detectably contaminated by the similar complex $[\text{Fe}(\text{CN})_6]^{3-}$, which might act as an oxidative quencher. The evidence supports reductive quenching of $^3\text{Zncyt}$ by the $[\text{Fe}(\text{CN})_6]^{4-}$ ion. The anion radical Zncyt^- is not detected, probably because it is rapidly consumed in the back reaction with the $[\text{Fe}(\text{CN})_6]^{3-}$ ion. To act as reductive quenchers for $^3\text{Zncyt}$, chemicals must have favorable electrostatic properties, redox potential, and reactivity. These requirements are discussed, so that further studies of this new reaction may be possible.

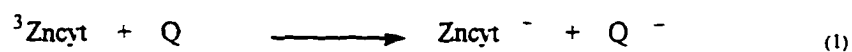
Introduction

Various metalloproteins act as electron carriers and redox enzymes in photosynthesis, respiration, nitrogen fixation, nonmetal metabolism, DNA biosynthesis, DNA repair, detoxification of various compounds, and other biological processes. To understand biological functions of metalloproteins, one must understand their chemical reactivity. Despite vigorous current research,¹⁻⁶ molecular mechanisms of electron-transfer reactions of metalloproteins are only partially understood.

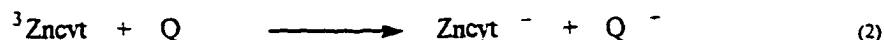
Much of this chemical research has involved heme proteins, such as myoglobins, hemoglobins, and cytochromes *c*. The proteins of the last family are prototypical electron-carriers. Their oxidoreduction reactions with various chemical and biochemical agents have been much studied, and their three-dimensional structures are known in detail.⁷

Almost all metals and metalloids form porphyrin complexes. Because heme is a kind of porphyrin, some of this diversity has touched the proteins.⁸ Derivatives of myoglobin,⁹⁻¹⁶ hemoglobin,¹⁷⁻²⁵ and cytochrome *c*²⁵⁻⁴³ containing various metals in the place of iron have been prepared and characterized. Owing to their interesting spectroscopic, photophysical, and photochemical properties, these so-called reconstituted proteins have proven very useful. Cytochrome *c* noninvasively reconstituted with zinc(II), called simply zinc cytochrome *c* and designated Zncyt,³⁶⁻³⁹ has been widely used in determination of interprotein distances⁴¹⁻⁴³ and in kinetic studies of electron-transfer reactions.⁴⁴⁻⁵⁵ It has absorption maxima at 423 (Soret), 549, and 585 nm; a fluorescent (singlet) excited state with the lifetime of 3.2 ns; and fluorescence maxima at 590 and 640 nm. Especially useful for kinetic studies is the lowest-lying triplet excited state, designated ³Zncyt. Because its lifetime is unusually long – between 7 and 15 ms, depending on preparation and experimental conditions⁵⁶⁻⁶⁰ – electron-transfer reactions of the triplet state can be studied relatively easily.

All of the previous studies known to us have dealt with *oxidative* quenching by various quenchers, designated Q. Among them are organic compounds,³⁹ transition-metal complexes, and metalloproteins.⁴⁴⁻⁵⁵ The products of these reactions, represented by eq 1, are zinc cytochrome *c* cation radical, designated Zncyt⁺, and the reduced form of the quencher, designated Q⁻. This study deals with *reductive* quenching, represented by eq 2, products of which are zinc cytochrome *c* anion radical, designated Zncyt⁻, and the oxidized



form of the quencher, designated Q^- . To our knowledge, this is the first investigation of the reaction in eq 1. It is needed for a better understanding of electron-transfer reactions of zinc cytochrome *c*.



Experimental Procedures

Chemicals. Distilled water was further demineralized and purified to a resistance greater than $15 \text{ M } \Omega \cdot \text{cm}$. Horse-heart cytochrome *c* was obtained from Sigma Chemical Co. Iron was removed, the free-base protein purified, and zinc(II) ions inserted according to published procedures,^{36,38} as quickly as possible. Zinc cytochrome *c* was always handled in the dark. Glutathione and the reduced form of nicotinamide adenine dinucleotide phosphate (NADPH) were obtained from Sigma Chemical Co. Trimethanolamine, trimethylamine, and *trans*-1,2-diaminocyclohexane-*N,N,N',N'*-tetraacetate (designated CDTA)⁶¹ were obtained from Aldrich Chemical Co. The complex salt $[\text{Ru}(\text{NH}_3)_6]\text{Cl}_2$ was obtained from Alfa Products, Inc. Disodium salt of ethylenediaminetetraacetic acid (Na_2EDTA), $\text{K}_4[\text{Fe}(\text{CN})_6]$, and all the other chemicals were obtained from Fischer Chemical Co. All chemicals were of reagent grade. They were used as received, unless stated otherwise. The compounds $[\text{Fe}(\text{CDTA})]$,⁶¹ $\text{K}_3[\text{Co}(\text{CN})_6]$,⁶² and methylviologen monocation radical,⁶³ designated MV^- , were prepared by published procedures.

Kinetics. The solvent was always sodium phosphate buffer. Experiments with EDTA were done at pH 6.5, whereas experiments with $[\text{Fe}(\text{CN})_6]^{4-}$ and $[\text{Fe}(\text{CN})_6]^{3-}$ were

done at pH 7.0. Flash kinetic spectrophotometry, so-called laser flash photolysis, on the microsecond scale was done with a standard apparatus.^{53,54} The sample solution in a 10-mm cuvette was thoroughly deaerated by gentle flushing with ultrapure wet argon, obtained from Air Products Co. A Phase-R (now Lumenex) DL1100 laser containing a 50 mM solution of rhodamine 590 in methanol delivered 0.4-ms pulses of excitation light. The monochromatic monitoring beam from a tungsten-halogen lamp was perpendicular to the excitation beam. The absorbance-time curves were analyzed with kinetic software obtained from OLIS, Inc. Each signal was an average of six pulses. Appearance and disappearance of the triplet state, $^3\text{Zncyt}$, were monitored at 460 nm, where the transient absorbance is greatest. The concentration of Zncyt was always 10 mM. The concentration of $^3\text{Zncyt}$ depended on the excitation power, but was always kept well below the concentration of the quencher. The only exceptions were studies of oxidative quenching by the $[\text{Fe}(\text{CN})_6]^{3-}$ ion; in these control experiments the concentration of $\text{K}_3[\text{Fe}(\text{CN})_6]$ was kept below 1.0 mM.

Purity of $\text{K}_3[\text{Fe}(\text{CN})_6]$. Our method is a modification of the standard one.⁶⁴ To a solution of 8.9 g of $\text{K}_3[\text{Fe}(\text{CN})_6]$ in 100 mL of water were added, in this order, 20 mL of a 0.25 M solution of KI, 2.0 mL of 1.00 M H_2SO_4 , 10.0 g of $\text{ZnSO}_4 \cdot 7\text{H}_2\text{O}$, and 2.0 mL of a saturated starch solution; the solvent was always water. Color of the final mixture indicated the purity of the complex salt. Blue color is diagnostic of the $[\text{Fe}(\text{CN})_6]^{3-}$ ion.

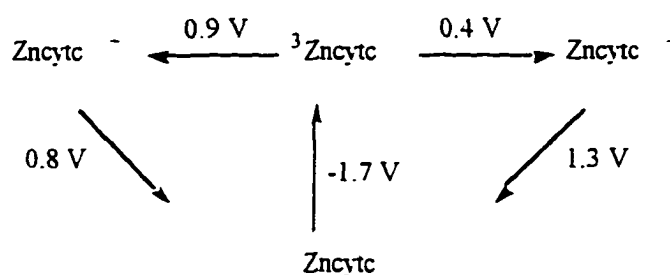
Results and Discussion

The Triplet State, $^3\text{Zncyt}$. The excitation by laser of the porphyrin p-system can be considered a promotion of an electron from the HOMO to the LUMO, with the inversion of

the electron spin. The natural decay is a return to the ground state. Because the excited (triplet) and the ground (singlet) states differ in spin multiplicity, the lifetime of $^3\text{Zncyt}$ is long, i.e., the decay is slow. Our rate constant for the natural decay is $100 \pm 10 \text{ s}^{-1}$, consistent with previously published values.⁵⁵⁻⁶⁰ This rate constant is independent of ionic strength in the entire range studied, from 2.5 mM to 1.00 M.⁵³

Redox Potentials and Quenching Modes. Redox potentials for four of the five redox couples shown in Scheme 1 were obtained from the literature or calculated directly from the accepted values in the literature.^{39,44} The value of 0.8 V was determined by differential pulse voltammetry.³⁹ The same value was obtained for zinc tetraphenylporphyrin.⁶⁵ This similarity between the heme protein reconstituted with zinc(II) and a simple zinc(II) porphyrin⁶⁵ shows that the redox potentials are not markedly affected by the protein matter surrounding the zinc(II) porphyrin molecule. The value of 1.7 V in Scheme 1 is the experimental result for the excitation energy.⁴⁴ Then the value of 0.9 V follows from the thermodynamic cycle. The value of 1.3 V was determined experimentally for different zinc(II) porphyrins,⁶⁵⁻⁶⁷ and we used it also for the protein; this method was justified above. Finally, the value of 0.4 V follows from the thermodynamic cycle. All the values are defined with respect to the normal hydrogen electrode, at pH 7.0 and 25 °C. The number of significant figures reflects our conservative analysis of redox potentials. By convention, redox potentials should be given as *reduction* potentials. Consistent adherence to this useful practice would, however, make our discussion confusing. For example, *reduction* potential of -0.9 V pertains to the half-reaction $\text{Zncyt}^- + e^- \rightarrow ^3\text{Zncyt}$, which we do not study (and which would be difficult to effect in any case). Because we study the

reverse of this half-reaction, it is more convenient to use the potential of 0.9 V. *All the potentials in Scheme 1 correspond to the half-reactions shown by the arrows, those that we actually study.* Because two of them are reductions, their potentials (0.8 and 0.4 V) are true reduction potentials.



Scheme 1. Potentials (versus normal hydrogen electrode) for the redox half-reactions (at pH 7.0 and 25 °C) of zinc cytochrome *c* that are shown by the arrows.

The main conclusion from Scheme 1 is that ${}^3\text{Zncyt}$ is both a stronger reductant and a stronger oxidant than Zncyt. Electron excitation simultaneously creates a high-lying electron that can be removed relatively easily by an oxidative quencher (as in eq 1) and a low-lying "hole" that can be "filled" relatively easily by a reductive quencher (as in eq 2). The values 0.9 and 0.4 V in Scheme 1 show that, in a thermodynamic sense, ${}^3\text{Zncyt}$ is a stronger reductant than oxidant. This is probably the reason why oxidative quenching of this

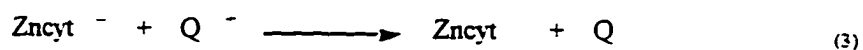
triplet state is well known, whereas reductive quenching, to our knowledge, has not been reported.

Optical Absorption of the Anion Radical Zncyt⁻. We did not find in the literature the optical absorption spectrum of this anion radical and had to infer its likely spectroscopic properties from those of closely related compounds and their ion radicals. This method is validated by the following facts. Ultraviolet-visible absorption spectra of zinc tetraphenylporphyrin and of zinc heme in Zncyt^c are very similar,⁶⁷⁻⁶⁹ and the cation radicals of both show an absorption maximum at 675 nm.⁷⁰ The triplet states of both zinc 5,10,15,20-tetra(N-methylpyridinium-4-yl)porphyrin, designated [Zn(TMPyP)]⁺, and zinc cytochrome *c* show maximum absorbance at 460 nm.⁷¹ Zinc porphyrin complexes usually have one axial ligand, i.e., the coordination number of five. This axial ligand in zinc myoglobin seems to be histidine,²⁵ as in the native (iron-containing) form of this protein. According to the latest study, by optical and NMR spectroscopic methods, the zinc(II) atom in zinc cytochrome *c* has the coordination number of six, i.e., two axial ligands—a methionine and a histidine residue.³⁸ Again, this is the same coordination as in the native (iron-containing) form of cytochrome *c*. Although these two reconstituted heme proteins differ in axial ligation, they have very similar absorption spectra.¹³ Evidently, the electronic structure of zinc porphyrin is not grossly perturbed by the substituents in the porphyrin group, the axial ligands, and the surrounding protein matter.

Now we consider the properties of known porphyrin anion radicals. The anion radical of metal-free (so-called free-base) cytochrome *c* was produced by pulse radiolysis; it has a broad absorption band at 700 nm. Photoreduction of zinc porphyrin by ascorbic acid

and photoreduction of zinc tetraphenylporphyrin by benzoin, both in aqueous solution, gave stable species that showed a characteristic absorption band at 620 nm.^{68,69} This species, however, is not the porphyrin anion radical but a product of its protonation or of some other chemical transformation.⁷² Chemical⁶⁸ and electrochemical⁶⁷ reductions of zinc tetraphenylporphyrin in nonaqueous solutions produced the anion radical, which showed absorption maxima at 455 and 710 nm. Experiments with pulse radiolysis established that anion radicals of several zinc porphyrins show broad absorption maxima around 700-730 nm.⁷³⁻⁷⁵ Photochemical studies of various zinc porphyrins also showed that the corresponding anion radicals absorb light at 700 nm.⁷⁰ For all of these reasons, we expected also the zinc cytochrome *c* anion radical, designated Zncyt⁻, to show marked absorbance at around 700 nm.

Requirements for Reductive Quenching. Because the relevant potential in Scheme 1 is 0.4 V, the *reduction* potential of the couple Q⁻/Q must be lower (i.e., less positive or more negative) than 0.4 V, so that the reaction in eq 2 be spontaneous. Since the anion radical Zncyt⁻ is a strong reductant – the relevant potential in Scheme 1 is 1.3 V – the back reaction in eq 3 must be contended with. The condition for its suppression, that the reductant Q have the reduction potential lower (more negative) than -1.3 V, cannot be met in aqueous



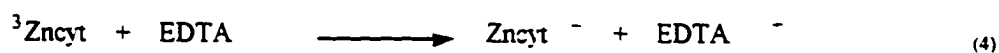
solution. Because the undesirable reaction in eq 3 has a large thermodynamic driving force and is likely to be fast, the anion radical Zncyt⁻ can be detected only as a transient intermediate, if at all.

In addition to the thermodynamic requirements outlined above, there must also exist kinetic requirements for the occurrence and detection of reductive quenching in eq 2. We learned about these requirements in a series of unsuccessful attempts at reductive quenching of $^3\text{Zncyt}$. These experiments are worth mentioning, briefly. The parenthetical values that follow are reduction potential at pH 7.0 for the redox couples the reductant member of which is given.⁷⁶

Glutathione (-0.23 V) and NADPH (-0.32 V) failed at the concentration of 1.0 mM, presumably because their redox reactions involve transfer of atoms as well as electrons; the rate constant for reductive quenching by both reagents is less than $1 \times 10^5 \text{ M}^{-1} \text{ s}^{-1}$. The iron(II) complex $[\text{Fe}(\text{CDTA})]$ (0.090 V)⁶¹ and the methylviologen monocation radical (-0.40 V), used at the concentration of 10 mM, proved unstable. Even though we observed quenching of $^3\text{Zncyt}$ in experiments with these two reagents, we could not be sure that it was due entirely to the reduction, as in eq 2. Even partial autooxidation of these reagents is intolerable, because their oxidized forms could effect the reaction in eq 3. Ferromyoglobin (0.047 V) at the concentration of 50 mM failed to quench, presumably because it is an oxygen carrier and intrinsically a poor redox agent;¹⁶ the rate constant is less than $2 \times 10^6 \text{ M}^{-1} \text{ s}^{-1}$. The positively-charged complex $[\text{Ru}(\text{NH}_3)_6]^{2+}$ (0.060 V) failed at the concentration of 20 mM, presumably because it and Zncyt repel each other at the low ionic strength (40 mM) used in these experiments; the rate constant is less than $5 \times 10^6 \text{ M}^{-1} \text{ s}^{-1}$. When $[\text{Ru}(\text{NH}_3)_6]^{2+}$ concentration was 20 mM to 1.0 mM $^3\text{Zncyt}$ was quenched, but the cation Zncyt^+ was observed as well. This oxidative quenching (eq 1) may be due to the impurity $[\text{Ru}(\text{NH}_3)_6]^{3+}$, which remained after the recrystallization of $[\text{Ru}(\text{NH}_3)_6]\text{Cl}_2$ from water. Horse-heart

ferrocytochrome *c* (0.25 V) failed at the concentration of 50 mM, probably because both it and its zinc derivative bear the net charge of +6 at pH 7.0; indeed, the electron self-exchange reaction of the native (iron) protein is relatively slow.⁷ The rate constant for reductive quenching is less than $2 \times 10^6 \text{ M}^{-1} \text{ s}^{-1}$. The absence of oxidative quenching by ferrocytochrome *c* was confirmed in this laboratory.⁷⁷ The upper limits mentioned above are conservative, and therefore probably high, estimates. These failed attempts were nevertheless useful, for they taught us how to choose effective reductive quenchers, so that quenching can occur during the lifetime of $^3\text{Zncyt}$, which is 10 ms.

Reductive Quenching of $^3\text{Zncyt}$ by EDTA. Reductive quenching of zinc porphyrins by EDTA, as in eq 2, is known;⁷⁸⁻⁸¹ the rate constant for a particular zinc porphyrin is $1.7 \times 10^5 \text{ M}^{-1} \text{ s}^{-1}$ at pH 5.0 and ionic strength of 50 mM. Our experiments with zinc cytochrome *c* gave positive results. The lifetime of the triplet state, $^3\text{Zncyt}$, is shortened in the presence of EDTA; one of many such experiments is shown in Fig 1. The observed rate constant, however, was only $200 \pm 20 \text{ s}^{-1}$ when the concentration of EDTA (added as its disodium salt) was 10 mM. At lower concentrations of EDTA the quenching was noncompeti-tive with natural decay, whereas higher concentrations perturbed the pH value and ionic strength of the reaction mixture. After the observed rate constant is corrected for the natural decay ($100 \pm 10 \text{ s}^{-1}$), the bimolecular rate constant for the reaction in eq 4 can be estimated at $100 \text{ s}^{-1}/0.010 \text{ M} = 1 \times 10^4 \text{ M}^{-1} \text{ s}^{-1}$. This is a reasonable value. Zinc heme inside cytochrome *c* is approximately ten times less reactive than free zinc porphyrin, mentioned



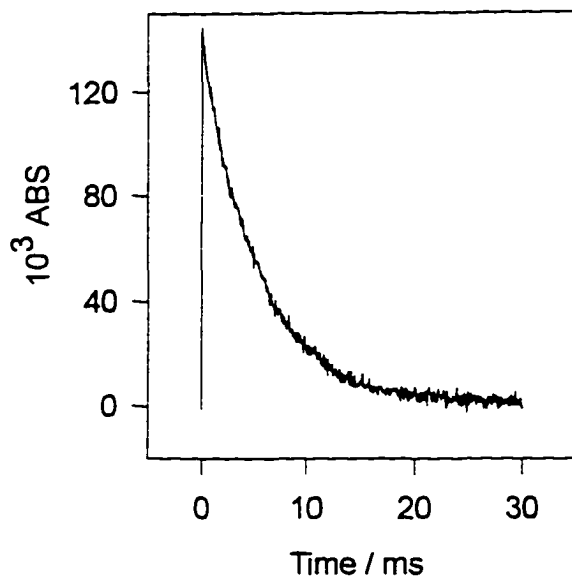


Figure 1. Reductive quenching by EDTA anion of the triplet state of zinc cytochrome *c*, designated as $^3\text{Zn}(\text{cyt})$, monitored at 460 nm. The solution was made 10 μM in zinc cytochrome *c* and 10 mM in Na_2EDTA , and the solvent was a sodium phosphate buffer at pH 6.5 and ionic strength of 5.0 mM. The relative concentrations of the ions HEDTA^{3-} and $\text{H}_2\text{EDTA}^{2-}$ were 7:1.

above. The considerable reactivity of zinc heme in the protein may be due to its partial exposure on the protein surface.³⁸

Rapid decomposition of the cation radical $\text{EDTA}^{\cdot+}$ suppresses the reaction in eq 5, and the anion radical $\text{Zncyt}^{\cdot-}$ is expected to be detectable. Although thermal oxidation according to eq 5 is not the only reaction that consumes this anion radical, its detection was worth attempting.



Indeed, monitoring at 690 nm, a wavelength at which $\text{Zncyt}^{\cdot-}$ is expected to absorb, consistently showed a transient species with a correct time profile; for a typical experiment, see Figure 2. Despite repeated attempts we could not record a complete absorption spectrum of the transient anion radical. At wavelengths less than 600 nm all three species— Zncyt , ${}^3\text{Zncyl}$, and $\text{Zncyt}^{\cdot-}$ —have very strong and overlapping absorption bands.

The evidence for reductive quenching so far is positive, but not compelling. We have to rule out nonredox modes of quenching and chemical degradation of zinc cytochrome *c*. Incubation of 10 mM zinc cytochrome *c* and 10 mM EDTA for 24 h did not affect the UV-visible spectrum of the protein. Clearly, even EDTA present in large excess over the protein cannot remove the zinc(II) ions from the heme or otherwise degrade the active site. At pH 6.5, the dominant forms of the quencher are the trianion, HEDTA^{3-} , and the dianion, $\text{H}_2\text{EDTA}^{2-}$; their relative concentrations are approximately 7:1. Concentration of carboxylate anions in a 50 mM solution of sodium acetate is approximately two times higher than their concentration in a 10 mM solution of EDTA, both at pH 6.5. That addition of 50 mM sodium acetate to the buffered 10 mM solution of zinc cytochrome *c* does not affect the

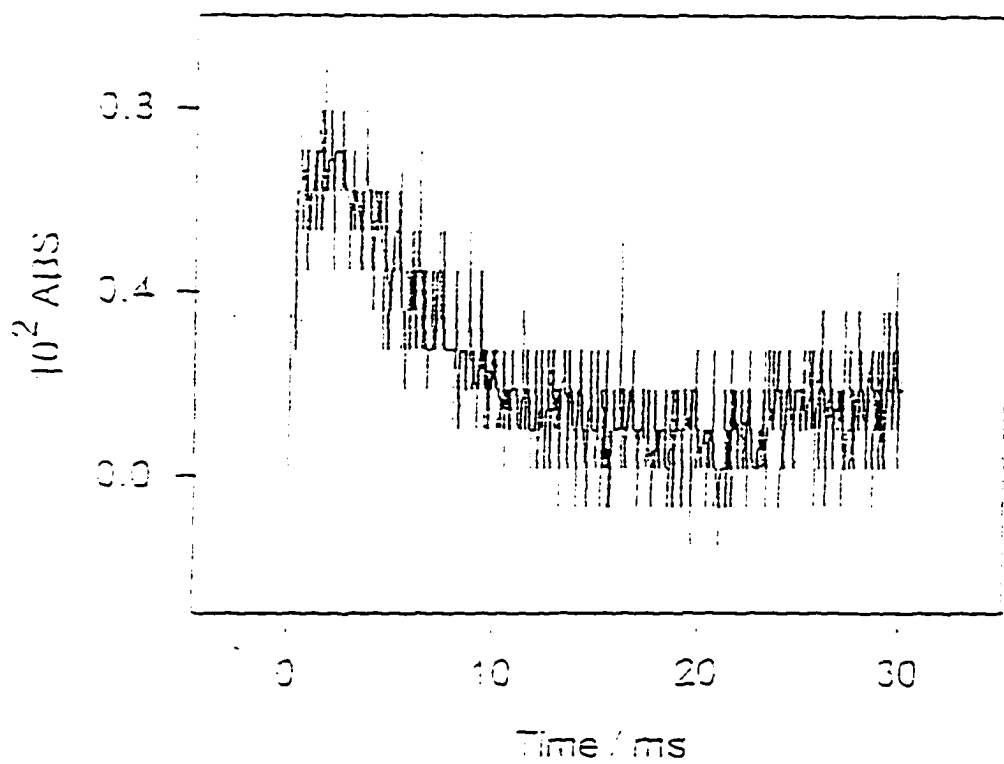


Figure 2. Transient absorption of zinc cytochrome c anion radical, monitored at 690 nm.

The conditions are the same as Figure 1.

lifetime of the triplet state proves that quenching is not caused by mere binding of EDTA anions to the positively-charged surface of Zncyt. Identity of cytochrome *c* conformation in the crystal containing a very high concentration of salt⁸² and in solution of low ionic strength,⁸³ as determined by X-ray diffraction and by NMR spectroscopy, proves that bound counterions are unlikely to cause significant structural changes that would affect the lifetime of the triplet state.

Trimethanolamine and trimethylamine, commonly used as so-called sacrificial reductants in photoinduced electron-transfer reactions, did not affect the lifetime of ³Zncyt. The former quenches the triplet state of a zinc porphyrin with a rate constant of $4.0 \times 10^3 \text{ M}^{-1} \text{ s}^{-1}$,⁷⁰ and probably so does the latter; the exact value is not available. Because of the shielding by the protein, the corresponding rate constant for zinc cytochrome *c* must be even lower than that for the free zinc porphyrin. For any quenching to compete with natural decay (100 s^{-1}) of ³Zncyt at the 1.0 mM concentration, the quenching rate constant must be greater than $1 \times 10^4 \text{ M}^{-1} \text{ s}^{-1}$. These two amines actually exist in solution as ammonium cations, with electroneutral substituents. They electrostatically repel zinc cytochrome *c* and cannot quench the triplet state before it decays naturally. These findings show that the negative charge of the EDTA anions is essential for quenching.

Photochemical and pulse-radiolytic studies of various zinc porphyrins found the anion radical to be unstable in aqueous solution.^{69,72} Dimerization, disproportionation, and protonation ultimately yield stable zinc dihydro-porphyrins.⁸⁴ In our experiments, 500 successive laser pulses did not produce any detectable changes in the UV-visible spectrum of zinc cytochrome *c*. The anion radical Zncyt⁻ seems to be formed, but it is prevented by the

protein envelope from dimerizing and ultimately yielding the hdroporphyrin species. We have no evidence for the reaction(s) consuming the small amount of Zncyt^- that is transiently formed.

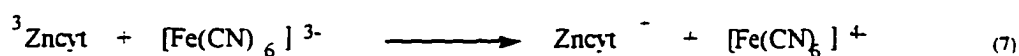
Reductive Quenching of $^3\text{Zncyt}$ by the $[\text{Fe}(\text{CN})_6]^+$ Ion. The experiments with EDTA described above indicated that negatively-charged quenchers are the correct choice for zinc cytochrome *c*, which has a positively-charged surface patch and bears a net positive charge. The $[\text{Fe}(\text{CN})_6]^+$ ion fits this requirement and is thermodynamically capable of reducing $^3\text{Zncyt}$ – the reduction potential of the $[\text{Fe}(\text{CN})_6]^{3-}/[\text{Fe}(\text{CN})_6]^+$ couple is 0.35 V. Indeed, we found fast quenching. The slope of the plot in Figure 3 is $(1.5 \pm 0.3) \times 10^8 \text{ M}^{-1} \text{ s}^{-1}$. It remained to be determined whether this rate constant corresponds to the reaction in eq 6. Before it, we considered three other conceivable mechanisms of quenching of $^3\text{Zncyt}$ in the presence of the $[\text{Fe}(\text{CN})_6]^+$ ion.



First, the ion $[\text{Fe}(\text{CN})_6]^+$ is known to bind electrostatically to the surface of cytochrome *c*.⁸⁵ Although there is no evidence that this binding perturbs the protein conformation, we considered the possibility that it may enhance radiationless decay of the triplet state $^3\text{Zncyt}$. We used the redox-inactive ion $[\text{Co}(\text{CN})_6]^{3-}$, which otherwise resembles the $[\text{Fe}(\text{CN})_6]^+$ ion in interactions with cytochrome *c*.⁸⁵ The triplet state $^3\text{Zncyt}$ decayed with the same rate constant, $100 \pm 10 \text{ s}^{-1}$, in the presence and in the absence of the $[\text{Co}(\text{CN})_6]^{3-}$ ion. Evidently, quenching in Figure 3 is not due to electrostatic association of the protein and the $[\text{Fe}(\text{CN})_6]^+$ ion.

Second, energy transfer requires overlap between the emission spectrum of $^3\text{Zncyt}$ (maxima at 590 and 640 nm)³⁶ and the absorption spectrum of the $[\text{Fe}(\text{CN})_6]^{3-}$ ion (the maximum at 330 nm). Because there is no significant overlap, energy transfer can be ruled out as a cause of fast quenching.

Third, the $[\text{Fe}(\text{CN})_6]^{3-}$ ion is an efficient oxidative quencher of $^3\text{Zncyt}$, as in eq 7. Without attempting a detailed study of this reaction, we examined it under conditions under which it would occur if $\text{K}_4[\text{Fe}(\text{CN})_6]$ were contaminated with $\text{K}_3[\text{Fe}(\text{CN})_6]$.



Since under these conditions the $[\text{Fe}(\text{CN})_6]^{3-}$ ion would not be present in excess over $^3\text{Zncyt}$, we investigated the reaction in eq 7 under approximately equimolar, not the pseudo-first-order, conditions. The rate constant of $(5 \pm 3) \times 10^9 \text{ M}^{-1} \text{ s}^{-1}$ is an approximate one, but it is adequate for the purpose of these control experiments. For the quenching at $(1.5 \pm 0.3) \times 10^8 \text{ M}^{-1} \text{ s}^{-1}$, shown in Figure 3, to be caused by the $[\text{Fe}(\text{CN})_6]^{3-}$ ion, this impurity would have to constitute approximately 3% or more of the reagent-grade $\text{K}_4[\text{Fe}(\text{CN})_6]$, at concentrations of this salt shown in Figure 3. Although improbable, this possibility had to be considered.

The assay for the $[\text{Fe}(\text{CN})_6]^{3-}$ ion was negative. Control experiments showed this analytical method to be sensitive to the $[\text{Fe}(\text{CN})_6]^{3-}$ concentration that is 0.10% of the $\text{K}_4[\text{Fe}(\text{CN})_6]$ concentration used in the assay. Quenching of $^3\text{Zncyt}$ with recrystallized $\text{K}_4[\text{Fe}(\text{CN})_6]$ occurs with the rate constant identical, within the error bounds, to the one reported above.

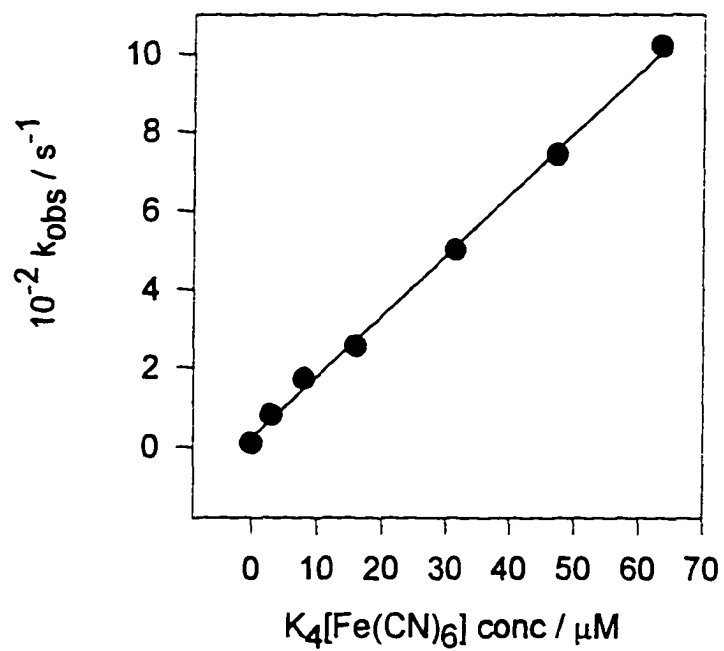


Figure 3. Reductive quenching by the $[Fe(CN)_6]^{4-}$ ion of the triplet state of zinc cytochrome c, designated 3Zn(cyt), in a sodium phosphate buffer at pH 7.0 and ionic strength of 40 mM.

We cautiously conclude that the results in Figure 3 are attributable to reductive quenching, represented by eq 6. This "forward" reaction has a thermodynamic driving force of only ca. 0.1 eV, and the subsequent thermal back-reaction in eq 8 has a driving force of ca. 0.9 eV. This simple consideration suggests that the back reaction is faster than the forward reaction, and that the intermediate Zncyt^- cannot accumulate. The concentration



of this reactive anion radical remains undetectably low, and it could not be observed in transient-absorption experiments at wavelength around 700 nm. Such detection apparently succeeded – see Figure 2 – in reductive quenching of $^3\text{Zncyt}$ with EDTA, when the back reaction was suppressed.

Conclusions

Photoinduced electron-transfer reactions of simple zinc porphyrins proved to be intricate, and ion radicals involved in them were detected with difficulty. In zinc cytochrome *c* the protein envelope modulates the reactivity of the heme group, but the anion radical may be involved, and its detection should be possible when the relative rates of its appearance and disappearance are favorable. In view of the wide and growing use of zinc-substituted heme proteins in kinetic, mechanistic, and spectroscopic studies, their electron-transfer reactions should be studied thoroughly.

Acknowledgment. This work was supported by the NSF under Grant MCB-9222741 and by an A. P. Sloan Research Fellowship to N. M. K.

References

- (1). Hoffman, B. M.; Natan, M. J.; Nocek, J. M.; Wallin, S. A. *Struct. Bonding* **1991**, *75*, 86.
- (2). McLendon, G.; Hake, R. *Chem. Rev.* **1992**, *92*, 481.
- (3). Winkler, J. R.; Gray, H. B. *Chem. Rev.* **1992**, *92*, 369.
- (4). Mauk, A. G. *Struct. Bonding* **1991**, *75*, 131.
- (5). Kostić, N. M. *Metal Ions Biol. Syst.* **1991**, *27*, 129.
- (6). Willie, A.; McLean, M.; Liu, R.-Q.; Hilgen-Willis, S.; Saunders, A. J.; Pielak, G. J.; Sligar, S. G.; Durham, B.; Millett, F. *Biochemistry* **1993**, *32*, 7519.
- (7). Moore, G. R.; Pettigrew, G. W. *Cytochromes c: Evolutionary, Structural and Physicochemical Aspects*; Springer-Verlag: Berlin, 1990.
- (8). Chien, J. C. W. *J. Am. Chem. Soc.* **1978**, *100*, 1310.
- (9). Papp, S.; Vanderkooi, J. M.; Owen, C. S.; Holtom, G. R.; Phillips, C. M. *Biophys. J.* **1990**, *58*, 177.
- (10). Kaposi, A. D.; Vanderkooi, J. M. *Proc. Natl. Acad. Sci. U.S.A.* **1992**, *89*, 11371.
- (11). Kaposi, A. D.; Fidy, J.; Stavrov, S. S.; Vanderkooi, J. M. *J. Phys. Chem.* **1993**, *97*, 6319.
- (12). Karas, J. L.; Lieber, C. M.; Gray, H. B. *J. Am. Chem. Soc.* **1988**, *110*, 599.
- (13). Axup, A. W.; Albin, M.; Mayo, S. L.; Crutchley, R. J.; Gray, H. B. *J. Am. Chem. Soc.* **1988**, *110*, 435.
- (14). Cowan, J. A.; Gray, H. B. *Inorg. Chem.* **1989**, *28*, 2074.

- (15). Casimiro, D. R.; Wong, L.-L.; Colon, J. L.; Zewert, T. E.; Richards, J. H.; Chang, I.-J.; Winkler, J. R.; Gray, H. B. *J. Am. Chem. Soc.* **1993**, *115*, 1485.
- (16). Cheng, J.; Zhou, J. S.; Kostić, N. M. *Inorg. Chem.* **1994**, *33*, 1600.
- (17). Leonard, J. J.; Yonetani, T.; Callis, J. B. *Biochemistry* **1974**, *13*, 1460.
- (18). Peterson-Kennedy, S. E.; McGourty, J. L.; Hoffman, B. M. *J. Am. Chem. Soc.* **1984**, *106*, 5010.
- (19). Peterson-Kennedy, S. E.; McGourty, J. L.; Kalweit, J. A.; Hoffman, B. M. *J. Am. Chem. Soc.* **1986**, *108*, 1739.
- (20). McGourty, J. L.; Peterson-Kennedy, S. E.; Ruo, W. Y.; Hoffman, B. M. *Biochemistry* **1987**, *26*, 8302.
- (21). Natan, M. J.; Hoffman, B. M. *J. Am. Chem. Soc.* **1989**, *111*, 6468.
- (22). Gingrich, D. J.; Nocek, J. M.; Natan, M. J.; Hoffman, B. M. *J. Am. Chem. Soc.* **1987**, *109*, 7533.
- (23). Simolo, K. P.; McLendon, G. L.; Mauk, M. R.; Mauk, A. G. *J. Am. Chem. Soc.* **1984**, *106*, 5012.
- (24). Magner, E.; McLendon, G. *Biochem. Biophys. Res. Commun.* **1989**, *159*, 472.
- (25). Chien, J. C. W. *J. Phys. Chem.* **1978**, *82*, 2171.
- (26). Erecinska, M.; Vanderkooi, J. M. *Meth. Enzymol.* **1978**, *53*, 165.
- (27). Findlay, M. C.; Chien, J. C. W. *Eur. J. Biochem.* **1977**, *76*, 79.
- (28). Findlay, M. C.; Dickinson, L. C.; Chien, J. C. W. *J. Am. Chem. Soc.* **1977**, *99*, 5168.
- (29). Dickinson, L. C.; Chien, J. C. W. *Biochemistry* **1975**, *14*, 3526.
- (30). Dickinson, L. C.; Chien, J. C. W. *Biochem. Biophys. Res. Commun.* **1974**, *58*, 236.

- (31). Chien, J. C. W.; Dickinson, L. C.; Mason, T. L. *Biochem. Biophys. Res. Commun.* **1975**, *63*, 853.
- (32). Dickinson, L. C.; Chien, J. C. W. *Inorg. Chem.* **1976**, *15*, 1111.
- (33). Dickinson, L. C.; Gibson, H. L.; Chien, J. C. W. *Eur. J. Biochem.* **1978**, *88*, 239.
- (34). Chien, J. C. W.; Dickinson, L. C. *J. Biol. Chem.* **1978**, *253*, 6965.
- (35). Dickinson, L. C.; Chien, J. C. W. *J. Biol. Chem.* **1977**, *252*, 6156.
- (36). Vanderkooi, J. M.; Adar, F.; Erecinska, M. *Eur. J. Biochem.* **1976**, *64*, 381.
- (37). Angiolillo, P. J.; Vanderkooi, J. M. *Biophys. J.* **1995**, *68*, 2505.
- (38). Anni, H.; Vanderkooi, J. M.; Mayne, L. *Biochemistry* **1995**, *34*, 5744.
- (39). Magner, E.; McLendon, G. *J. Phys. Chem.* **1989**, *93*, 7130.
- (40). Moore, G.; Williams, R. J. P.; Chien, J. C. W.; Dickinson, L. C. *J. Inorg. Biochem.* **1980**, *13*, 1.
- (41). Vanderkooi, J. M.; Landesberg, R.; Haydon, G.; Owen, C. *Eur. J. Biochem.* **1977**, *81*, 339.
- (42). Vanderkooi, J. M.; Glatz, P.; Casadei, J.; Woodrow, G. V., III *Eur. J. Biochem.* **1980**, *110*, 189.
- (43). Koloczek, H.; Horie, T.; Yonetani, T.; Anni, H.; Maniara, G.; Vanderkooi, J. M. *Biochemistry* **1987**, *26*, 3142.
- (44). Conklin, K. T.; McLendon, G. *J. Am. Chem. Soc.* **1988**, *110*, 3345.
- (45). Conklin, K. T.; McLendon, G. *Inorg. Chem.* **1986**, *25*, 4804.
- (46). Zhou, J. S.; Hoffman, B. M. *Science* **1994**, *265*, 1693.
- (47). Zhou, J. S.; Nocek, J. M.; DeVan, M. L.; Hoffman, B. M. *Science* **1995**, *269*, 204.

- (48). Zhou, J. S.; Kostić, N. M. *J. Am. Chem. Soc.* **1991**, *113*, 6067.
- (49). Zhou, J. S.; Kostić, N. M. *J. Am. Chem. Soc.* **1991**, *113*, 7040.
- (50). Zhou, J. S.; Kostić, N. M. *J. Am. Chem. Soc.* **1992**, *114*, 3562.
- (51). Zhou, J. S.; Kostić, N. M. *Spectrum* **1992**, *5(2)*, 1.
- (52). Zhou, J. S.; Kostić, N. M. *Biochemistry* **1992**, *31*, 7543.
- (53). Zhou, J. S.; Kostić, N. M. *Biochemistry* **1993**, *32*, 4539.
- (54). Zhou, J. S.; Kostić, N. M. *J. Am. Chem. Soc.* **1993**, *115*, 10796.
- (55). Qin, L.; Kostić, N. M. *Biochemistry* **1994**, *33*, 12592.
- (56). Elias, H.; Chou, M. H.; Winkler, J. R. *J. Am. Chem. Soc.* **1988**, *110*, 429.
- (57). Vos, K.; Lavalette, D.; Visser, A. J. W. G. *Eur. J. Biochem.* **1987**, *169*, 269.
- (58). Dixit, S. N.; Waring, A. J.; Vanderkooi, J. M. *FEBS Lett.* **1981**, *125*, 86.
- (59). Horie, T.; Maniara, G.; Vanderkooi, J. M. *FEBS Lett.* **1985**, *177*, 287.
- (60). Dixit, B. P. S.N.; Moy, V. T.; Vanderkooi, J. M. *Biochemistry* **1984**, *23*, 2103.
- (61). Cassatt, J. C.; Marini, C. P.; Bender, J. W. *Biochemistry* **1975**, *14*, 5470.
- (62). Bigelow, J. H. *Inorg. Synth.* **1946**, *2*, 225.
- (63). Szentrimay, R.; Yeh, P.; Kuwana, T. In *Electrochemical Studies of Biological Systems*; Sawyer, D. T., Ed.; ACS Symposium Series 38; American Chemical Society: Washgton, DC, 1977; p 143.
- (64). Vogel, A. I. *Vogel's Textbook of Quantitative Chemical Analysis*; 5th ed.; Longman: London, 1989; sec. 10.124.
- (65). Hodge, J. A.; Hill, M. G.; Gray, H. B. *Inorg. Chem.* **1995**, *34*, 809.
- (66). Richoux, M.-C.; Abou-Gamra, Z. M. *Inorg. Chim. Acta* **1986**, *118*, 115.

- (67). Lanese, J. G.; Wilson, G. S. *J. Electrochem. Soc.* **1972**, *119*, 1039.
- (68). Closs, G. L.; Closs, L. E. *J. Am. Chem. Soc.* **1963**, *85*, 818.
- (69). Seely, G. R.; Calvin, M. *J. Chem. Phys.* **1955**, *23*, 1068.
- (70). Hurst, J. K.; Lee, L. Y. C.; Grätzel, M. *J. Am. Chem. Soc.* **1983**, *105*, 7048.
- (71). Le Roux, D.; Mialocq, J.-C.; Anitoff, O.; Folcher, G. *J. Chem. Soc., Faraday Trans. 2* **1984**, *80*, 909.
- (72). Seely, G. R.; Talmadge, K. *Photochem. Photobiol.* **1964**, *3*, 195.
- (73). Neta, P.; Scherz, A.; Levanon, H. *J. Am. Chem. Soc.* **1979**, *101*, 3624.
- (74). Neta, P. *J. Phys. Chem.* **1981**, *85*, 3678.
- (75). Levanon, H.; Neta, P. *J. Phys. Chem.* **1982**, *86*, 4532.
- (76). *CRC Handbook of Biochemistry*, 2nd ed.; Chemical Rubber Co.: Cleveland, 1970; p. J33.
- (77). Qin, L.; Kostić, N. M. submitted to *Biochemistry*.
- (78). Kalyanasundaram, K.; Grätzel, M. *Helv. Chim. Acta* **1980**, *63*, 478.
- (79). Harriman, A.; Porter, G.; Richoux, M.-C. *J. Chem. Soc., Faraday Trans. 2* **1981**, *77*, 833.
- (80). Harriman, A.; Richoux, M.-C. *J. Photochem.* **1981**, *15*, 335.
- (81). Handman, J.; Harriman, A.; Porter, G. *Nature* **1984**, *307*, 534.
- (82). Bushnell, G. W.; Louie, G. V.; Brayer, G. D. *J. Mol. Biol.* **1990**, *214*, 585.
- (83). Qi, P. X.; Di Stefano, D. L.; Wand, A. J. *Biochemistry* **1994**, *33*, 6408.
- (84). Harel, Y.; Meyerstein, D. *J. Am. Chem. Soc.* **1974**, *96*, 2720.
- (85). Moore, G. R.; Eley, C. G. S.; Williams, G. *Adv. Inorg. Bioinorg. Mech.* **1984**, *3*, 1.

CHAPTER 4**EFFECTS OF MUTATIONS IN PLASTOCYANIN ON THE KINETICS OF THE PROTEIN REARRANGEMENT GATING THE ELECTRON-TRANSFER REACTION WITH ZINC CYTOCHROME C. ANALYSIS OF THE REARRANGEMENT PATHWAY**

Chengyu Shen and Nenad Kostić

Abstract

We study, by flash kinetic spectrophotometry on the microsecond time scale, the effects of viscosity on the kinetics of oxidative quenching of the triplet state of zinc cytochrome *c*, $^3\text{Zncyt}$, by the wild-type form and the following nine mutants of cupriplastocyanin: Leu12Glu, Leu12Asn, Phe35Tyr, Gln88Glu, Tyr83Phe, Tyr83His, Asp42Asn, Glu43Asn, and the double mutant Glu59Lys/Glu60Gln. The unimolecular rate constants for the quenching reactions within the persistent diprotein complex, which predominates at low ionic strength, and within the transient diprotein complex, which is involved at higher ionic strength, are equal irrespective of the mutation. Evidently, the two complexes are the same. In both reactions the rate-limiting step is rearrangement of the diprotein complex from a configuration optimal for

docking to the one optimal for the subsequent electron-transfer step, which is fast. We investigate the effects of plastocyanin mutations on this rearrangement, which gates the overall electron-transfer reaction. Conversion of the carboxylate anions into amide groups in the lower acidic cluster (residues nos. 42 and 43), replacement of Tyr 83 with other aromatic residues, and mutations in the hydrophobic patch in plastocyanin do not significantly affect the rearrangement. Conversion of a pair of carboxylate anions into a cationic and a neutral residue in the upper acidic cluster (residues nos. 59 and 60) impedes the rearrangement. Creation of an anion at the position no. 88, between the upper acidic cluster and the hydrophobic patch, facilitates the rearrangement. The rate constant for the rearrangement smoothly decreases as the solution viscosity increases, irrespective of the mutation. Fittings of this dependence to the modified Kramers's equation and to an empirical equation show that zinc cytochrome *c* follows the same trajectory on the surfaces of all the plastocyanin mutants, but that the obstacles along the way vary as mutations alter the electrostatic potential. All of the kinetic effects and noneffects of mutations consistently suggest that in the protein rearrangement the basic patch of zinc cytochrome *c* moves from a position between the two acidic clusters to a position at or near the upper acidic cluster.

Abbreviations: cyt, cytochrome *c*; cyt(III), ferricytochrome *c*; cyt(II), ferrocyclochrome *c*; pc, plastocyanin; pc(II), cupriplastocyanin; pc(I), cuproplastocyanin; Zncyt, zinc cytochrome *c*; ³Zncyt, triplet (excited) state of zinc cytochrome *c*; Zncyt^{•+}, cation radical of zinc cytochrome *c*; Znpc, zinc plastocyanin.

Introduction

Electron-transfer reactions of metalloproteins are involved in photosynthesis, respiration, and many other biological processes. Chemical research into molecular mechanisms of these important reactions is best done with well-characterized proteins and their pairs.¹⁻¹⁴ The heme protein cytochrome *c*^{15, 16} and the blue copper protein plastocyanin,¹⁷⁻²⁰ designated *cyt* and *pc*, are well suited to quantitative studies because their three-dimensional structures in both oxidized and reduced states and in both crystal and solution are precisely known.

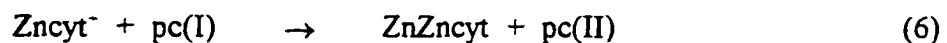
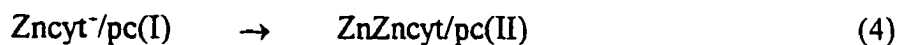
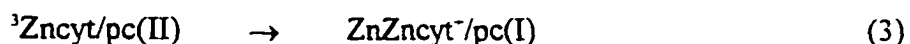
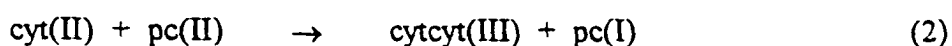
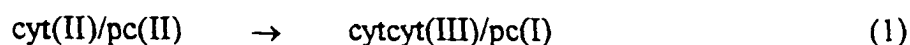
A pair of metalloproteins can associate in multiple configurations.^{9, 21-31} A configuration that optimizes binding need not optimize the subsequent electron-transfer reaction. The rate of this reaction within the complex may be controlled by the rate of some structural change; in this case the redox reaction is said to be gated.³²⁻³⁸ The phenomenon of gating is common with proteins and is found in various biochemical processes.

In the chemical equations below the slash mark represents protein association, i.e., the diprotein complex. The Roman numerals are the oxidation states of iron and copper. In zinc cytochrome *c* the oxidation state of zinc is always II, and an electron is given and accepted by the porphyrin ring.

Because zinc cytochrome *c* and the wild-type cupriplastocyanin bear respective net charges of +6 and -8 at pH 7.0, and because they contain oppositely-charged surface patches, these two proteins associate in solution at low ionic strength. Much evidence shows that in the complexes *cyt/pc* the basic (positive) patch around the exposed heme edge abuts the broad acidic (negative) patch in plastocyanin.^{26, 39-43}

Studies in our laboratories and by others of the unimolecular reaction in eq 1⁴⁴⁻⁴⁶ and of the bimolecular reaction in eq 2⁴⁷ showed that ferrocyanochrome *c* reduces cupriplastocyanin from the acidic patch, but not from the initial binding site within this large patch. Similar conclusions were reached in studies of reactions analogous to those in eqs 1 and 2, but involving ferrocyanochrome *f* instead of ferrocyanochrome *c*.⁴⁸⁻⁵⁰

Kinetic studies of thermal reactions, which involve the proteins in their ground electronic states, are relatively complicated. The reaction in eq 1 has to be initiated by external reduction of the complex *cyt(III)/pc(II)*, and the reaction in eq 2 involves both protein association and subsequent electron transfer. Replacement of iron(II) with zinc(II) in the heme does not significantly perturb the surface of cytochrome *c* and its interactions with other proteins.⁵¹⁻⁵³ Use of zinc cytochrome *c* in the studies of photoinduced reactions, those in eqs 3-6, obviates the need for external reducing agents and permits detailed studies of the most interesting step in



the reactions — electron transfer within the diprotein complex.^{41-43, 54-60} The reactions in eqs 3 and 5, in which the triplet state of the porphyrin is the electron donor, are termed forward reactions. Those in eqs 4 and 6, in which the cation radical of the porphyrin is the electron acceptor, are termed back reactions.

The thermal reactions in eqs 1 and 2 have the driving force of only ca. 0.10 eV and are true redox reactions; the rate-limiting step in them is electron transfer. Raising the driving force assists the electron transfer but does not affect the structural dynamics of the proteins. The photoinduced forward reactions in eqs 3 and 5 have the driving force of ca. 1.2 eV; in them the protein rearrangement is the rate-limiting step, the one actually observed in kinetic experiments. In conclusion, the reactions in eqs 3 and 5 are gated.

Kinetic studies^{41, 57, 58, 61} began to reveal the interplay between the structural rearrangement and the electron transfer. The gating process seems to be configurational fluctuation of the diprotein complex, during which the two proteins remain docked in the same general orientation but slide on each other's surface or wiggle with respect to each other. A theoretical analysis by an established method⁶² of electron-transfer paths between the heme and blue copper sites in various configurations of the cyt(II)/pc(II) complex confirmed the experimental findings by showing that the configuration that optimizes the surface interactions does not optimize the heme-copper electronic coupling.⁶³ Motions of the cytochrome *c* molecule, whose basic patch explores the area within or near the broad acidic patch in plastocyanin, enhance this electronic coupling. In this way configurational fluctuation improves the intrinsic electron-transfer reactivity. Analysis of enthalpy of activation (ΔH^\ddagger) for the reaction in eq 3 in terms of solvation effects⁶¹ answered some but not nearly all the questions concerning the

dynamic process of gating. All the previous studies of the reactions in eqs 3-6 have been done with wild-type plastocyanin. Now we report a systematic comparison of the wild-type form and nine mutants of spinach plastocyanin in the reaction in eq 3 at different viscosities. Analysis of kinetic results reveals a likely trajectory for the cytochrome *c* motion on the plastocyanin surface.

Materials and Methods

Chemicals. Distilled water was demineralized to a resistivity greater than $17 \text{ M } \Omega \cdot \text{cm}$. Chromatography resins and gels were purchased from Sigma Chemical Co. and Pharmacia. Nitrogen, HF, and ultrapure argon were purchased from Air Products Co. All other chemicals were purchased from Fisher Chemical Co.

Buffers. All buffers were made fresh from the solid salts $\text{NaH}_2\text{PO}_4 \cdot \text{H}_2\text{O}$ and $\text{Na}_2\text{HPO}_4 \cdot 7 \text{H}_2\text{O}$ and had ionic strength (μ) of 2.5 or 10 mM and pH of 7.00 ± 0.05 at 293 K. In all of these preparations we took into consideration dependence of the pK_a of H_2PO_4^- on ionic strength.

Temperature and Viscosity. Temperature was kept at $20.0 \pm 0.2 \text{ }^\circ\text{C}$ with a 30-L circulating bath Forma Scientific CH/P 2067. Viscosity was adjusted by adding glycerol to the buffered solution, up to the concentration of 80% w/w.

Zinc Cytochrome *c*. Horse-heart cytochrome *c* was purchased from Sigma Chemical Co. The iron-free (so-called free-base) form was made, purified, and reconstituted with zinc(II) by a modification⁵¹ of the original procedure.^{77, 78} The product, zinc cytochrome *c*, was handled at $4 \text{ }^\circ\text{C}$, in the dark. Two of the criteria of purity were the absorbance ratios $A_{423}/A_{549} > 15.4$ and $A_{549}/A_{585} < 2.0$. The absorptivity is $\epsilon_{423} = 2.43 \times 10^5 \text{ M}^{-1} \text{ cm}^{-1}$.⁷⁸

Plastocyanin. Recombinant wild-type protein from spinach and nine of its mutants were prepared by my lab mate, Mr. Milan M. Cmogorac. The properties of these proteins are listed in table 1. The amount of holo-plastocyanin was determined spectrophotometrically, under oxidizing conditions, on the basis of the absorptivity $\epsilon_{595} = 4900 \text{ M}^{-1}\text{cm}^{-1}$.⁶⁴

Only the fractions of the highest purity were used in this study. Despite the most careful handling, the mutants contained some apo and zinc forms, which could not be oxidized with $\text{K}_3[\text{Fe}(\text{CN})_6]$. Solutions in a 100 mM Tris buffer were made 100 and 150 μM in the mutants, 100 and 200 μM in CuSO_4 , and 150 mM in NaCl. Incubation overnight and repeated chromatography, as described above, temporarily lowered the absorbance quotient A_{280}/A_{595} from 1.8-2.0 to 1.5-1.6; the quotient increased later. Because traces of zinc(II) ions are present in reagent-grade chemicals, some zinc form of the mutants had to be tolerated. The properties of the mutants are given in Table 1.

Flash Kinetic Spectrophotometry. So-called laser flash photolysis at the resolution of one point per μs was done with a standard apparatus.⁵⁴⁻⁵⁷ The triplet state $^3\text{Zncyt}$ was created by 0.4- μs pulses of light from a Phase-R (now Luminex) DL1100 laser containing the dye Rhodamine 590. The concentration of zinc cytochrome *c* was always 10 μM . Appearance and disappearance of $^3\text{Zncyt}$ and Zncyt^- were monitored at 460 and 675 nm, respectively.

Concentration of the triplet state depended on the intensity of the laser pulse and was ca. 1.0 μM , much lower than the cupriplastocyanin concentration, which was normally 50 μM . Kinetic conditions for the pseudo-first order were thus achieved. The protein solutions, prepared with deaerated buffers, were thoroughly deaerated further in the stream of wet argon, without frothing, for 10 min after each addition of plastocyanin. At each set of conditions

multiple traces were recorded: The change of absorbance with time was analyzed with the software SigmaPlot v1.02, from Jandel Scientific, Inc.

Kinetic Effects of Viscosity. Because we are interested in the effects of solution viscosity on the unimolecular component of quenching, the reaction in eq 3, we did these experiments in the sodium phosphate buffer at the low ionic strength of 2.5 mM and with the high cupriplastocyanin concentration of 50 μM . The relative viscosity (η/η_0) of the buffered solution was adjusted with glycerol.⁶³ These experiments with the wild-type form and mutants of plastocyanin were done like the previous experiments with the wild-type form only.⁵⁷ Given $\eta_0 = 1.002$ cp for water at 25 °C and the fact that the buffered solutions were dilute, the relative viscosity is practically equal to the absolute viscosity (η).

Fittings of Data. Least-squares averaging, with SigmaPlot v1.02, of the results from separate fittings of kinetic traces obtained by successive flashes gave better results than fittings of averaged traces. The former method lessens the undue influence of so-called outliers on the average result. The correlation coefficient of the rate constant was greater than 0.990. The error margins for all results include two standard deviations and correspond to the confidence limit greater than 95%; they are rounded to one significant figure, for clarity.

Results

Natural Decay of the Triplet State, $^3\text{Zncyt}$. The rate constant for this monoexponential process is 100 ± 10 s⁻¹ regardless of ionic strength. When the buffer at the ionic strength of 2.5 mM is made 80% w/w in glycerol, the rate constant decreases to 75 ± 10 s⁻¹. When the

Table 1. Properties of Recombinant Plastocyanin

| pc(II) mutant | A_{280}/A_{695} ratio | | | % Znpc | amplitude of the 3rd phase |
|-----------------------|-------------------------|---------------------------------------|-------|--------|----------------------------------|
| | calculated | lowest obtained in purification | final | | |
| wild type | 1.1 | 1.08 | 1.34 | 15 | 19 |
| Leu 12 Gln | 1.1 | 1.15 | 3.22 | 58 | 64 |
| Leu 12 Asn | 1.1 | 1.13 | 1.90 | 32 | 41 |
| Phe 35 Tyr | 1.5 | 1.41 | 1.83 | 16 | 23 |
| Gln 88 Gln | 1.1 | 1.08 | 1.38 | 18 | 22 |
| Glu 59 Lys/Gln 60 Gln | 1.1 | 1.15 | 1.39 | 14 | 17 |
| Tyr 83 Phe | 0.8 | 0.78 | 1.06 | 21 | 26 |
| Tyr 83 His | 0.8 | 0.77 | 2.16 | 53 | 64 |
| Asp 42 Asn | 1.1 | 1.08 | 1.38 | 14 | 22 |
| Glu 43 Gln | 1.1 | 1.08 | 1.38 | 17 | 22 |

rate constant ceased to decrease during the passing of argon, the sample solution was considered deaerated.

Quenching of $^3\text{Zncyt}$ by Cupriplastocyanin. The mechanism for the electron transfer is shown in Scheme 1. The subscripts in the symbols for the intracomplex rate constants k_f (for the unimolecular reaction) and k_r (for the bimolecular reaction) are reminders that both of these are so-called forward reactions, which are defined above. The two subscripts are not identical because the persistent complex, which exists at low ionic strength, and the transient complex, which is involved at higher ionic strength, are not necessarily identical. We retain these symbols from our previous publications, for the sake of consistency.

At the ionic strength of 100 mM the overall quenching is monoexponential, i.e., the reaction is purely bimolecular.⁵⁴ At the intermediate, but already low, ionic strength of 10 mM the quenching by Asp42Asn and by the double mutant Glu59Lys/Glu60Gln remains monoexponential. Quenching by the wild-type form and by seven of the mutants is biexponential. The only component of quenching by the former two mutants, and the slower component in the case of the wild-type form and the seven other mutants, corresponds to the bimolecular reaction in Scheme 1. The faster component, which is evident with the latter eight but not with the former two quenchers, corresponds to the unimolecular reaction in Scheme 1. Relative amplitude of the bimolecular component decreases, while that of the unimolecular component increases from 0 to ca. 70%, as the cupriplastocyanin concentration is raised to 50 μM .

We succeeded in observing directly the unimolecular component of the quenching (k_f) by all the mutants when we lowered the ionic strength to 2.5 mM. The overall quenching is

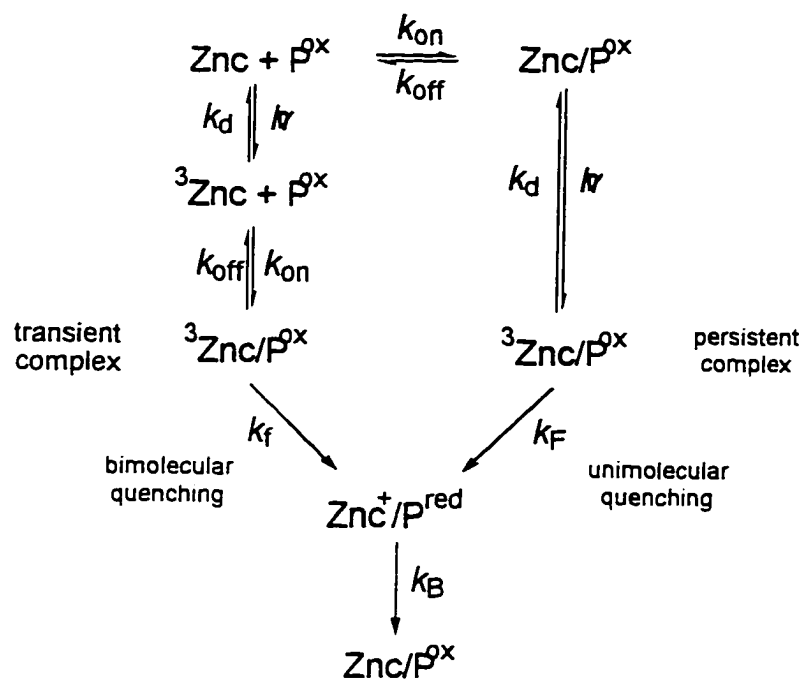
practically biexponential for the wild-type form and the following six mutants: Phe35Tyr, Gln88Glu, Asp42Asn, Glu43Asn, Tyr83Phe, and the double mutant Glu59Lys/Glu60Gln. The quenching is clearly triexponential for the following three mutants: Leu12Glu, Leu12Asn, and Tyr83His. The third phase was accepted or rejected on the basis of the standard deviation and the statistical null hypothesis with a confidence level of 95%. The relative amplitudes varied, but the unimolecular component dominated the overall quenching when the quencher concentration was 40 μM .

The Slowest Component of Quenching and the Magnitude of Transient

Absorbance. The slowest component, the third phase, was prominent for the mutants Leu12Glu, Leu12Asn, and Tyr83His, at the ionic strength of 2.5 mM. When this component was observed, its rate constant was more than 3000 times higher than that for the natural decay and ca. ten times lower than that for the bimolecular component. This component resembles the bimolecular component of quenching. Its amplitude (contribution to the total transient absorbance) is negligible at the lowest concentrations of cupriplastocyanin but becomes a major (ca. 40%) or even dominant (ca. 60%, in the case of Leu12Glu) fraction of the total amplitude at the higher concentrations of cupriplastocyanin.

Kinetic experiments at the ionic strength of 2.5 mM gave identical results when performed in cuvettes made of quartz and of polystyrene. Evidently, the third phase of quenching is not due to adsorption of proteins to the quartz surface.

Scheme 1.



$$k_{\text{obs}} = \frac{k_{\text{on}} k_f [\text{P}^{\text{ox}}]}{k_{\text{off}} + k_f + k_{\text{on}} [\text{P}^{\text{ox}}]}$$

$$K_a = \frac{k_{\text{on}}}{k_{\text{off}}}$$

Table 2. Kinetics of protein rearrangement of the diprotein complex $^3\text{Zncyt/pc(II)}$ from the docking configuration into the electron-transfer configuration.

| location | mutant | local charge ^a | | $10^{-5} k_F$, s^{-1} |
|-----------------------------|------------------------|---------------------------|--------|-----------------------------|
| | | Wt | mutant | |
| | Wild Type | | | 2.1 ± 0.1 |
| <i>hydrophobic patch</i> | Leu 12 Glu | 0 | 1- | 1.6 ± 0.2 |
| | Leu 12 Asn | 0 | 0 | 2.4 ± 0.5 |
| | Phe 35 Tyr | 0 | 0 | 2.0 ± 0.2 |
| <i>between the patches</i> | Gln 88 Glu | 0 | 1- | 3.1 ± 0.3 |
| <i>upper acidic cluster</i> | Glu 59 Lys, Glu 60 Gln | 2- | 1+ | 0.16 ± 0.02 |
| <i>between the clusters</i> | Tyr 83 Phe | 0 | 0 | 2.0 ± 0.2 |
| | Tyr 83 His | 0 | 0/1+ | 1.6 ± 0.4 |
| <i>lower acidic cluster</i> | Asp 42 Asn | 1- | 0 | 2.4 ± 0.2 |
| | Glu 43 Asn | 1- | 0 | 2.2 ± 0.3 |

We estimated the concentration of zinc plastocyanin in the samples of the mutants. We set $\epsilon_{597} = 4,900 \text{ M}^{-1}\text{cm}^{-1}$ for all the mutants⁶⁴⁻⁶⁶ and calculated the expected absorbance at 280 nm for those mutants that differ from the wild-type protein in aromatic residues.⁶⁷ The calculated absorbance quotients A_{597}/A_{280} for each mutant agreed nicely with the lowest value recorded during the purification. The amount of zinc plastocyanin correlates well with the amplitude of the third phase. See Table 1.

In most experiments the magnitude of the signal (the transient absorbance of $^3\text{Zncyt}$ at 460 nm) was in the range 0.080-0.14. Given the noise level of ca. 0.005 absorbance units, these signals allowed for good precision and reliable fittings. The three aforementioned mutants that contained large fractions of zinc proteins presented a problem, however. At the ionic strength of 2.5 mM, upon each addition of these mutants the transient absorbance became smaller. It decreased to ca. 0.020, the lowest value measurable with acceptable accuracy, before the mutant concentration increased to 40 μM . The problem became easier when the ionic strength was raised 10 mM and disappeared at the ionic strength of 100 mM. Fortunately, at all ionic strengths the absorbance remained constant upon repeated flashing. This finding is correct, because the back reactions in eqs 4 and 6 regenerate zinc cytochrome *c*.

Kinetic Effects of Viscosity. As the representative findings in Figure 1 show, the intramolecular rate constant k_f smoothly decreases and levels off as the solution viscosity increases.

Discussions

Plastocyanin Mutants. The structure of poplar plastocyanin, determined by crystallography,⁶⁸ closely resembles the structure of the bean protein in solution, determined by nmr spectroscopy.⁶⁹ The acidic patch of carboxylate groups consists of two clusters, on either side of Tyr83. The lower cluster, residues 42-45, is larger than the upper cluster, residues 59-61. The hydrophobic patch, made up mostly of nonpolar residues, surrounds His87, a ligand to the copper atoms. These structural features are shown schematically in Figure 2

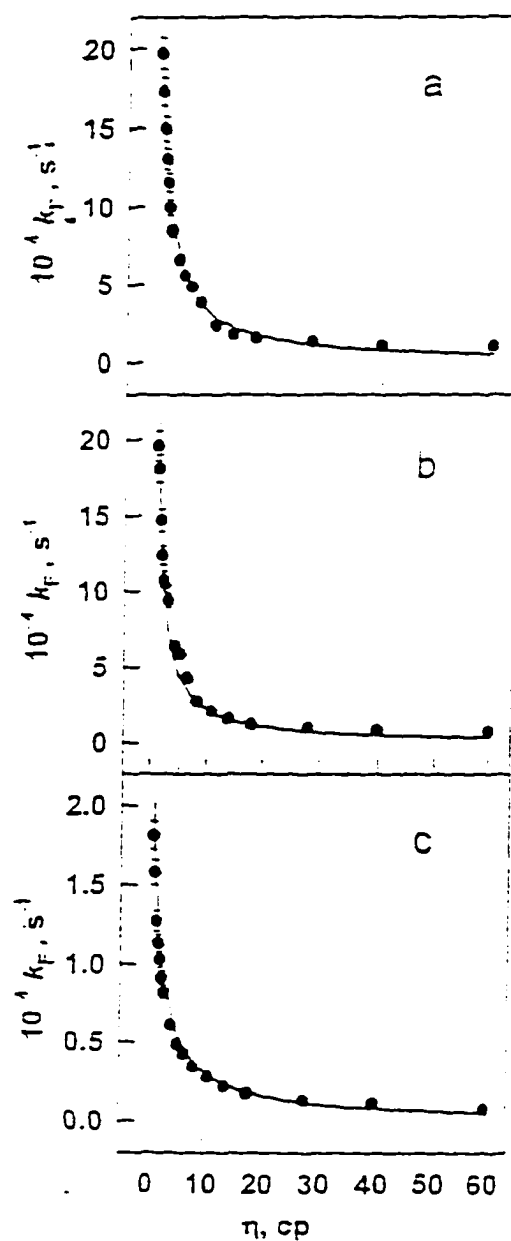


Figure 1. Dependence on solution viscosity of the unimolecular rate constant k_F for the rearrangement of the diprotein complex $^3\text{Zncyt}/\text{pc}(\text{II})$ from the docking configuration into the electron-transfer configuration. Viscosity (η) of a sodium phosphate buffer having pH 7.00 = 0.05 and ionic strength of 2.5 mM at 293 K was adjusted with glycerol. (a) Wild-type cupriplastocyanin; (b) single mutant Asp42Asn; (c) double mutant Glu59Lys/Glu60Gln. The lines are fittings to eq 10. The error bars include two standard deviations.

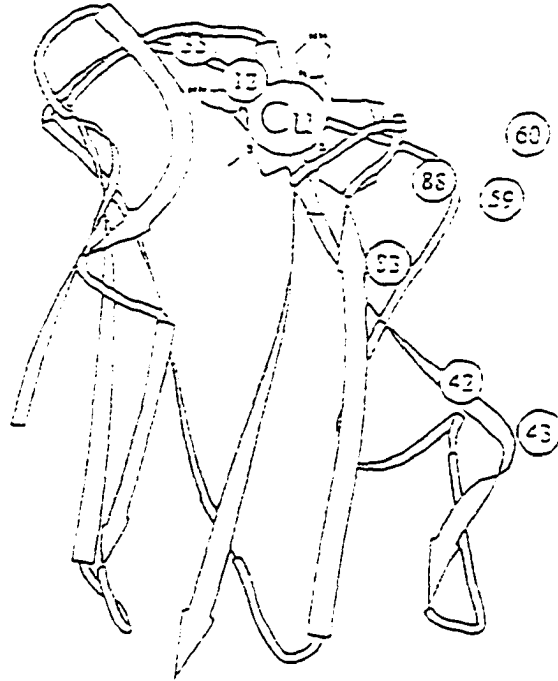


Figure 2. The structure of wild-type plastocyanin showing the copper atom, its four ligands, locations of the mutated residues. All the circled numerals mark the α -carbon atoms, except no. 60, which marks the g -carbon atom in order to avoid overlap.

Before this study, plastocyanin mutants were used to investigate reactions with the two physiological partners of this protein. Mutations in the hydrophobic patch (Gly10, Leu12, and Ala90) hinder the electron transfer to photosystem I,^{66, 70} whereas the mutation Asp42Asn apparently hinders the association but not the subsequent electron-transfer step.⁶⁶ It is accepted that cuproplastocyanin uses its acidic patch for recognition of, and its hydrophobic patch for transferring an electron to, photosystem I.⁷⁰ Conversion into amides of certain carboxylate anions in the acidic patch hinders electron transfer from cytochrome *c* and cytochrome *f*, as in eq 2, but conversion of others has no significant effect.^{48, 66, 71} The mutants Tyr83Phe and Tyr83Leu were compared with the wild-type cupriplastocyanin in their reactions with ferrocyanochrome *f* and ferrocyanochrome *c*, respectively.^{47, 72} The reaction with ferrocyanochrome *c* is only partially analyzed, and this study is a contribution to its full understanding. Even though the two proteins are not physiological partners, the mechanism of their reaction is interesting because it shows the essence of gating.

We work with the nine mutants listed in Table 1. They have been characterized by UV-vis spectrophotometry, EPR spectroscopy, and isoelectric focusing; their redox potentials have been determined; and they have been used in previous kinetic studies with proteins other than cytochrome *c*.⁶⁶ Nonpolar, neutral Leu12 was changed into two polar residues — the neutral Asn and the anionic Glu. The nonpolar, conserved Phe35 was changed into the somewhat polar Tyr. The mutation Gln88Glu introduced a negative charge between the hydrophobic and acidic patches. The anionic residues Asp42 and Glu43 in the acidic patch were neutralized by conversion into the amides. In the double mutation the pair of anions Glu59 and Glu60 were converted into a cation and a neutral residue, Lys and Gln. The prominent residue Tyr83,

which separates the two acidic clusters, was replaced with two aromatic residues — the nonpolar Phe and the polar His. All of the aforementioned estimates of charge at pH 7.0 are based on assumptions that the side chains under consideration have normal pK_a values.

Mechanism of Quenching and the Rate Constants. Previous studies in this laboratory^{57, 58} with the natural plastocyanin from French bean gave much evidence for redox quenching of $^3\text{Zncyt}$, that is, for Scheme 1. Systematic experiments at ten ionic strengths spanning the interval 2.5 mM to 3.00 M showed that at $\mu \leq 10$ mM the reaction can be made to occur mostly by a unimolecular mechanism, within the persistent complex, whereas at $\mu > 40$ mM the reaction occurs solely by a bimolecular mechanism, within the transient complex. Equality of the corresponding rate constants, $k_F = (2.5 \pm 0.4) \times 10^5 \text{ s}^{-1}$ and $k_T = (2.8 \pm 0.6) \times 10^5 \text{ s}^{-1}$, was an early evidence that, in the case of wild-type plastocyanin, the two complexes are the same or that they rearrange into another complex common to both reaction pathways in Scheme 1. Equality of the corresponding activation parameters ΔH^\ddagger (13 ± 2 and 13 ± 1 kJ/mol) and ΔS^\ddagger (-97 ± 4 and -96 ± 3 J/Kmol) is firm evidence that the two complexes are the same, i.e., that the wild-type plastocyanin associates with zinc cytochrome *c* similarly at different ionic strengths.⁶¹ In both complexes, however, electron transfer is gated by a rearrangement, which was quantitatively studied by analyzing the dependence of k_F on solution viscosity.^{41, 57} The aforementioned intracomplex rate constant actually corresponds to the rate-limiting rearrangement process; the electron-transfer step is faster than that and is not directly observed.

In this study, working with the recombinant protein, we reproduced the previous results for the wild-type plastocyanin. Reassured by this reproducibility, we compared the reactivity of the nine mutants. The rate constant k_F was observed directly at $\mu = 2.5$ mM.

We explained above the third phase in the quenching reaction, found only at the ionic strength of 2.5 mM. Since zinc plastocyanin is redox-inactive and incapable of directly quenching $^3\text{Zncyt}$,⁵⁴ its effect must be indirect. It competes with the quencher, cupriplastocyanin, for association with zinc cytochrome *c*. The reactive species, $^3\text{Zncyt}$, must dissociate from zinc plastocyanin and reassociate with cupriplastocyanin.

Ionic strength affects the degree of protein association, i.e., the concentration of the diprotein complex. Ionic strength, however, does not seem to affect the electron-transfer properties of this complex, even though it is clearly a dynamic system. In studies of various protein pairs the dependence of the observed rate constant on ionic strength has been taken as evidence for rearrangement of the protein complex.¹³ This reasoning may be correct in particular cases, but intuitive equating of stability and rigidity is ambiguous.

Kinetic Effects of Viscosity. One of the effects of the solvent is to modulate protein motion. We know of only several prior studies of protein reactions in which viscosity was varied.^{27, 73-76} Studies from this laboratory^{41, 57, 58} showed that buffered mixtures of water and several viscous liquids, glycerol among them, do not perturb the spectroscopic and photophysical properties of zinc cytochrome *c* and plastocyanin. These studies also showed that the smooth dependences of the kind shown in Figure 1 and Table 3 are caused by changes in viscosity, not in other properties of the solution.

Analysis of the Viscosity Effects. According to Kramers's theory,⁷⁵ the rate of crossing a diffusive barrier in a unimolecular reaction is inversely proportional to viscous friction. A configurational change of a diprotein complex depends on the friction of the proteins with each other and with the solvent. In the empirical eq 8 the two frictions are considered additive. The

constant c has units of frequency, s is protein friction and has units of viscosity, h is solvent viscosity, and E is the barrier separating the configurations of the diprotein complex.

Combination of eq 8 with eq 9 from the theory of transition states yields eq 10 for the modified Kramers's theory. The term $(1 + h) RT$ corresponds to the constant c in eq 8. Because the empirical eq 11 proved useful in a previous study,⁵⁸ we use it again. The parameter d defines the dependence of the rearrangement rate on the solution viscosity. It is related, but not equal, to the protein friction (s) in eq 8. Fitting of the rate constant (k_F) and the viscosity (h) to either eq 10 or eq 11 gave the free energy of activation for the rearrangement (ΔG^\ddagger) and the friction parameter σ or δ .

$$k_F = \frac{c}{\sigma + \eta} \exp \frac{-E}{RT} \quad (8)$$

$$k = \frac{k_B T}{h} \exp \frac{-\Delta G^\ddagger}{RT} \quad (9)$$

$$k_F = \frac{k_B T}{h} \times \frac{1 + \eta}{\sigma + \eta} \exp \frac{-\Delta G^\ddagger}{RT} \quad (10)$$

$$k_F = \frac{k_B T}{h} \eta^{-\delta} \exp \frac{-\Delta G^\ddagger}{RT} \quad (11)$$

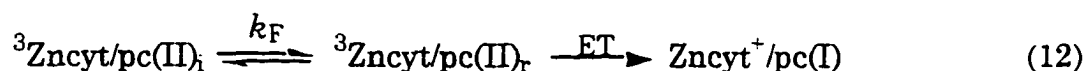
The two fittings gave the results in Table 3, which are consistent with each other and with those in Table 2. The wild-type plastocyanin and the mutants behave alike. The higher value of ΔG^\ddagger for the double mutant can be attributed to electrostatic repulsion between the basic patch in cytochrome c and the pair of residues in the upper cluster whose combined charge was reversed from -2 in the wild-type protein to +1 in the double mutant. Although the rate

constant k_F is slightly higher for Gln88Glu than for other mutants (Table 2), the parameter ΔG^\ddagger is approximately the same, within the error margins of the fitting, for all the single-residue mutants (Table 3). The large kinetic effect of the double mutation is clearly evident in the ΔG^\ddagger value. The relatively small variation of the friction parameters s and d among the various forms of plastocyanin indicates that solution viscosity similarly affects configurational dynamics of diprotein complexes containing these various forms. In other words, zinc cytochrome *c* follows more or less the same trajectory on the surfaces of all the plastocyanin mutants, but the obstacles along the way vary as mutations alter the electrostatic potential. This finding justifies the following analysis of the rearrangement pathways in terms of the rate constants.

Table 3. Fittings to Two Equations of the Dependence on Solution Viscosity of the Rate Constant k_F for the Rearrangement of the Diprotein Complex $^3\text{Zncyt/pc(II)}$ from the Docking Configuration into the Electron-Transfer Configuration. This Rearrangement Gates the Electron-Transfer Reactions in eqs 3 and 5. For the Conditions, see Table 2

| mutant | eq 10 | | eq 11 | |
|-------------------|---------------------------------|---------------|---------------------------------|---------------|
| | ΔG^\ddagger , kJ/mol | σ | ΔG^\ddagger , kJ/mol | δ |
| wild type | 43 ± 1 | 0.7 ± 0.2 | 43 ± 1 | 0.8 ± 0.1 |
| Leu12Asn | 43 ± 1 | 1.2 ± 0.2 | 43 ± 1 | 0.7 ± 0.1 |
| Phe35Tyr | 43 ± 1 | 0.9 ± 0.2 | 43 ± 1 | 0.7 ± 0.1 |
| Gln88Glu | 43 ± 1 | 1.5 ± 0.2 | 43 ± 1 | 0.6 ± 0.1 |
| Glu59Lys/Glu60Gln | 49 ± 1 | 0.7 ± 0.2 | 49 ± 1 | 0.9 ± 0.1 |
| Tyr83Phe | 43 ± 1 | 0.9 ± 0.2 | 43 ± 1 | 0.7 ± 0.1 |
| Asp42Asn | 43 ± 1 | 0.7 ± 0.2 | 43 ± 1 | 0.8 ± 0.1 |
| Glu43Asn | 43 ± 1 | 1.3 ± 0.2 | 43 ± 1 | 0.7 ± 0.1 |

Kinetics of the Rearrangement. As explained above, the rate constants k_F in Table 2 pertain to the configurational fluctuation that is gating the faster electron-transfer reaction. Equation 12 shows the conversion of the initial (i) to the rearranged (r) configuration and subsequent electron transfer. The wild-type and mutant forms of plastocyanin can be compared on the basis of the k_F values, for the persistent complex in Scheme 1. The small effects of replacing Leu12 with other residues are most likely due to conformational perturbations of the active site, which are evident in changes of the redox potential and the EPR and UV-vis spectra of these mutants.⁶⁶ Indeed, those atoms of Leu12 in the wild-type protein that are replaced in the mutant are located only 4 Å from the copper atom.



Only two mutants, Gln88Glu and the double mutant Glu59Lys/Glu60Gln, truly differ from the wild-type protein in the kinetics of rearrangement. In the analysis of these differences, we assume that mutation alters the energetics of rearrangement, but not the initial docking configuration and the rearrangement trajectory. This assumption is justified by the results in Figure 1 and Table 3. These results, which were discussed above, show that solution viscosity identically affects the complexes ${}^3\text{Zncyt/pc(II)}$ containing the wild-type form and all the mutants of plastocyanin.

The rate constants k_F in Table 2 clearly show that mutations in the lower cluster do not affect the rearrangement, whereas those in the upper cluster and at the position no. 88. Although the electrostatic changes in the lower cluster are smaller than those in the upper one, the kinetic results are precise enough and the pattern consistent enough to warrant our

conclusion. Moreover, the direction of change agrees with the electrostatic considerations. Decreasing negative charge in the upper cluster weakens the attraction for the basic patch of cytochrome *c*; increasing positive charge in the upper cluster repels the basic patch; and introducing a negative charge at position no. 88 attracts the basic patch of cytochrome *c*. Moreover, the residue Gln88 is involved in the most efficient electron-tunneling path in the configuration n/eq.⁶³ Both the effects and the noneffects of mutations consistently point at the northern equatorial (n/eq) configuration, or one similar to it, as the reactive one.

The reversal of local charges brought about by the double mutation has a great effect on the protein association, (results from Mr. Milan Crnogorac) Neutralization of a single charge of Asp42 or Glu43, in the lower cluster, has a lesser but significant effect. In these two cases the concentration of the complex ³Zncyt/pc(II) was too low for the reaction k_f to be observed. (Fortunately, all the mutants, including these two, showed the unimolecular component at the ionic strength of 2.5 mM.) Single mutations in positions 42 and 43, however, do not detectably alter the kinetics of rearrangement, as the rate constants k_f show. Introduction of a negative charge in between the acidic and the hydrophobic patch, in the mutant Gln88Glu, does not affect the protein association but does assist their rearrangement in the associated state. Evidently, the residue no. 88 is not involved in the initial docking of the proteins but is involved in the configurational fluctuation.

In studies of dynamic metalloprotein complexes relationships are sometimes sought, and claimed, between association constants and rate constants. This reasoning may be correct in a given case, but intuitive equating of stability and reactivity is ambiguous. Position of an equilibrium between free proteins and their complex is a matter of thermodynamics, whereas

the rate at which this equilibrium is established and the rate at which the complex may rearrange or react are matters of kinetics.

Conclusions and Prospects

A recent analysis of electron-tunneling paths between the heme and the blue copper site indicated two likely pathways for the rearrangement of the diprotein complex cyt/pc from the configuration optimal for the docking *interaction* to the configuration optimal for the electron-transfer *reaction*.⁶³ This theoretical study guided us in the present experimental study. The effects of viscosity on the protein rearrangement involving the wild-type form and nine mutants of cupriplastocyanin showed which of the two pathways is likely for this rate-limiting rearrangement of the complex ³Zncyt/pc(II). On the basis of this study, we will design new plastocyanin mutants and explore in greater detail the dynamics of configurational fluctuations that gate the interprotein electron-transfer reaction.

Acknowledgements. We thank Anita Samuelsson for the purification of the mutants, Maja M. Ivkovic'-Jensen for sharing her kinetic results with us. This work was supported by the U.S. National Science Foundation, through Grant MCB-9222741, and by the Swedish Natural Science Research Council.

References

- (1) Hoffman, B. M., Natan, M. J., Nocek, J. M., and Wallin, S. A. *Struct. Bond.* **1991**, *75*, 86.
- (2) Mauk, A. G. *Struct. Bond.* **1991**, *75*, 131.
- (3) Pelletier, H. and Kraut, J. *Science* **1992**, *258*, 1748.
- (4) Chen, L., Durley, R. C. E., Mathews, F. S., and Davidson, V. L. *Science* **1994**, *264*, 86.
- (5) Chen, L., Poliks, R., Hamada, K., Chen, Z., Mathews, F. S., Davidson, V. L., Satow, Y., Huizinga, E., Vellieux, F. M. D., and Hol, W. G. J. *Biochemistry* **1992**, *31*, 4959.
- (6) McLendon, G. *Struct. Bond.* **1991**, *75*, 160.
- (7) McLendon, G. *Met. Ions Biol. Syst.* **1991**, *27*, 183.
- (8) McLendon, G. and Hake, R. *Chem. Rev.* **1992**, *92*, 481.
- (9) Zhou, J. S. and Hoffman, B. M. *Science* **1994**, *265*, 1693.
- (10) Zhou, J. S., Nocek, J. M., DeVan, M. L., and Hoffman, B. M. *Science* **1995**, *269*, 204.
- (11) Therien, M. J., Chang, J., Raphael, A. L., Bowler, B. E., and Gray, H. B. *Struct. Bond.* **1991**, *75*, 110.
- (12) Winkler, J. R. and Gray, H. B. *Chem. Rev.* **1992**, *92*, 369.
- (13) Kostić, N. M. *Met. Ions Biol. Syst.* **1991**, *27*, 129.
- (14) Pettigrew, G. W. and Moore, G. R. *Cytochrome c: Biological Aspects*, Springer-Verlag, 1987, Berlin.
- (15) Moore, G. R. and Pettigrew, G. W. *Cytochrome c: Evolutionary, Structural, and Physicochemical Aspects*, Springer Verlag, 1990, Berlin.
- (16) Scott, R. A. and Mauk, A. G., Ed. *Cytochrome c: A Multidisciplinary Approach*, University Science Books, Sausalito, 1996, California.

- (17) Redinbo, M. R., Yeates, T.O., and Merchant, S. *J. Bioenerg. Biomembr.* **1994**, *26*, 49.
- (18) Gross, E. L. *Photosyn. Res.* **1993**, *37*, 103.
- (19) Sykes, A.G. *Adv. Inorg. Chem.* **1991**, *36*, 377.
- (20) Sykes, A.G. *Struct. Bond.* **1991**, *75*, 177.
- (21) Wendoloski, J. J., Matthew, J. B. Webber, P. C. and Salemm, F. R. *Science* **1987**, *238*, 794.
- (22) Northrup, S. H., Boles, J. O., and Reynolds, J. C. L. *Science* **1988**, *241*, 67.
- (23) Rodgers, K. K., Pochapsky, T. C., and Sligar, S. G. *Science* **1988**, *240*, 1657.
- (24) Burch, A. M., Rigby, S. E. J., Funk, W. D., MacGilliwray, R. T. A., Mauk, M. R., Mauk, A. G., and Moore, G. R. *Science* **1990**, *247*, 831.
- (25) Wallin, S. A., Stemp, E. D. A., Everest, A. M., Nocek, J. M., Netzel, T. L., and Hoffman, B. *M. J. Am. Chem. Soc.* **1991**, *113*, 1842.
- (26) Roberts, W. A., Freeman, H. C., Getzoff, E. D., Olson, A. J., and Tainer, J. A. **1991**, *J. Biol. Chem.* *266*, 13431.
- (27) Nocek, J. M., Stemp, E. D. A., Finnegan, M. G., Koshy, T. I., Johnson, M. K., Margoliash, E., Mauk, A. G., Smith, M., and Hoffman, B. *M. J. Am. Chem. Soc.* **1991**, *113*, 6822.
- (28) Willie, A., Steyton, P. S., Sligar, S. G., Durham, B., and Millett, F. *Biochemistry* **1992**, *31*, 7237.
- (29) McLendon, G., Zhang, Q., Wallin, S. A., Miller, R. M., Billestone, W., Spears, K. G., and Hoffman, B. *M. J. Am. Chem. Soc.* **1993**, *115*, 3665.
- (30) Harris, T. K. and Davidson V. L. *Biochemistry* **1993**, *32*, 14145.
- (31) Mauk, M. R., Ferrer, J. C., and Mauk, A. G. *Biochemistry* **1994**, *33*, 12609.
- (32) Hoffman, B. M., and Ratner, M. A. *J. Am. Chem. Soc.* **1987**, *109*, 6237.

- (33) Hoffman, B. M., and Ratner, M. A. *J. Am. Chem. Soc.* **1988**, *110*, 8267.
- (34) Brunschwig, B. S. and Sutin, N. *J. Am. Chem. Soc.* **1989**, *111*, 7454.
- (35) Hoffman, B. M., Ratner, M. A., and Wallin, S. A. *Adv. Chem. Ser.* **1990**, *226*, 125.
- (36) Feitelson, J. and McLendon, G. *Biochemistry* **1991**, *30*, 5051.
- (37) Walker, M. C. and Tollin, G. *Biochemistry* **1992**, *31*, 2798.
- (38) Sullivan, E. P., Jr., Hazzard, J. T., Tollin, G., and Enemark, J. H. *J. Am. Chem. Soc.* **1992**, *114*, 9662.
- (39) King, J. C., Binstead, R. A., & Wright, P. E. *Biochim. Biophys. Acta* **1985**, *106*, 262.
- (40) Bagby, S.; Driscoll, P. C.; Goodall, K. G.; Redfield, C.; and Hill, H. A. O. *Eur. J. Biochemistry* **1990**, *188*, 413.
- (41) Zhou, J. S. and Kostić, N. M. *J. Am. Chem. Soc.* **1992**, *114*, 3562.
- (42) Zhou, J. S. and Kostić, N. M. *Biochemistry* **1992**, *31*, 7543.
- (43) Zhou, J. S. and Kostić, N. M. *The Spectrum* **1992**, *5*, No. 2, 1.
- (44) Peerey, L. M. and Kostić, N. M. *Biochemistry* **1989**, *28*, 1861.
- (45) Peerey, L. M., Brothers, H. M., II, Hazzard, J. T., Tollin, G., and Kostić, N. M. *Biochemistry* **1991**, *30*, 9297.
- (46) Meyer, T. E., Zhao, C. G., Cusanovich, M. A., and Tollin, G. *Biochemistry* **1993**, *32*, 4552.
- (47) Modi, S., He, S., Gray, J. C., and Bendall, D. S. *Biochim. Biophys. Acta* **1992**, *1101*, 64.
- (48) Modi, S., Nordling, M., Lundberg, L. G., Hansson, O., and Bendall, D. S. *Biochim. Biophys. Acta* **1992**, *1102*, 85.
- (49) Qin, L. and Kostić, N. M. *Biochemistry* **1992**, *31*, 5145.

- (50) Qin, L., & Kostić, N. M. *Biochemistry* **1993**, *32*, 6273.
- (51) Ye, S., Shen, C., Cotton, T. M., and Kostić, N. M. *J. Inorg. Biochem.* **1997**, *65*, 219.
- (52) Angiolillo, P. J.; and Vanderkooi, J.M. *Biophys. J.* **1995**, *68*, 2505.
- (53) Anni, H., Vanderkooi, J. M., and Mayne, L. *Biochemistry* **1995**, *34*, 5744.
- (54) Zhou, J. S. and Kostić, N. M. *J. Am. Chem. Soc.* **1991**, *113*, 6067
- (55) Zhou, J. S. and Kostić, N. M. *J. Am. Chem. Soc.* **1991**, *113*, 7040
- (56) Zhou, J. S. and Kostić, N. M. *Biochemistry* **1993**, *32*, 4539
- (57) Zhou, J. S. and Kostić, N. M. *J. Am. Chem. Soc.* **1993**, *115*, 10796.
- (58) Qin, L. and Kostić, N. M. *Biochemistry* **1994**, *33*, 12592.
- (59) Qin, L. and Kostić, N. M. *Biochemistry* **1996**, *35*, 3379.
- (60) Kostić, N. M. in *Metal-Containing Polymeric Materials*, Pitman, 1996, C.U., Jr. et al., Ed., Plenum Publishing, New York.
- (61) Ivković-Jensen, M. and Kostić, N. M. *Biochemistry*, **1996**, *35*, 15095.
- (62) Onuchic, J. N., Beratan, D. N., Winkler, J. R., and Gray, H. B. *Ann. Rev. Biophys. Biomol. Struct.* **1992**, *21*, 349.
- (63) Ullmann, G. M. and Kostić, N. M. *J. Am. Chem. Soc.* **1995**, *117*, 4766.
- (64) Katoh, S., Shiratori, I., and Takamiya, A. *J. Biochem. (Tokyo)* **1962**, *51*, 32.
- (65) Sigfridsson, K., Hansson, Ö., Karlsson, B. G., Baltzer, L., Nordling, M., and Lundberg, L. *G. Biochim. Biophys. Acta* **1995**, *1228*, 28.
- (66) Sigfridsson, K., Young, S., and Hansson, Ö. *Biochemistry* **1996**, *35*, 1249.
- (67) Gill, S. C. and Von Hippel, P. H. *Anal. Biochem.* **1989**, *182*, 319.

- (68) Guss, J. M. and Freeman, H. C. *J. Mol. Biol.* **1983**, *169*, 521. (74) Beece, D.; Eisenstein, L., Frauenfelder, H., Good, D., Marden, M. C., Reinisch, L., Reynolds, A. H., Sorensen, L. B., and Yue, K. T. *Biochemistry* **1980**, *19*, 5147.
- (69) Moore, J. M., Lepre, C. A., Gippert, G. P., Chazin, W. J., Case, D. A., and Wright, P. E. *J. Mol. Biol.* **1991**, *221*, 533.
- (70) Haehnel, W., Jansen, T., Gause, K., Klösgen, R. B., Stahl, B., Michl, D., Huvermann, B., Karas, M., and Herrmann, R. G. *EMBO J.* **1994**, *13*, 1028.
- (71) Lee, B. H., Hibino, T., Takabe, T., Weisbeek, P. J., and Takabe, T. *J. Biochem. (Tokyo)* **1995**, *117*, 1209.
- (72) He, S., Modi, S., Bendall, D. S.; and Gray, J. C. *EMBO J.* **1991**, *10*, 4011.
- (73) Gavish, B. and Werber, M. M. *Biochemistry* **1979**, *18*, 1269.
- (74) Kramers, H. A. *Physica (Utrecht)* **1940**, *7*, 284.
- (75) Khoshtariya, D. E., Hammerstad-Pedersen, J. M., & Ulstrup, J. *Biochim. Biophys. Acta* **1991**, *1076*, 359.
- (76) Ansari, A.; Jones, C. M.; Henry, E. R.; Hoffrichter, J.; and Eaton, W. A. *Science* **1992**, *256*, 1796.
- (77) Vanderkooi, J. M. and Erecinska, M. *Eur. J. Biochem.* **1975**, *60*, 199.
- (78) Vanderkooi, J. M., Adar, F., and Erecinska, M. *Eur. J. Biochem.* **1976**, *64*, 381.

GENERAL CONCLUSIONS

We characterized zinc-substituted cytochrome c by circular dichroism and resonance Raman spectra. Our analyses show that replacement of iron(II) or iron(III) by zinc(II) in cytochrome c cause little structural perturbation of the protein conformation and a large change of ligation at the active site. One of the axial ligands in native cytochrome c, most likely Met 80, does not seem to be coordinated in the zinc form of the protein.

The electron-transfer reactions in sol-gel glass is very interesting. The metalloproteins are stable in glass, but they may behave differently from in aqueous solution. The surface charge of the glass plays a important role and the reactivities of doped protein are governed by the interactions among the protein, the glass, and the quencher. These findings are essential in the design of sol-gel glass derived biosensors.

The reactions of zinc cytochrome c with small redox quenchers in aqueous solution are studied. We proposed the first example of reductive quenching of zinc cytochrome c, by hexacyanoferrate(II) anion and by conjugated bases of ethylenediaminetetraacetic acid.

The electron-transfer reactions between zinc cytochrome c and plastocyanin are also studied. We studied the effects of plastocyanin mutation on the rate of diprotein complex rearrangement. Viscosity effects are also studied and the activation parameters for diprotein complex arrangement obtained.

ACKNOWLEDGMENTS

I would like to thank Professor Nenad kostić for excellent mentorship throughout my graduate career. I am also thankful to the members of my research group, past or present, for their friendship and many stimulating scientific discussions. Finally, I wish to thank my parents for their years of support and encouragement.